

ABSTRACT

Title of Document:

MASS SPECTROMETRIC ANALYSIS OF
CYTOPLASMIC RIBOSOMAL PROTEINS IN
DRUG RESISTANT AND DRUG SUSCEPTIBLE
HUMAN CELL LINES

Faith A. Hays, Doctor of Philosophy, 2006

Directed By:

Professor Catherine Fenselau
Department of Chemistry and Biochemistry

This study examines changes in cytoplasmic ribosomes that accompany drug resistance in MCF-7 breast cancer cells. Differences in ribosomal protein composition between drug susceptible and drug resistant cell lines were examined. Ribosomes were isolated from mitoxantrone susceptible and mitoxantrone resistant MCF-7 cells. The acid extracted ribosomal proteins were subjected to optimized 2DGE using a “zoom” strip (pI 7-11) for the first dimension separation. Further optimization of 2DGE included the use of a 15mM DTT wick at the cathode end of the focusing tray, decreasing the protein loading amount and using large format gels for the second dimension. Forty-nine ribosomal proteins were identified in the drug susceptible cell line. Two novel protein isoforms of the proteins RPS3 and one novel isoform of RPS10 were identified in the drug resistant cell line.

Methods for the extraction and detection of ribosomal proteins from the 2D gel were developed. The method of Mirza et.al. was modified and used to

extract ribosomal proteins from the gel. The detection of these proteins was optimized by the use of 50% ACN/1.0% TFA to solubilize the MALDI matrix. In addition, the extracted protein solution was mixed 1:1 with 5% Triton X-100. Intact molecular weights were determined for 41 ribosomal proteins using high performance MALDI-TOF mass spectrometry.

The average number of ribosomes per cell was determined for the drug susceptible, as well as the drug resistant cell line, and found to be unchanged.

**MASS SPECTROMETRIC ANALYSIS OF CYTOPLASMIC
RIBOSOMAL PROTEINS IN DRUG RESISTANT
AND DRUG SUSCEPTIBLE CELL LINES**

By

Faith A. Hays

Dissertation submitted to the Faculty of the Graduate School of the
University of Maryland, College Park, in partial fulfillment
of the requirements for the degree of
Doctor of Philosophy
2006

Advisory Committee:
Professor Catherine Fenselau, Chair
Professor Jonathan Dinman
Professor Peter Gutierrez
Professor Douglas Julin
Professor George Lorimer

© Copyright by
Faith A. Hays
2006

Dedication

My time and effort in graduate school as well as this thesis is dedicated to my son, Noah Hays. He inspires me to not allow anything to stand in the way of my accomplishments.

Acknowledgements

I would first like to acknowledge my friends and family for their support. I must start with Noah, who never lets me think about work too much when I'm not there. My mother, Barabara Hays, provides guidance and is always willing to help. Natasha Smith shows me what friendship means. Rachael Strong is always willing to listen. Sunny Wang inspires me to be strong. Cheryl Lane makes me laugh so hard. Barabara and Warren Freeman are my biggest cheerleaders. Suzanne Kilgore gives pure love and support.

The people of the lab, past and present, have provided the best working atmosphere and make me want to come to work on lazy days, sometimes. My co-workers, Jeff Whiteaker, Steve Swatkoski, Andrei Chertov and Scott Russell were always willing to provide perspective, and I thank them.

I would like to thank Dr. Catherine Fenselau for her commitment to see me through.

Table of Contents

Dedication	ii
Acknowledgements	iii
Table of Contents	iv
List of Tables	vi
List of Figures	vii
Chapter 1: Introduction	1
Ribosomes	1
<i>Ribosome Structure</i>	3
<i>Ribosome Function</i>	6
<i>The Reported Changes of Ribosomes and Ribosomal Proteins</i>	9
Proteomics	11
Two Dimensional Gel Electrophoresis	13
Mass Spectrometry	16
Post-Translational Modifications	19
<i>Bottom-Up Approach</i>	21
<i>Top-Down Approach</i>	22
Protein Identification and Bioinformatics	25
Hypothesis and Objectives	27
Chapter 2: Materials and Methods	28
Materials	28
Equipment	28
Methods	29
<i>Cell Culture and Harvest</i>	29
<i>Isolation of Ribosomes and Extraction of Ribosomal Proteins</i>	30
<i>Two-Dimensional Gel Electrophoresis</i>	32
<i>Image Analysis and Comparative Densitometry</i>	36
<i>In-Gel Digestion and Desalting</i>	36
<i>Mass Spectrometry</i>	38
<i>Protein Identification</i>	39
<i>Isolation of Protein Isoforms and Mass Measurement</i>	42
<i>Absolute Quantitation</i>	44
<i>Error Analysis</i>	45
Chapter 3: Results	47
Reproducible Method for Isolation and Purification of Ribosomal Proteins	47
Optimization of 2DGE and Protein Identification	47
Comparative Study between Parental and Mitoxantrone ^R MCF-7 Cells	63
Characterization of Protein Isoforms	69
Absolute Quantitation of Ribosomes	74
Chapter 4: Discussion	79
Characterization of the Ribosome	79
Bottom-Up Characterization of the Ribosome	80
Optimization of 2D Gel Analysis	80
Identification of Proteins	81
Sequence Coverage	87

Top-Down Characterization of the MCF-7 Ribosome	89
Optimization of Extraction of Ribosomal Proteins from Gels.....	91
MALDI Optimization for Molecular Mass Determination.....	93
Intact Molecular Weights.....	93
Implications for Multidrug Resistance in Breast Cancer.....	96
RPS3	97
RPS10	98
Conclusion	99
Bibliography.....	100

List of Tables

	Page
Table 3.1: Proteins identified using the bottom-up approach from 2D gels.....	54-55
Table 3.2: Sequence coverage of proteins using the bottom-up approach.....	56-62
Table 3.3: Relative quantitation of proteins with altered abundances.....	66
Table 3.4: Result of precision study of the MALDI-TOF.....	70
Table 3.5: Intact molecular weights of the ribosomal proteins.....	73
Table 4.1 The list of human ribosomal proteins in the SwissProt database.....	84-85
Table 4.2 In-silico digest of small molecular weight ribosomal proteins.....	88

List of Figures

	Page
Figure 1.1 Three step process of protein synthesis.....	8
Figure 1.2 Scheme for identification of proteins using a bottom-up approach.....	15
Figure 1.3 Ion path in the quadrupole time-of-flight mass spectrometer.....	18
Figure 1.4 Schematic representation of matrix-assisted laser desorption ionization.....	20
Figure 1.5 Dominant fragmentation pattern of a peptide.....	23
Figure 2.1 Scheme of 2DGE.....	34
Figure 2.2 Comparison of 2D gels from using the Compugen Z3 program.....	35
Figure 2.3 Protein identification using peptide mass fingerprinting.....	40
Figure 2.4 Protein identification using Tandem MS.....	41
Figure 2.5 Intact molecular weight determination.....	43
Figure 3.1 Evaluation of method 1 for isolation of ribosomal proteins.....	48
Figure 3.2 Evaluation of method 2 for isolation of ribosomal proteins.....	49
Figure 3.3 Evaluation of method 3 for isolation of ribosomal proteins.....	50
Figure 3.4 Comparison of 2D gel of ribosomal proteins before and after optimization.....	52
Figure 3.5 Annotated gel of ribosomal proteins.....	53
Figure 3.6 Zoomed views of the 2D gels of ribosomal proteins.....	64
Figure 3.7 Compugen image of the comparison of the parental cell line and the mitoxantrone resistant cell line.....	65
Figure 3.8 RPS3 protein abundance changes.....	67
Figure 3.9 RPS10 protein abundance changes.....	68
Figure 3.10 The intact molecular weight of the standard apomyoglobin.....	70
Figure 3.11 Overlay of the spectra from the precision study.....	72
Figure 3.12 Bar graph representation of the number of cell per harvest.....	76
Figure 3.13 Bar graph representation of the number of ribosome per harvest.....	77
Figure 3.14 Bar graph representation of the number of ribosomes per cell.....	78
Figure 4.1 A ClustLW sequence alignment of three isoforms of ribosomal protein S4.....	86

Chapter 1: Introduction

Ribosomes

Ribosomes synthesize all cellular proteins, making their role in cell growth and proliferation absolutely critical for survival. The ribosome is made up of ribosomal RNA (rRNA) and proteins. Initially the proteins were believed to be the catalysts in the polymerization of amino acids to form polypeptides, but it was discovered that the rRNA was functioning as the enzyme [1, 2]. In order for the ribosome to synthesize a protein, it requires: a template which dictates the sequence of amino acids, the amino acids themselves, and the energy to form the new peptide bonds.

The template from which the ribosome synthesizes the protein is in the form of messenger RNA (mRNA). Messenger RNA is a complementary transcript of the gene in the DNA blueprint. Messenger RNA contains codons, which are base pair triplets that code for a certain amino acid. In eukaryotic cells, the DNA and the ribosomes are spatially segregated. The mRNA serves to deliver the sequence information by traveling from the nucleus to the ribosome in the cytoplasm. In many cases the mRNA molecule is altered or modified during this transition.

In order to synthesize the protein using amino acid building blocks, a supply of activated amino acids is necessary. Ribosomes incorporate amino acids, which are activated by attachment to transfer RNA (tRNA) and ATP. The tRNA carries the amino acid to the ribosome and the GTP provides the energy to form the new peptide bond. The tRNA contains an anticodon,

which is complementary to the codon. This anticodon interacts with the codons on the mRNA molecule to ensure the correct amino acid is added to the polypeptide chain. Once the proofreading function is carried out, the amino acid is incorporated into the growing polypeptide chain.

Ribosomes are so abundant in actively growing cells, they can account for up to 30% of the dry weight of the cell. The specific amount of ribosomes in a cell depends on the activity of the cell or the tissue to which the cell belongs. With the exception of cells that have a secretory function, most ribosomes are found free in the cytoplasm of the cell.

Ribosomes are assembled in the nucleolus of the cell. Pre-rRNA is transcribed in the nucleus and extensively modified to yield the mature rRNA species in the nucleolus. Modification of the pre-rRNA in eukaryotes includes methylation of the sugar 2' hydroxyl group or pseudouridine formation. The ribosomal proteins, which are synthesized by cytoplasmic ribosomes, are transported to the nucleolus. The proteins associate with the maturing rRNA segments as they are being processed from the pre-rRNA. The current belief is that the individual pre-ribosomal subunits are transported out of the nucleus through the nuclear pore complex [3]. Further processing occurs in the cytoplasm which results in the mature ribosomal subunits.

Although ribosomal function has been conserved across nature, structural differences occur between prokaryotes and eukaryotes. For prokaryotic ribosomes, the RNA to protein ratio is about 2:1 by weight, the molecular mass is about 2.5×10^6 Da, and the diameter is about 200-250 Å.

Conversely, eukaryotic ribosomes have an RNA to protein ratio of about 1:1 by weight, the molecular mass is about 4×10^6 Da, and the diameter is about 250-300 Å [3, 4]. While chloroplasts and mitochondria are found in eukaryotes, their ribosomes do not resemble the 80S eukaryotic ribosomes. Chloroplast ribosomes strongly resemble the 70S ribosomes of eubacteria and blue-green algae. The characteristics of mitochondrial ribosomes depend on the organism from which they are derived, and are therefore more diverse.

Ribosome Structure

The ribosome is made up of two subunits, termed the large subunit and the small subunit. The intact ribosome, as well as each subunit, is characterized in terms of their sedimentation coefficient. For eukaryotes, the sedimentation coefficients are 80S for the intact ribosome and 60S and 40S for the large and small subunits respectively. For prokaryotes, the intact ribosome has a sedimentation coefficient of 70S while the large and small subunits have values of 50S and 30S respectively. The subunits are found separated in the cell unless actively translating an mRNA transcript. Extensive electron microscopy studies as well as cross-linking studies have been performed in order to determine the shape of the individual subunits as well as the intact ribosome [5, 6]. X-ray crystallography studies have also been performed, initially only on ribosomal subunits but eventually on intact

ribosomes from bacteria, to obtain a more detailed understanding of the interaction between the rRNA and ribosomal proteins.

The most recent crystal structure reported for a ribosome was published in *Science* in 2005 and was for the intact 70S ribosome of the *E. coli* at 3.5Å resolution [7]. Previously, structures were reported for the 70S ribosome for *T. thermophilus* at 5.5Å [8] in addition to two versions of the crystal structure of *T. thermophilus* small ribosomal subunit, one which was obtained at 3.0Å resolution[9], the other at 3.3 Å [10]. A 3.1Å resolution structure for the large subunit from *D. radiodurans* was reported in 2001 [11] and a 2.4Å resolution structure was reported for the large subunit of *H. marismortui* in 2000 [12]. Although ribosomes have remained fairly conserved evolutionarily, differences exist. The number of proteins observed in the ribosome and the length of the various rRNA molecules vary from species to species [4]. Ribosomes from multiple sources must be studied in order to understand the structural and functional effects of these changes in rRNA and proteins.

The rRNA determines the overall shape of the ribosomal subunits. The rRNA is also characterized by its sedimentation coefficient. Since the first work was done on *E. coli* ribosomes, the sedimentation coefficients assigned to the rRNA species are only accurate for *E. coli*. The small subunit contains one rRNA molecule which is 16S in *E. coli* or 16S-like in other organisms. The 16S-like rRNA in human cytoplasmic ribosomes is 1880 nucleotides long. The large subunits of bacteria consist of a 23S rRNA. The

large subunit of eukaryotes contains two, strongly interacting rRNA species: the 23S-like and the 5.8S. The 23S-like rRNA contains about 5,025 nucleotides in the human cytoplasmic ribosome, while the 5.8S contains about 160. In all prokaryotes and eukaryotes, the large subunit also contains a 5S rRNA, which is about 120 nucleotides long.

The eukaryotic ribosome contains about 75-80 proteins [13]. Most of the proteins are extremely basic with a pI range of about 9-13. There are a few exceptions with pI values about 6 [4]. The molecular weights of the majority proteins are in the range of 10kDa to 30kDa. Two eukaryotic ribosomal proteins have molecular weights in the range of 50-60kDa, while there are 10 small proteins which have molecular weights under 10kDa. The small subunit of the eukaryotic ribosome contains about 30 proteins, while the large subunit contains about 50. The *E. coli* ribosome contains 55 total proteins, which helps explain the difference in the rRNA to protein ratio in prokaryotes versus eukaryotes. Almost all of the proteins are present in a single copy per ribosome. The *E. coli* ribosomal proteins were named based on a gel electrophoresis experiment performed in 1970 by Kaltschmidt and Wittman [14]. The subunits were separated and a 2D electrophoresis experiment was performed. The proteins were numbered starting from one at the top of the gel and counting down to the bottom. Similar experiments were run for different species and therefore ribosomal proteins across the species had their own nomenclatures according to the electrophoretic map. For this reason, the protein number corresponding to a protein in *E. coli* has no

association with a protein of the same number in humans. When it was discovered that ribosomal proteins were relatively conserved, homologies were determined, and family groups were assigned. Thirty-one proteins of the *E. coli* ribosome share sequence homology with eukaryotic proteins [15]. In order to gain understanding of how a given protein interacts with the rRNA, cross-linking studies and disassembly studies have been performed [6, 16, 17].

Ribosome Function

Protein synthesis occurs in three distinct steps: initiation, elongation and termination, which are illustrated in Figure 1.1. Initiation is the stage in which the ribosomal subunits come together with an mRNA molecule, the initiator tRNA, and some elongation factors. Elongation occurs as the mRNA transcript is “read” and amino acids are added to the initiating amino acid to form the polypeptide chain. Termination involves the end of the elongation process and dissociation of the translational components.

Each step contains multiple interactions allowing the ribosome to continue incorporating amino acids. The initiator complex is formed as the 40S subunit binds to an mRNA molecule as can be seen in panel A of Figure 1.1. The initiator tRNA, which contains a methionine residue, is activated by binding to a molecule of ATP. An important characteristic of the initiator tRNA is that it has preferable affinity for the P (peptidyl tRNA) site and it is not

recognized by elongation factor 1, which is usually involved in bringing aminoacyl-tRNA's to the ribosome.

Initiation factors are bound to the ribosome in a complex with GTP and subsequently released by GTP hydrolysis. For example, initiation factor 2 (IF-2) assembles with the ribosome as a complex of aminoacyl-tRNA and GTP and catalyzes the binding of aminoacyl-tRNA to the P site in the ribosome. The initiator complex is bound to the start codon on the mRNA molecule. Initiation factor-3 prevents association of the large subunit with the small subunit until all of the other factors are in place. The 60S subunit binds to the complex, and the initiation factor is released from the complex. The rate limiting step of initiation is the binding of an mRNA to the 40S subunit because of the selection of the mRNA molecule as well as the correct positioning of the start codon. The ribosome is ready to accept a tRNA molecule into the A (aminoacyl tRNA) site and begin the elongation process.

Elongation consists of a series of steps which are repeated until the stop codon of the mRNA has been reached. Panel B of Figure 1.1 illustrates the sequence. In the first step, the tRNA carrying an amino acid is bound to the A site, with the aid of the elongation factor 1-GTP (EF-1-GTP) complex. The GTP is hydrolyzed and EF-1 is released. The specificity of the tRNA that binds is dependent on the template codon because the codon on the mRNA and the anticodon on the tRNA must be complementary to each other.

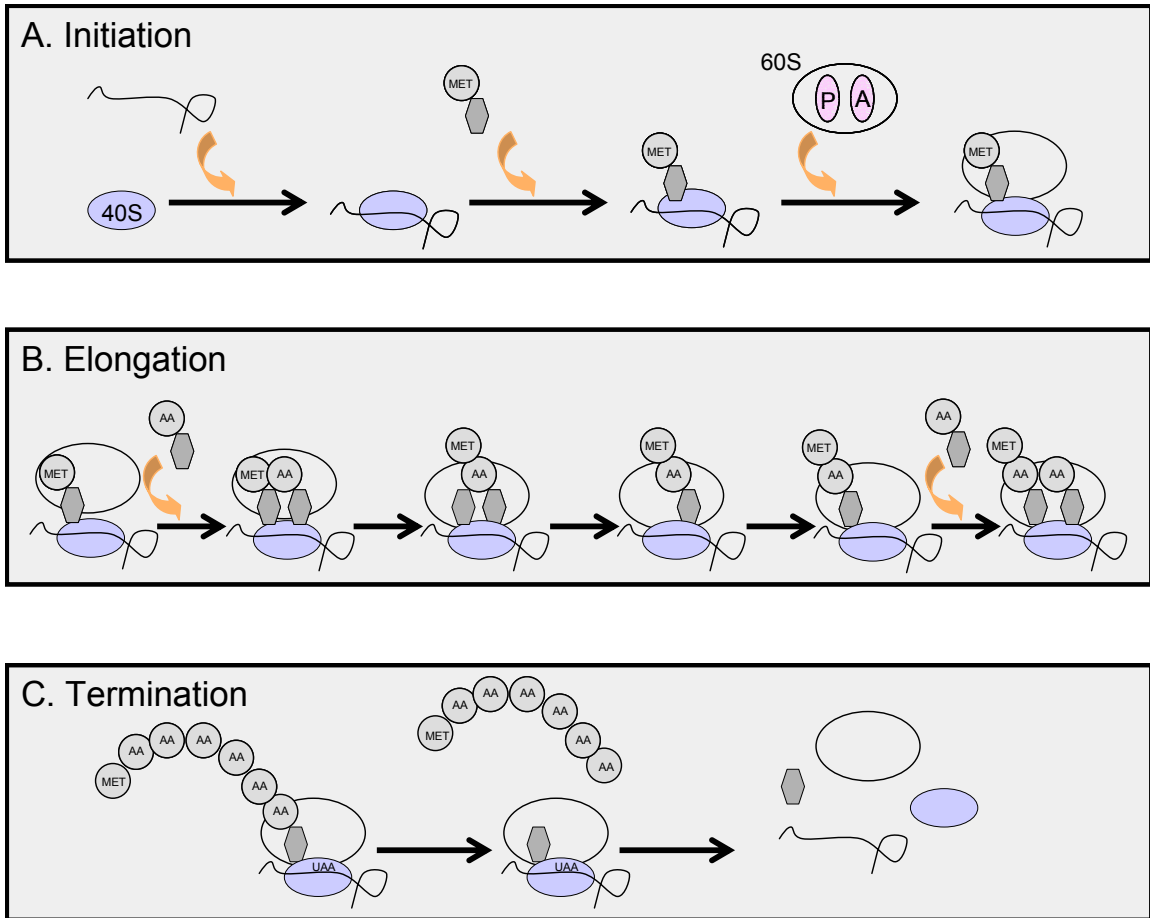


Figure 1.1 Three step process of protein synthesis

Initiation involves all of the components involved in protein synthesis coming together in an ordered manner. The small ribosomal subunit interacts with the mRNA and initiator tRNA before the large subunit is recruited (**A**). Elongation involves the incorporation of amino acids into the polypeptide chain by the repetition of multiple steps (**B**). Termination occurs when the stop codon enters the reading frame. This initiates hydrolysis of the polypeptide chain and dissociation of the ribosome (**C**).

A transfer reaction occurs in which the polypeptide chain on the tRNA in the P site is transferred to the tRNA in the A site. This peptidyltransferase reaction is catalyzed by the large subunit of the ribosome. The NH₂ group of the amino acid bound to the aminoacyl-tRNA performs a nucleophilic attack on the carboxyl group of the amino acid on the peptidyl-tRNA. This reaction results in a peptide bond forming between the peptide chain and the amino acid. The deacylated tRNA in the P site is ejected from the ribosome and the newly formed peptidyl-tRNA is translocated from the A site to the P site. Simultaneously, the ribosome shifts the distance of one codon from the 5' towards the 3' on the mRNA revealing a new codon in the empty A site. Elongation factor-2 (EF-2) complexed with GTP catalyzes this translocation reaction and again, hydrolysis of GTP results in the release of EF-2. Each time this sequence is repeated, one amino acid is added to the polypeptide chain with the consumption of one molecule of aminoacyl-tRNA, two molecules of GTP and two water molecules.

Termination occurs as a result of a stop codon on the mRNA moving into the reading frame. The stop codon does not have a cognate aminoacyl-tRNA; therefore the polypeptide chain is ended. The presentation of the stop codon in the reading frame attracts proteins called release factors. Their function is to bind to the ribosome and induce hydrolysis of the polypeptide from the peptidyl-tRNA in the P site. In eukaryotes, there is one release factor, RF1, which recognizes all of the potential stop codons, UAA, UAG or UGA. It appears that the RF1 simulates tRNA binding in the A site. Instead

of an amino acid from the aminoacyl-tRNA performing a nucleophilic attack on the peptidyl-tRNA polypeptide, a water molecule performs the attack. This hydrolysis reaction releases the polypeptide chain. RF1 is released as a result of GTP hydrolysis followed by the release of the final deacylated tRNA. The ribosome subunits dissociate as can be seen in Panel C of Figure 1.3 [3, 4].

The Reported Changes of Ribosomes and Ribosomal Proteins

Although the rRNA is the catalyst in the synthesis of polypeptide chains, ribosomal proteins still have an important function by providing the structure for the rRNA. Changes in the ribosome have been observed on different levels. For instance, the observation was made that the number of active ribosomes per cell differed as a result of drug resistance [18]. Eukaryotic ribosomal proteins are encoded by more than one gene, indicating that multiple isoforms of the proteins can exist and have been shown to be present in 80S ribosomes [19]. The particular protein isoforms present in the ribosome depends in part on the developmental stage of the organism.

It has been demonstrated that the protein complement of ribosomes is heterogeneous for a specific organism, depending on the functionality and tissue of origin [20, 21]. In addition, a myriad of reports exist on the differential gene expression of ribosomal proteins [22-28] as well as altered abundance of ribosomal proteins [29, 30] in diseased states. While increased expression or abundance of ribosomal proteins may not indicate a change in

the structure of the ribosome, it does indicate a potential deregulation of the very coordinated process of ribosomal protein synthesis.

Ribosomal proteins have also been observed to change in both abundance and structure in antibiotic resistant bacteria [31]. Gregory and Dahlberg showed that alterations in ribosomal proteins are responsible for erythromycin resistance in *E. coli* even though the proteins had no direct contact with the drug [32]. It was determined that resistance was conferred through perturbation of the surrounding 23S rRNA as a result of the protein changes. Large subunit ribosomal protein mutations have been observed as a result of resistance to a drug that induces frameshifting of the mRNA on the small subunit [33]. This indicates that the change in structure of the ribosomal proteins of the large subunit create conformational rearrangements of the small subunit.

Ribosomal proteins are known to be heavily altered by such post-translational modifications (PTM) as: methionine loss, N-terminal acetylation; lysine acetylation; methylation and phosphorylation [33-42]. It is unclear, however, what role the post-translational modifications play in ribosomal proteins. In a few cases, PTM's are known to be regulated by developmental stage. These include the reduction in the number of glutamic acid residues on the C-terminus of ribosomal protein S6 [15]. Another example is the phosphorylation state of RPS6. This modification is thought to regulate cell growth because the number of phosphorylations on the protein is proportional to the level of protein synthesis [43]. The phosphorylation of RPS6 is coupled

to extracellular signaling pathways, which are deregulated in cancer cells [44, 45].

Proteomics

In order to study protein changes in a complex such as the ribosome, traditional biochemical techniques would be time consuming because one protein is analyzed at a time. Proteomic methods are more efficient because they are designed to characterize many proteins at one time. The term “proteome” refers to the dynamic protein complement of the genome, which is static. The proteins expressed in a cell change depending on the stage of growth and function of the cell. In addition, the DNA sequence does not predict post translational modifications or processing that proteins may experience to alter activity. Although it has been determined that the human genome consists of 25,000 genes, with alternative splicing and post translational modifications, it is estimated that over 100,000 populations of proteins exist in the cell [46].

The proteome is a theoretical set of proteins, because it is impossible to determine all of the proteins present in a cell at one time. Sample complexity, dynamic range of the concentrations of the proteins and a lack of technology are among the challenges. The dynamic range of the proteins in a cell varies greatly. Some proteins are present in just a few copies per cell, whereas others are present in as high as 10^6 copies per cell [46].

Fractionating the proteins of a cell is one way of reducing the sample complexity. Many types of fractionation have been employed in proteomic studies, such as various liquid chromatographic methods and subcellular fractionation. Subcellular fractionation allows the global cellular changes as a result of acquired drug resistance to be determined by studying one fraction at a time. The end result is the ability to hypothesize cellular mechanisms based on changes in the individual fractions. The issue of dynamic range can be addressed by fractionating as well, but other strategies such as removal of extremely abundant proteins will allow the less abundant proteins to be detected.

Comparative proteomics is a useful method in which a control state can be compared to an altered state of a system in order to find differences that result. For example, in this work on acquired drug resistance, a drug susceptible cell line is the control state, while a drug resistant cell line is the altered state. The protein differences that are discovered between the two may give insight into the mechanisms of drug resistance. The proteins are evaluated on two different levels: the relative abundance of the protein and the post-translational modification changes of the proteins. The scheme for identifying post-translational modifications can be seen in Figure 1.2.

Two-Dimensional Gel Electrophoresis

Modern two-dimensional polyacrylamide gel electrophoresis (2DGE) is a method in which proteins are separated in the first dimension by their

isoelectric point and in the second dimension by molecular weight. This two-dimensional separation provides better resolution of individual proteins from complex mixtures than methods such as 1D gels or liquid chromatography. 2DGE is a powerful technique because a visual comparison can be made between the control and experimental gels. This visual comparison gives the ability to compare abundance profiles and determine differences in the profiles.

When 2DGE was applied to the ribosomal proteins, both the first and second dimension separated the proteins based on charge. This elicited a diagonal pattern of protein spots. A method was introduced by O'Farrell in 1975 in which the proteins were separated by charge in the first dimension, as before [47]. The second dimension included the addition of sodium dodecyl sulfate in order to remove the charge differences of the proteins as a variable and separate proteins based on molecular weight. This optimization improved the resolution of the proteins even further. In addition to allowing more proteins to be separated in one experiment, the effective area of the gel was increased.

The introduction of immobilized pH gradient (IPG) strips for isoelectric focusing, which create a gradient with a resolution of 0.001 pH units, also contributed greatly to the reproducibility and resolution of the proteins [48]. Performing 2DGE on ribosomal proteins presents a unique challenge because of the basicity of the proteins. A number of reasons contribute to the poor resolution and reproducibility of 2D gels of basic proteins [49-56].

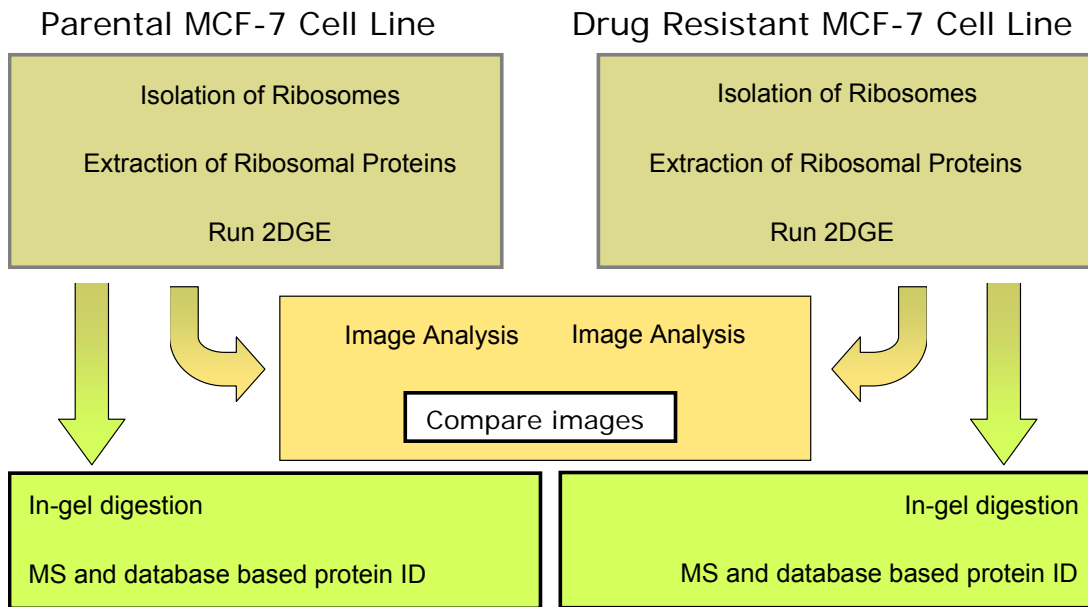


Figure 1.2 Scheme for identification of proteins using a bottom-up approach

Most involve the isoelectric focusing step of the first dimension. Reducing agents are added to the buffer to keep the proteins reduced. Often times, the reducing agent migrates toward the anode of the focusing chamber depleting the cathode end of reducing agent. The proteins are therefore susceptible to both inter and intra-molecular oxidation. This effect results in horizontal streaking due to the many populations of proteins with different disulfide bonds.

Mass Spectrometry

Mass spectrometry is a method in which the mass of an analyte can be determined giving valuable information on the structure of the analyte. The mass spectrometer can be separated into 3 regions: an ionization source, an analyzer and a detector. The source ionizes the analyte so that it can be detected as well as vaporizing it so that it can be separated in a vacuum by the analyzers. The analyzer separates the charged, airborne analytes based on their m/z , where m is the mass and z is the charge of the analyte. The detector converts the electronic signal that results from the charged, m/z separated analytes colliding with the detector plate into a mass spectrum.

Mass spectrometry became an integral tool for protein studies in the late 1980's with the invention and application of the matrix-assisted laser desorption ionization mass spectrometry (MALDI-MS) and electrospray ionization mass spectrometry (ESI-MS) techniques. These methods are able to generate large molecular weight ions. They produce volatile ions of non-

volatile biomolecules, such as proteins, allowing the biomolecule to remain intact during ionization, separation and detection.

The presented work was performed on two different types of mass spectrometers, which will be discussed briefly. The configuration of the Applied Biosystems *Q-star Pulsar i* can be seen in Figure 1.3. Electrospray ionization was first applied to mass spectrometry of large biomolecules by Nobel laureate John Fenn in 1989 [57]. The analyte is mixed in a conducting solution, which is then sprayed across a high potential from a conducting metal-coated needle.

The solution forms fine droplets which contain solvent and analyte, leaving the gaseous analyte ions. ESI often produces analytes which are multiply charged as a result of multiple protonations or deprotonations.

The Q-star can be operated in different modes depending on the information sought. In the scanning mode, the instrument scans all m/z ratios in a given range. The ions introduced from the electrospray source travel through the two quadrupoles and are pulsed into the time-of-flight tube. The m/z is related to the time it takes to reach the detector. Small ions reach the detector faster than large ones.

The second mode, which is used to perform tandem mass spectrometry, is called product ion scanning. In this case, a selected precursor ion is selected in the first quadrupole and subjected to collisionally induced dissociation using an inert gas in the second quadrupole. The fragments are then pulsed into the time-of-flight tube and analyzed.

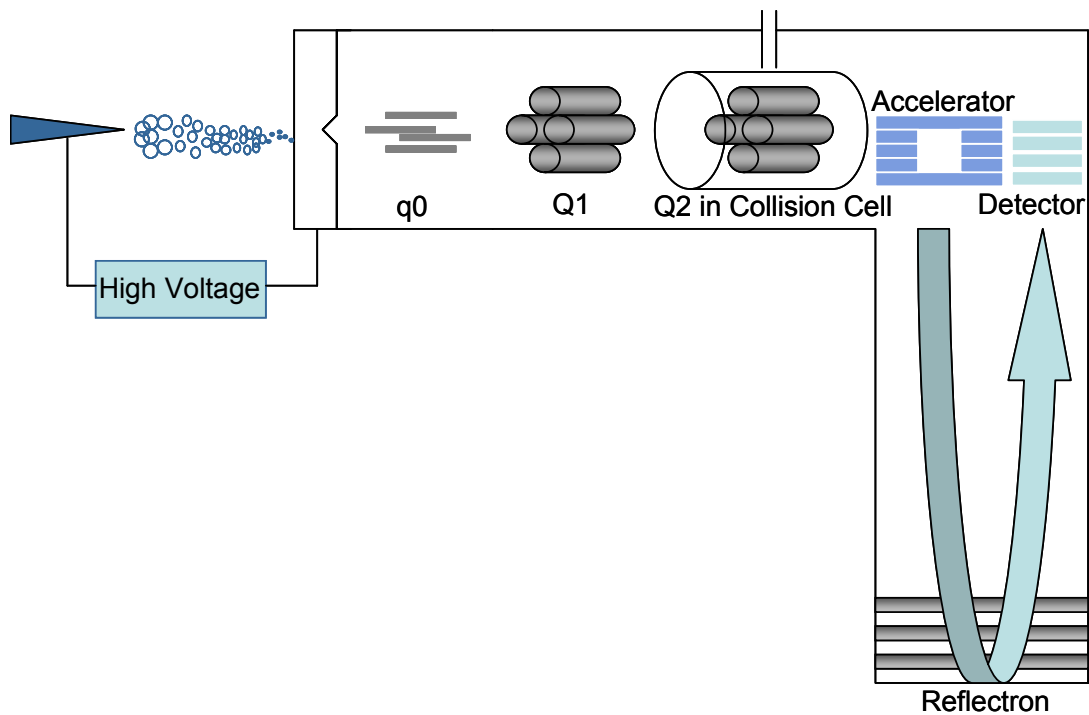


Figure 1.3 Ion path in the quadrupole time-of-flight mass spectrometer

High voltage is applied which creates fine mist containing analyte. The solvent is evaporated leaving volatile ions. Q0 focuses the ions, while Q1 separates them. A collision cell surrounds Q2, which is used for tandem mass spectrometry. The ions are accelerated into the time-of-flight region. The reflectron increases the effective length of the time-of-flight tube.

The configuration of the Shimadzu AXIMA-CFR+ can be seen in Figure 1.4. Matrix assisted laser desorption ionization (MALDI) was introduced as a mass spectrometric ionization technique in 1988 by both Karas and Hillenkamp; and Tanaka [57-59]. In MALDI, a UV absorbing matrix is co-crystallized with an analyte on a sample target plate. A laser pulse is applied to the target and the analyte and matrix are desorbed creating gaseous molecules. The analyte is ionized by protonation in collision with the laser activated matrix. The ions are then pulsed into the time-of-flight tube and analyzed. Ions formed by MALDI are generally singly charged.

Tandem mass spectrometry can also be performed on the AXIMA using a method called post-source decay (PSD). Larger molecules are unstable in the field free region of the time-of-flight tube. Fragmentation occurs as a result of this instability. The precursor ion is selected by allowing the ion package of interest to be transmitted through an ion gate. Initially, the PSD ions of a certain precursor ion are traveling at the same velocity. These ions are reaccelerated at the reflectron, which allows for their separation [60].

Post Translational Modifications

Post translational modifications (PTM's) are alterations to a protein structure made enzymatically after the proteins are translated. Modifications can also be made co-translationally. They include the covalent addition of small and large groups, disulfide bond formation, or the cleavage of a segment of the protein.

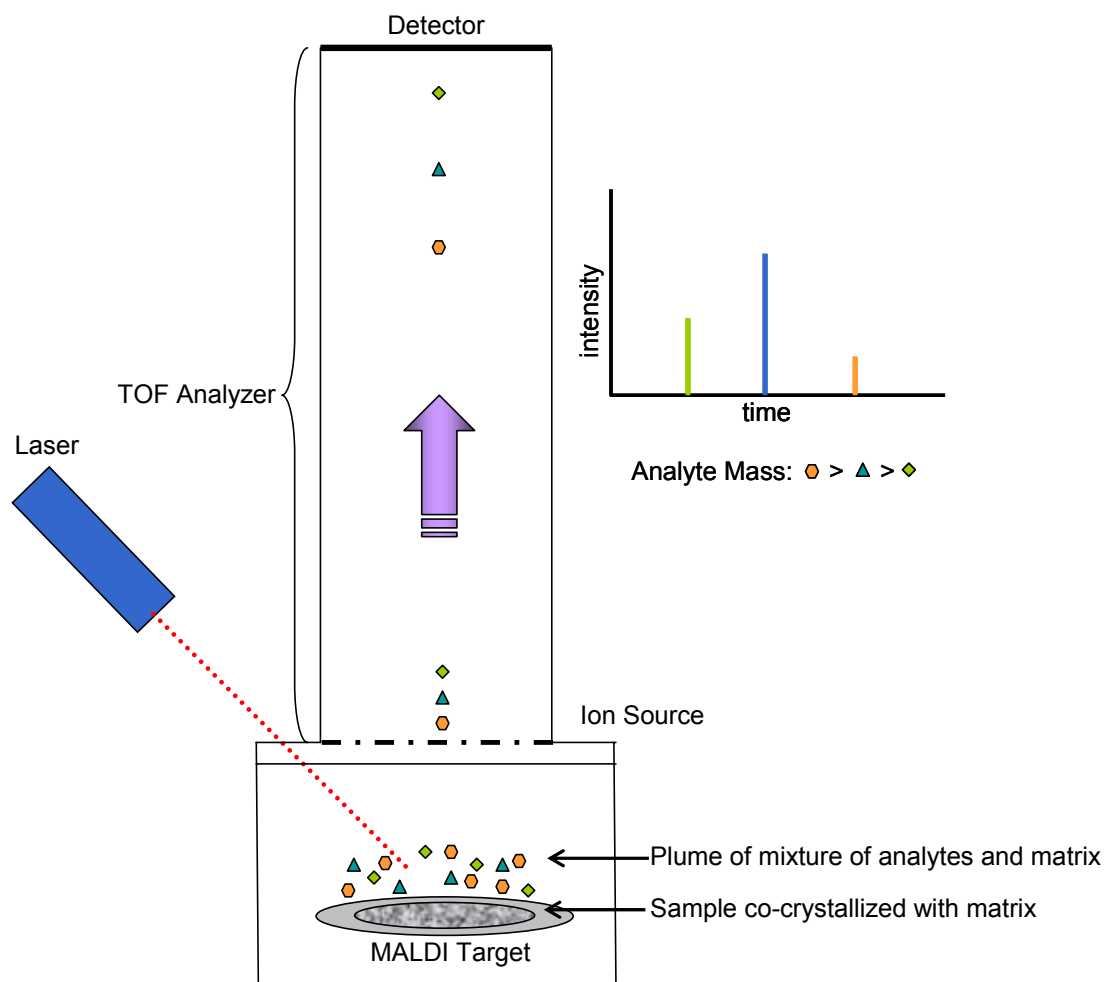


Figure 1.4 Schematic representation of matrix-assisted laser desorption ionization and flight path of the ions

Ions are formed when the analyte and matrix molecules collide in the plume created by the laser. The ions are then accelerated into the time-of-flight region, where they are separated based on their mass to charge ratio (m/z). Less kinetic energy is transferred to the larger ions therefore it takes longer for them to hit the detector. This is observed in the hypothetical spectrum.

PTM's contribute to the tertiary and quaternary structure of a protein, and affect its function. Commonly observed effects of PTM's are the alteration of the activity of the protein, localization of the protein within a system, turnover of the protein, and protein-protein interactions [61-71]. Proteomic methods have allowed the characterization of many proteins in one experiment. Initially these methods were applied to the identification of proteins, but now methods are being developed to characterize the modifications present on proteins.

“Bottom-up” Proteomics

The use of mass spectrometry as a tool for determining protein identification using peptides is termed “bottom-up” proteomics. The idea is that the protein is cut apart, and from the bottom up, the pieces are put together to determine the sequence.

Tandem mass spectrometry allows isolation of a tryptic peptide that can be fragmented in the instrument and the ionized pieces detected to determine the partial sequence of the peptide [72, 73]. Peptides most commonly break at the amide bond between amino acids, as illustrated in Figure 1.5. If the charge is retained on the amino-terminal fragment, it is called a “b” ion. If the charge is retained on the carboxy-terminal fragment, it is called a “y” ion [74]. If multiple b and y ions are detected for a peptide, the sequence can be determined to help identify the peptide. When this analysis

is performed for multiple peptides from a protein, that protein can be identified.

Using a bottom-up approach, PTM's can be identified by the observation of a shift in the mass of a peptide. For instance, if a protein is phosphorylated, the peptide containing the phosphate group will have an increase in mass of 80Da. The phosphate group can be localized to a particular amino acid residue by mass shifts in the fragmentation pattern. These assessments can be made by the investigation, and some search programs attempt to accommodate PTM's. In order for this approach to identify the PTM's in a protein, the modified peptide must be observed. Ideally, all peptides must be found to provide complete coverage of the protein sequence [75]. The greatest weakness of this method is that incomplete sequence coverage of the protein is usually obtained. Commonly, not all proteolytic peptides are detected in the spectrum, which means that modifications or mutations can go undetected.

Another approach has been devised to complement the "bottom-up" approach in an attempt to increase sequence coverage and determine the protein modifications.

"Top-Down" Proteomics

"Top-down" proteomics is a more recent application for determining protein structure. In this approach, the intact protein is introduced into the

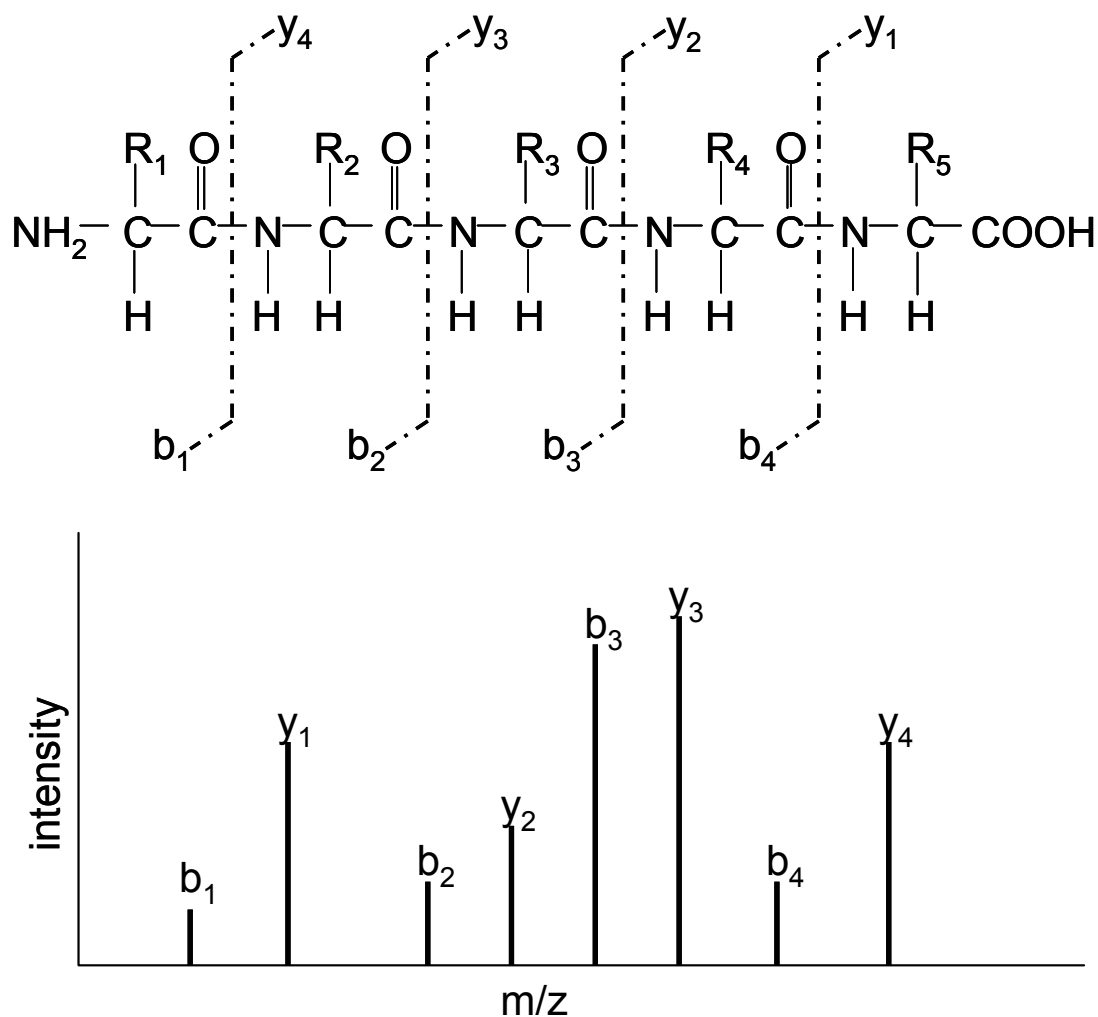


Figure 1.5 Dominant fragmentation pattern of a peptide and the resultant hypothetical mass spectrum

Tandem mass spectrometry fragments proteolytic peptides in the gas phase. In the Q-star, this is achieved with collision induced dissociation (CID). In the AXIMA, this is achieved using post source decay. In both cases, the amide bond is most commonly broken. If the amino-terminal fragment retains the charge, it is termed a “b” ion. If the carboxy-terminal fragment retains the charge, it is termed a “y” ion.

mass spectrometer and an intact molecular weight is determined. The intact protein is then fragmented in the mass spectrometer [75-84]. The intact molecular weight of the protein can indicate the presence of post-translational modifications or mutations in the primary sequence if it varies from the calculated molecular weight. The molecular weights of the fragments localize the position of any modifications in the structure of the protein.

A method that is receiving considerable attention currently for the identification and localization of PTM's integrates top-down, bottom up approaches [38, 41, 85]. In this case, the protein is identified by peptide analysis (bottom up). Next the intact molecular weight of the intact protein is determined (top down) and compared to the theoretical molecular mass of the protein. Differences in mass may indicate the presence of modifications. Several computer programs are available [86, 87] to provide tentative identification of modifications. The modification is localized by gas phase fragmentation, bottom up.

Obtaining 100% sequence coverage is difficult using either the top-down or bottom-up approach [70]. In the bottom up approach, the peptides may be lost in the sample preparation steps preceding mass spectrometry. In the top-down approach, the spectra are very complicated and not all of the fragment peaks are observed. The methods are complementary, and therefore by using both, the better the likelihood of obtaining good sequence coverage.

Protein Identification and Bioinformatics

The information generated from mass spectrometry experiments can be used to identify proteins using two approaches. Both approaches involve the proteolytic digestion of a somewhat purified protein. In peptide mass fingerprinting, a mass spectrum is generated in which the peaks in the spectrum correspond to ionized peptides which can be searched against a database to identify the protein. This peptide map is often generated using a MALDI-TOF instrument because the generated spectra contain only singly charged peptides, which simplifies the search. High sequence coverage, meaning a large representation of the sequence of the protein, must be obtained in order to unambiguously identify the protein using this method. The search engine compares the peptide list with peptide lists of in-silico digests products of the proteins in the specified database. A score is generated which reflects the probability that the observed match between the observed peaks with the theoretical peaks is a chance event [88, 89]. Weaknesses of this approach are that the protein must be relatively pure. In addition, it is possible to have peptides from two different proteins with the same molecular weight, which confounds identification of the protein. A second approach to protein identification involves acquiring tandem mass (MS/MS) spectrometry data. In this method, a peptide is selected to be fragmented using either PSD or CID. The fragments correspond to amino acid losses and the peptide can therefore be pieced back together to obtain a microsequence. The microsequence or combination of microsequences is

then searched against the database for protein identification. The spectra generated from CID are generally complicated, containing many y and b ions, as well as ions that result from other fragmentation patterns. The most facile method of identifying the protein is to submit the MS/MS spectra to a search engine. The search engine scans against protein sequence databases using various algorithms which calculate theoretical mass spectra and the overlap between the experimental and theoretical spectra is compared. A score which reflects the statistical significance of the match between the observed and theoretical masses is calculated and assigned to the match [90].

Hypothesis and Objectives

Understanding the mechanisms of acquired drug resistance can lead to better treatments for cancer and therefore better outcomes. Ribosomes perform a critical function in the cell by synthesizing all of the proteins. We hypothesize that characterizing the content and structure of the ribosomal proteins of drug susceptible and drug resistant MCF-7 cells will provide insight into the involvement of the ribosome in multidrug resistance. With this hypothesis, we have the following aims:

1. Determine a reproducible method for isolation and purification of ribosomal proteins
2. Optimize 2D gels of ribosomal proteins so that protein changes can be observed and identify the proteins visualized in the array
3. Perform a gel-based comparative study between drug susceptible MCF-7 cell line and mitoxantrone resistant MCF-7 cell line
4. Characterize the protein isoforms which were determined to have altered abundances in the comparative study using both the “bottom-up” and “top-down” mass spectrometric approaches
5. Perform absolute quantification study to evaluate the number of ribosomes per cell in the drug susceptible MCF-7 cell line and mitoxantrone resistant MCF-7 cell line

Chapter 2: Materials and Methods

Materials

Parental and mitoxantrone resistant cell lines were provided by Dr. Ken Cowan at the National Institutes of Health, National Cancer Institute. The DC protein assay kit, the Protean II pre-cast gels (8-16% Tris-HCl), and the Bio-Safe coomassie blue were purchased from Bio-Rad (Hercules, California). The immobilized pH gradient strips (IPG 18cm pH 7-11), the IPG buffer were purchased from GE Healthcare (Piscataway, New Jersey). The quick-seal ultracentrifuge tubes were purchased from Beckman Coulter (Fullerton, CA). Sequence grade modified porcine trypsin was obtained from Promega Corporation (Madison, Wisconsin). Ammonium bicarbonate, calcium chloride, 3-[(3-cholamidopropyl) dimethylammonio]-1-propanesulfonate (CHAPS), dithiothreitol (DTT), Eagle's minimal media (MEM), fetal bovine serum, glycerol, iodoacetamide, magnesium chloride, penicillin streptomycin antibiotic solution, phosphate buffered saline (PBS), potassium chloride, sucrose, thiourea, trifluoroacetic acid (TFA), Trizma base, cell culture grade trypsin, sodium dodecyl sulfate (SDS), and urea were obtained from Sigma Aldrich (St. Louis, Missouri).

Equipment

The Optima LE-80K preparative ultracentrifuge and the DU 530 UV-Vis spectrophotometer were from Beckman Coulter (Fullerton, CA). The

mechanical homogenizer was purchased from Kinematica (Littau, Lucerne (Switzerland)). The protein isoelectric focusing cell was obtained from GE Healthcare (Piscataway, New Jersey). The second dimension gel apparatus and the GS-800 densitometer were obtained from Bio-Rad (Hercules, California). The hematocytometer and cover slips were purchased from Hauser Scientific (Horsham, PA). The Alphashot-2 YS-2 microscope was from Nikon (Japan). The speed-vac was from Thermo-Savant (Holbrook, NY). The electrospray ionization mass spectrometer was from Applied Biosystems (Foster City, CA), and the matrix-assisted laser desorption ionization mass spectrometer was from Shimadzu Corporation (Nishinokyo-Kuwabara-cho, Nakagyo-ku, Kyoto (Japan)).

Methods

Cell Culture and Harvest

All cell lines used in this work were cultured in house. The cells were grown in 150 cm² flasks (Corning Incorporated, Corning, New York) in Eagle's Minimal Essential Media (MEM) supplemented with 10% fetal bovine serum and 1% penicillin streptomycin antibiotic solution. The cells were sustained in an incubator at a temperature of 37°C with 5% carbon dioxide. At confluence the cells were harvested. Cells were washed with 15mL of 10mM phosphate buffered saline (PBS), followed by the addition of 3mL of cell culture grade trypsin. After a five minute incubation period, 10mL of MEM was added to the flasks to stop tryptic activity by changing the pH. Cells were suspended by repeatedly pipetting the solution up and down while rinsing the walls. The

suspension was transferred to pre-weighed centrifugation tubes and centrifuged at 500g for 5 min. The cell pellet was washed by resuspending two times with PBS followed by centrifugation. The cell pellet was weighed and subjected to subcellular fractionation.

Isolation of Ribosomes and Extraction of Ribosomal Proteins

Three methods were evaluated for the isolation of ribosomal proteins. The first method suggested suspension of the cell pellet in 3 volumes of homogenization buffer (20mM Tris-HCl, pH 7.5; 5mM MgCl₂; 100mM KCl; 5mM β-mercaptoethanol; 250mM Sucrose) [91]. The pellet was homogenized by 80 strokes of a chilled glass homogenizer. The nuclei, mitochondria and cellular debris were removed by centrifugation at 12,000g for 10 minutes. Triton X-100 was added to a final concentration of 1%, and mixed with the post-mitochondrial supernatant. The mixture was layered over an equal volume of the homogenization buffer with 1.0M Sucrose and centrifuged at 260,000g for 2 hours at 4°C.

In the second method [92], the cells were lysed using a lysis buffer containing 1% Triton X-100; 1% sodium deoxycholate; 5mM Tris-HCl, pH 7.5; 1.5mM KCl; 2.5mM MgCl₂. The lysate was centrifuged at 12000g for 5 minutes to remove the nuclei, mitochondria and cellular debris. The supernatant is brought to 28mL of final volume, and placed in a Beckman Quick-Seal tube. The mixture is underlayered with 6mL of Buffer A (20mM Tris-HCl; 100mM KCl; 5mM MgCl₂; 1mM DTT; 700mM Sucrose), followed by 6mL

of Buffer B (20mM Tris-HCl; 500mM KCl; 5mM MgCl₂; 1mM DTT; 1.6M Sucrose). This was centrifuged for 16 hours at 215,000g.

The final method that was evaluated and used for all subsequent analyses did not contain any detergent, which is difficult to remove from the proteins [93]. The cell pellet was suspended in 2 volumes of homogenization buffer (50mM Tris-HCl, pH 7.5; 5mM MgCl₂, 25mM KCl, 200mM Sucrose). The suspension was homogenized by 20 strokes in the Kinematica mechanical homogenizer. The homogenate rested for 1 minute and was homogenized again for 20 strokes. The nuclei, mitochondria and cellular debris were removed by centrifugation at 10,000g for 10 minutes. Homogenization was repeated on the resultant pellet and the supernatants were pooled. The lysate was layered at a 1:1 (v/v) ratio over a 2M sucrose solution in the same buffer and subjected to centrifugation at 260,000g for 2 hours.

The ribosomal pellet was suspended in 1 ml of homogenization buffer without sucrose, and is made 10mM in MgCl₂ by the addition of 5μL of 1M MgCl₂ [92, 94]. This was followed by the addition of 0.7 volumes of ethanol. The ribosomes precipitate immediately, and the suspension was centrifuged at 7000 rpm for 10 minutes. The supernatant was removed and the ribosomes were resuspended in 250μL of homogenization buffer with no sucrose, followed by the addition of 25μL of 1M MgCl₂ and 550μL of glacial acetic acid. Following a 45 minute incubation period, the precipitated RNA was removed by centrifugation at 10,000 rpm for 10 minutes. The

supernatant was removed and placed in another tube with 4 volumes of acetone. The proteins immediately precipitated, but the suspension was placed in the freezer at -20°C for 2 hours to facilitate complete precipitation of the proteins. The mixture was centrifuged at 10,000 rpm for 10 minutes to pellet the proteins. The proteins were washed by the addition of 1 mL of acetone and centrifuged again. This wash step was repeated once.

Two-Dimensional Gel Electrophoresis

In order to insure a consistent amount of protein was loaded onto each gel, the Bio-Rad DC Protein Assay Kit (Hercules, CA) was used to determine protein concentration. The first gels were run using 11cm first dimension strips with a linear pI range of 3-10. At this time, 200 μg of protein was loaded per gel. The proteins were lined up vertically on basic side of the gel because they could not be resolved in the pI range. At this point, first dimension strips with a non-linear pI range of 7-11 were evaluated. Resolution of the proteins was achieved although the quality of the gels was still poor. In an attempt to improve resolution, larger format, 18cm gels were used. The spots were no longer running into each other. Resolution of the proteins on the gel was further improved by using 50 μg of protein per gel.

The first dimension of separation was started by a one hour incubation of the protein sample with 320 μL of rehydration solution, which contains 7M urea, 2M thiourea, 2% (w/v) CHAPS, 50mM DTT and 1% IPG buffer (GE Healthcare). The rehydration solution was pipetted into the focusing tray and

the IPG strip (pI range of 7-11, GE Healthcare) was laid on top of the solution. An electrode wick saturated by 6 μ L of 15mM DTT was placed under the strip at the cathode end of the focusing tray, while an electrode wick saturated with 6 μ L of deionized water was placed under the strip at the anode end of the tray. The strip was overlaid with mineral oil to prevent burning and the strip was passively rehydrated for 12 hours. The proteins were focused for 60,000 V-hr.

Upon completion of the first dimension focusing, the IPG strip was removed from the focusing tray and placed in equilibration buffer containing 0.375M Tris-HCl, pH 8.8, 6M Urea, 20% Glycerol, 2% sodium dodecyl sulfate (SDS) and 2% DTT for 10 minutes. The strip was removed from this buffer and placed in the same buffer without DTT, but containing 2.5% iodoacetamide for 10 minutes. The strip was placed on top of an 8-16% Tris-HCl SDS-PAGE pre-cast gel (Bio-Rad, Hercules CA). The strip was covered with agarose solution, running buffer was added, and current was applied as follows: 16mA for 30 minutes followed by 24mA for 5 hours. When the second dimension was completed, the gel was removed from the glass plates and placed in 50% water, 45% methanol and 5% acetic acid for 45 minutes to "fix" the proteins in the gel. The gel was then washed in water for 15 minutes followed by staining overnight by Bio-safe coomassie blue (Bio-Rad, Hercules, CA). The next day, the gel was destained by several water washing steps to eliminate background staining.

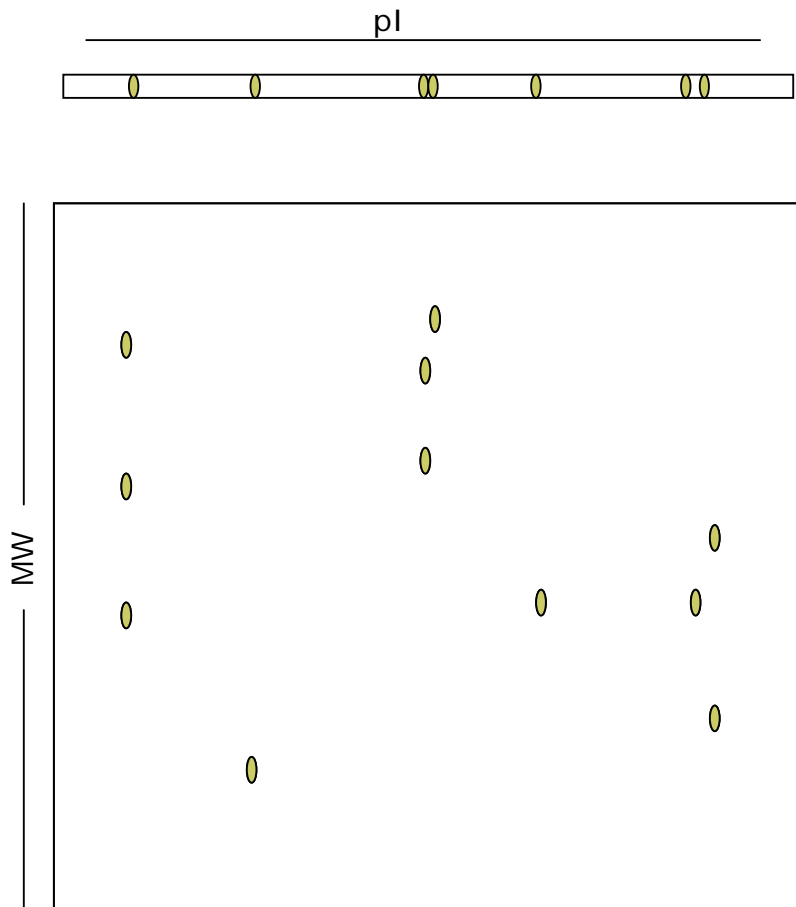


Figure 2.1 Scheme of 2DGE

The first dimension of this separation involves the migration of the proteins to their isoelectric point within an immobilized pH gradient (IPG). In the second dimension, sodium dodecyl sulfate is added to remove the intrinsic charge of the protein so that this separation is based only on molecular weight of the protein. In the first dimension, 7 spots are observed. In the second dimension, 11 spots are observed, so 4 more proteins were resolved using a two dimensional approach.

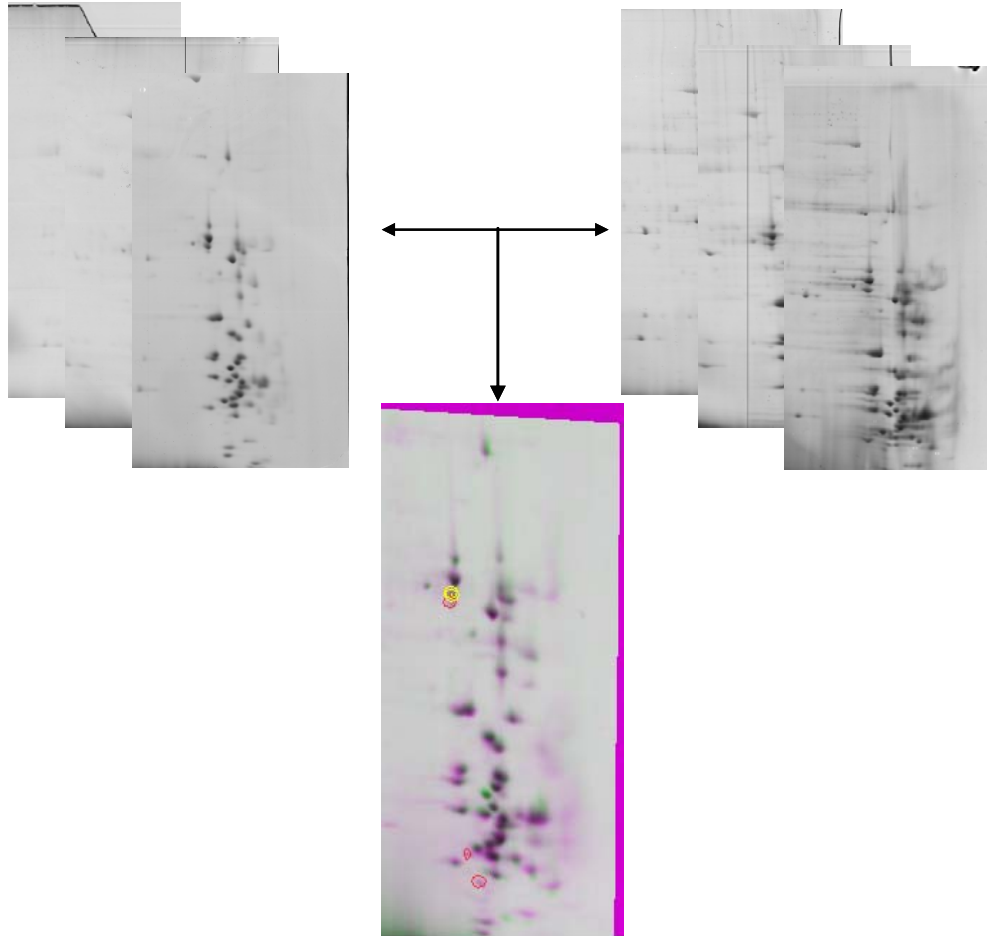


Figure 2.2 Comparison of 2D gels from using the Compugen Z3 program

Three gels were run for each of three harvests from each of the cell lines. The images of the three gels from one harvest were registered, resulting in one image. The registered image of the harvest 1 gels of the parental cell line was then overlaid with the registered image from harvest 1 of the mitoxantrone^R cell line, and the spots were matched. This was repeated two times using the registered images from the other two harvests. Red circles indicate the presence of the protein only in the drug resistant cell line. The yellow circle indicates a decrease in relative abundance in the drug resistant cell line.

Image Analysis and Comparative Densitometry

Images of the two-dimensional gels were obtained using a GS-800 densitometer and its associated software, PDQuest. Once the gels were scanned, the images were saved as TIFF files. Image analysis was performed after importing the TIFF files into the Compugen Z3 software as shown in Figure 2.2 (Compugen Limited, Tel Aviv, Israel).

Each gel image was registered and the spot intensities were measured and recorded. Three gel images from a harvest were overlaid and registered and saved as an image. The spot intensities were normalized between the images for differences in protein loading. This was also done for the drug resistant cell line. For comparative analysis, three gel pairs were evaluated. The pair of images was overlaid and the spots were matched as can be seen in Figure 2.2. The difference in the abundance between homologous spots in the two cells lines was calculated based on the quotient of their relative abundance in each gel. Spots with a differential abundance greater than a factor of two were considered to be physiologically relevant.

In-Gel Digestion and Desalting

In-gel digestion was performed using the method of Schevchenko et al. [95]. Once the gel was imaged, the spots were excised and placed into microcentrifuge tubes. The gel pieces were washed by alternately adding and removing water followed by water/acetonitrile (1:1) for 15 minutes each. Acetonitrile was added until the gel pieces shrunk and became white.

Following the removal of the acetonitrile, the gel pieces were rehydrated in 0.1M NH_4HCO_3 for 5 minutes. An equal volume of acetonitrile was added and incubated for 15 minutes. All of the liquid was removed and the gel pieces were dried down in a vacuum centrifuge. These washing steps were performed to remove the coomassie blue stain in the gel pieces.

The proteins were reduced by the addition of 10mM DTT in 0.1M NH_4HCO_3 to the dehydrated gel pieces following a 45 minute incubation at 56°C. The microcentrifuge tubes were allowed to come to room temperature and the excess liquid was removed. The proteins were alkylated by the addition of 55mM iodoacetamide in 0.1M NH_4HCO_3 for a 30 minute room temperature incubation in the dark. The iodoacetamide solution was removed and the gel washing steps were repeated to remove any residual stain and DTT and iodoacetamide from the gel pieces.

The gel pieces were dried down in the vacuum centrifuge and then rehydrated by the addition of digestion buffer (50mM NH_4HCO_3 , 5mM CaCl₂, 12.5 ng/ μL trypsin). The gel pieces were incubated for 45 minutes on ice while rehydrating. Any remaining solution is removed and replaced with a small volume of digestion buffer without the enzyme. The gel pieces were incubated overnight at 37°C.

The following day, 25mM NH_4HCO_3 was added and the gel pieces were incubated for 15 minutes. The same volume of acetonitrile was added and again incubated for 15 minutes. The supernatant was recovered and the extraction was repeated two times with the addition of 5% formic acid with a

15 minute incubation, followed by the addition of an equal volume of acetonitrile and another 15 minute incubation period. The extracts from each spot were pooled and dried down in a vacuum centrifuge.

The peptides were resuspended in 0.1% TFA and desalted using a C₁₈ ZipTip (Millipore, Bedford, MA). Briefly, the tip was equilibrated by twice aspirating and then dispensing 50% acetonitrile, followed by twice aspirating and then dispensing 0.1% TFA. The peptides were bound to the column by aspirating then dispensing the peptide mixture for 7-10 cycles. The salts were removed by washing with 0.1% TFA two times. The peptides were eluted by aspirating and then dispensing 0.1% TFA/50% acetonitrile for 3-5 cycles. The peptides were dried down and resuspended in electrospray solution (49% water/49% methanol/2% acetic acid). If the peptides were to be analyzed by the MALDI instrument, they were spotted directly on the MALDI plate in the elution solution.

Mass Spectrometry

The peptides were either analyzed on the Shimadzu AXIMA CFR⁺ MALDI with a nitrogen laser at a wavelength of 337nm, or on the Applied Biosystems Q-star Pulsar I using the Protana static nanospray source (Odense, Denmark). To obtain spectra from the AXIMA, 1-2µL of sample was applied to the MALDI target and allowed to dry. The matrix used for peptides was 5 mg/ml alpha-cyano and 1µL was applied to the dried sample. The AXIMA was set to scan from m/z range of 0-5000 using reflectron mode for

MS analysis. The laser power was set at 45 (arbitrary units), and 100 profiles were averaged at 10 laser shots per profile. Once the TOF spectrum was acquired, peptides were selected for post source decay (PSD) analysis or tandem mass spectrometry based on their intensity. If the intensity of the peptide was above 100mV, the quality of the PSD spectrum was good enough to provide reliable protein identification. PSD spectra were acquired by setting the ion gate to pass ions 5 m/z units above and below the m/z of the peptide of interest. The laser power ranged from about 50-60 (arbitrary units).

The Q-star instrument was set to scan m/z range 300-2000 for the MS analysis. In order to obtain the spectra, 2 μ L of the suspended peptides in electrospray solution were put into the capillary tip (Protana, Odense, Denmark), and sprayed into the instrument with the following parameters: the curtain gas was 25, the ionspray voltage was 900V and the detector was set at 2300 mV. Once a peptide list was generated, tandem MS was performed. The parameter that changed for tandem mass spectrometry was the collision gas. The amount of gas had to be modified based on the ease of fragmentation of the peptide. The collision gas range was between 20-50 (arbitrary units).

Protein Identification

A scheme for protein identification using peptide mass fingerprinting can be seen in Figure 2.3. The mass list of the peptides obtained from MS analysis

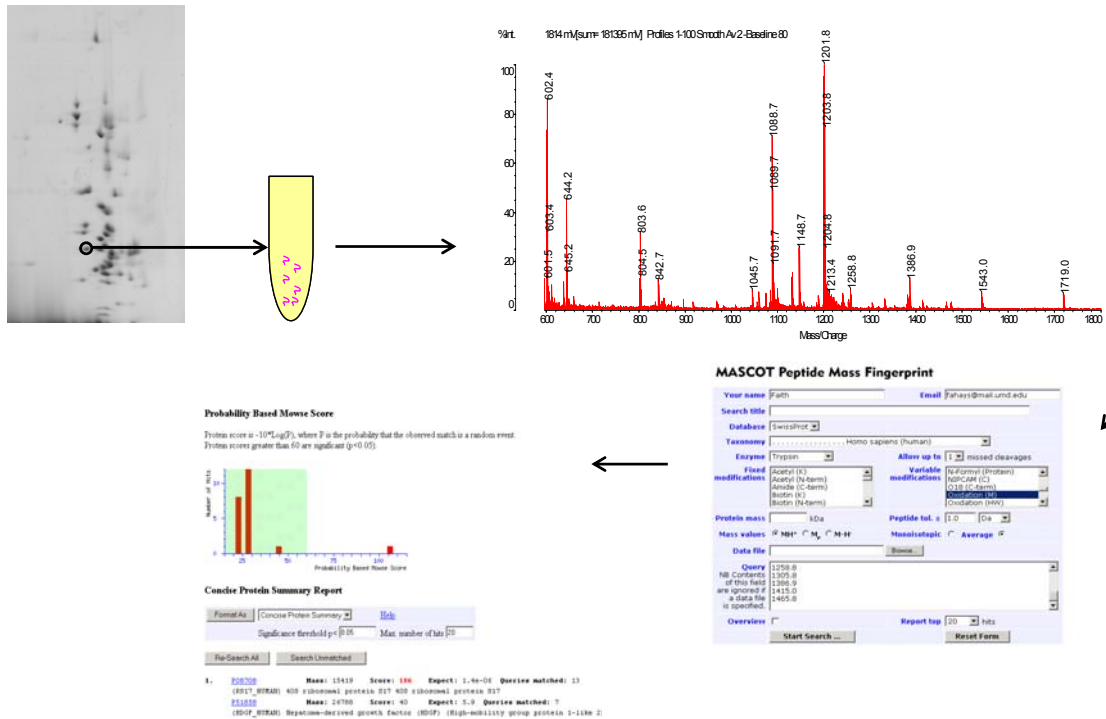
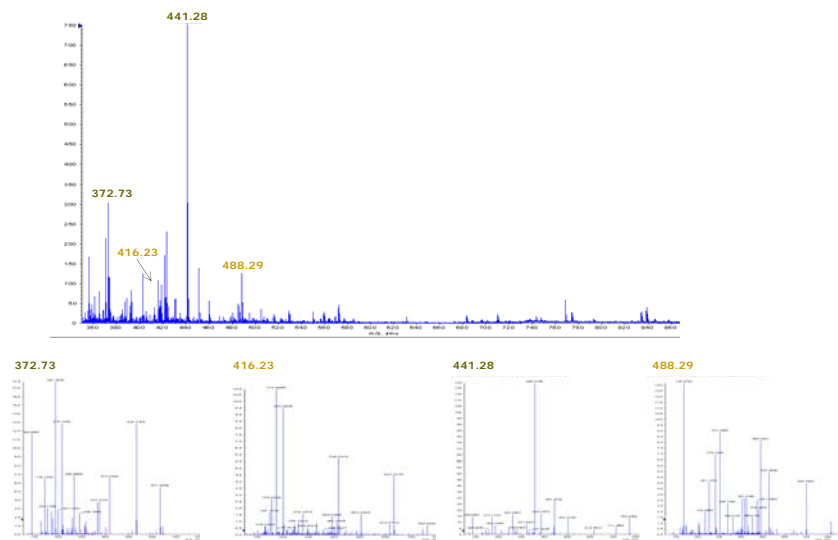


Figure 2.3 Protein identification using peptide mass fingerprinting

The protein is digested in the gel using trypsin. The resultant peptides are extracted from the gel, desalted and analyzed by mass spectrometry. The list of peptides is submitted to the MASCOT search engine using the SwissProt database. MASCOT returns a list of candidate proteins. A score greater than 60 is considered to be significant.



MASCOT MS/MS Ions Search

Your name: Faith | Email: fahays@umd.edu

Search title: d:\pe_sciex_data\Projects\Faith Mitox(R)\Data\spot 25A.ms.ms.wiff (all san

Database: SwissProt

Taxonomy: Homo sapiens (human)

Enzyme: Trypsin | Allow up to: 1 missed cleavages

Fixed modifications: Acetyl (K), Acetyl (N-term), Amide (C-term), Biotin (K), Biotin (N-term)

Variable modifications: N-Acetyl (Protein), N-Formyl (Protein), NIS-CAM (C), Oxidation (M)

Protein mass: kDa | ICAT:

Peptide tol. ±: 2.0 Da | MS/MS tol. ±: 0.8 Da

Peptide charge: 2+ | Monoisotopic: | Average:

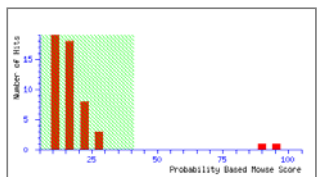
Data file: LOCALS-1\Temp\mas100.tmp | Browse

Data format: Mascot generic | Precursor: m/z

Instrument: IES-QUAD-TOF

Report top: 20 hits

Start Search ... | Reset Form



1. **F20200** | Mass: 17000 | Score: 95 | Query modified: 1
 (L12_10040) 605 ribosomal protein L12 605 ribosomal protein L12

Query	Observed	Ms (exp)	Ms (calc)	Delta	Miss	Sequence
1	372.7000	741.3814	743.4290	-0.8435	0	K.L12100L.R
2	441.3000	886.7654	888.1002	-0.8435	0	K.L12100L.R
3	876.4000	1674.7954	1674.7955	-0.0001	0	K.L12100L.R

2. **F20213-02-00-00** | Mass: 20100 | Score: 95 | Query modified: 2
 (L12_10040) 605 ribosomal protein L12 605 ribosomal protein L12 (L12-10040)

Query	Observed	Ms (exp)	Ms (calc)	Delta	Miss	Sequence
1	372.7000	741.3814	743.4290	-0.8435	0	K.L12100L.R
2	441.3000	886.7654	888.1002	-0.8435	0	K.L12100L.R
3	876.4000	1674.7954	1674.7955	-0.0001	0	K.L12100L.R

Protein View

Search for F20200 Score: 95
 (L12_10040) 605 ribosomal protein L12 605 ribosomal protein L12
 Found in search of C:\POCURE-1\ADIRI-1\LOCALS-1\Temp\mas100.tmp

Monomer mass (kDa): 17000 | Calculated pI value: 9.48
 NCBI BLAST search of F20200 against nr
 Unconnected [blast2seq](#) for porting into other applications

Taxonomy: [View NCBI](#)

Variable modifications: Carbamidomethyl (C), Oxidation (O)
 Cleavage by Trypsin: cuts C-term side of KR unless next residue is P
 Sequence Coverage: 100%

Matched peptides shown in **Bold Red**

```

1 MDPFPPFPRF EYVVLCTGG EYVATLALP EYVPLGKSPK EYVQIATK
94 GDSGLSTVY EYVPLGKQ EYVATLALP EYVATLALP EYVQIATK
104 SDHTTDEYV EYVPLGKQK EYVATLALP EYVATLALP EYVQIATK
154 IYDIDGAY EYVPLGK
  
```

Show predicted peptides also

Sort Peptides By: Rank Number Increasing Mass Decreasing Mass

Start - End	Observed	Ms (exp)	Ms (calc)	Delta	Miss	Sequence
25 - 49	441.3000	886.7654	888.1002	-0.8435	0	K.L12100L.R
62 - 67	372.7000	741.3814	743.4290	-0.8435	0	K.L12100L.R
131 - 146	876.4000	1674.7954	1674.7955	-0.0001	0	K.L12100L.R

Error (ppm) vs Mass (Da) plot showing error values near 0 ppm across a mass range of 700 to 1700 Da.

Figure 2.4 Protein identification using Tandem MS

The protein is digested in the gel using trypsin. The resultant peptides are extracted from the gel, desalted and analyzed by mass spectrometry. Tandem MS is performed on peptides selected from the TOF spectrum (top). The spectra are submitted to MASCOT. MASCOT returns a list of candidate proteins.

was submitted to the MASCOT search engine manually. A scheme for protein identification using sequence tags can be seen in Figure 2.4. A minimum of 2 multiply charged peptides were selected from the TOF spectrum and subjected to tandem mass spectrometry with either the AXIMA or the Q-star. The resulting sequence tags as well as the masses of the peptides were submitted to the SwissProt database through the MASCOT search engine using the BioExplore software associated with the mass spectrometer. MASCOT returned a list of candidate proteins with scores that represent a 95% confidence level associated with the potential identifications.

Isolation of Protein Isoforms and Mass Measurement

The scheme for intact molecular weight determination can be seen in Figure 2.5. The proteins from the spots of interest were extracted from the 2D gels using a method by Mirza et al [96]. The spots were cut from the fixed and stained gel and briefly washed with water. To destain, the water was removed and 10% acetic acid was added for 10 minutes. After acetic acid removal and water wash, the gel piece was washed in acetonitrile followed by methanol for 20 minutes each. A solution of formic acid/water/isopropanol (1/3/2) was added and the tubes were vortexed until the gel piece was colorless. The gel piece was washed in water then dehydrated by placing it in the speed-vac for 5 minutes. Ten microliters of extraction solution, (50% acetonitrile/0.1% TFA), was added and the tube was vortexed for 1 hour.

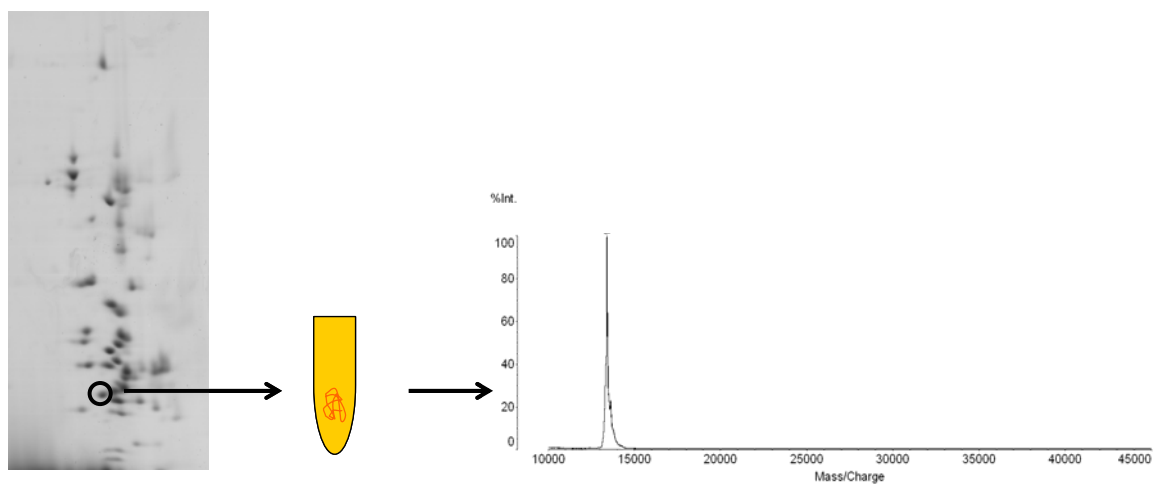


Figure 2.5 Intact molecular weight determination

The protein was extracted from the gel using the method described by Mirza et al. The protein was mixed with Triton X-100 and spotted on the MALDI plate. The intact molecular weight was measured.

MALDI analysis was performed on the extracted protein by mixing 1uL of the extract with 1uL of 5% Triton X-100. The 2uL mixture was spotted on the MALDI plate using the sandwich method with 10mg/mL of sinapinic acid in 50% ACN/1% TFA. The sandwich method entails spotting the matrix, letting it dry. The sample is then spotted on the plate and allowed to dry, followed by another spot of matrix. The settings for the instrument were as follows: linear mode; mass range was 10,000-40,000; laser power 100-105; and 250 profiles were averaged.

Absolute Quantification

Absolute quantification of the number of ribosomes in a cell was performed on both the parental MCF-7 cell line and the mitoxantrone resistant MCF-7 cell line. Three flasks of each cell line were grown to confluence. The cells were harvested as described earlier with careful attention to the amount of trypsin and media added in the last two steps. A 100µL aliquot was removed from the mixture of the suspended cells and used for cell counting. A hemacytometer was used to count the cells in the aliquot and calculate the total number of cells per harvest. The glass cover slip was placed on top of the hemacytometer and 6µL of suspended cells was placed under the cover slip. Using a microscope, the number of cells was counted manually in each square and all 16 squares were added together. The counting was repeated in another 16-square grid and the two values were averaged. This was repeated for two additional harvests for each cell line for a total of three

harvests per cell line. The averaged number was multiplied by 10,000 to give the number of cells per mL.

The isolation of ribosomes was performed as described above. Following centrifugation through the sucrose cushion, the pellet was recovered and the ribosomes were precipitated using ethanol as above. They were resuspended in water for optical density measurements. Using a Beckman DU 530 UV-Vis spectrophotometer, the OD₂₆₀ measurements were taken with 4 replicate measurements each at a 1X concentration and a 0.5X concentration. The widely accepted conversion factor of, 1 OD₂₆₀ unit is equal to 19 pmol of ribosomes [97], was used to calculate the total number of ribosomes per harvest. By determining the total number of cells per harvest and the total number of ribosomes per harvest, the total number of ribosomes per cell could be calculated.

Error Analysis

The number of cells per harvest as well as the number of ribosomes per harvest was calculated for each harvest. The number of ribosomes per cell was then calculated for each harvest and the standard deviation was determined using the following equation:

$$\frac{s_x}{x} = \sqrt{\left(\frac{s_c}{c}\right)^2 + \left(\frac{s_r}{r}\right)^2}$$

Where s_x is the standard deviation of the calculated value of the number of ribosomes per cell (x); s_c is the standard deviation of the cell count (c) and s_r

is the standard deviation of the measurement of the number of ribosomes per harvest (r).

While individual error bars are informative, they do not convey the inter-relatedness of datasets in a quantitative way. The ANOVA (analysis of variance) function can statistically compare the variation between groups. In this case, since two populations are being tested repeatedly, the two-factor ANOVA with replication was performed. This test was applied to compare the cell count between the parental and drug resistant cell lines; to compare the absorbances between the parental and drug resistant cell lines and to compare the calculated values of the number of ribosomes per cell for both the parental and drug resistant cell lines.

Chapter 3: Results

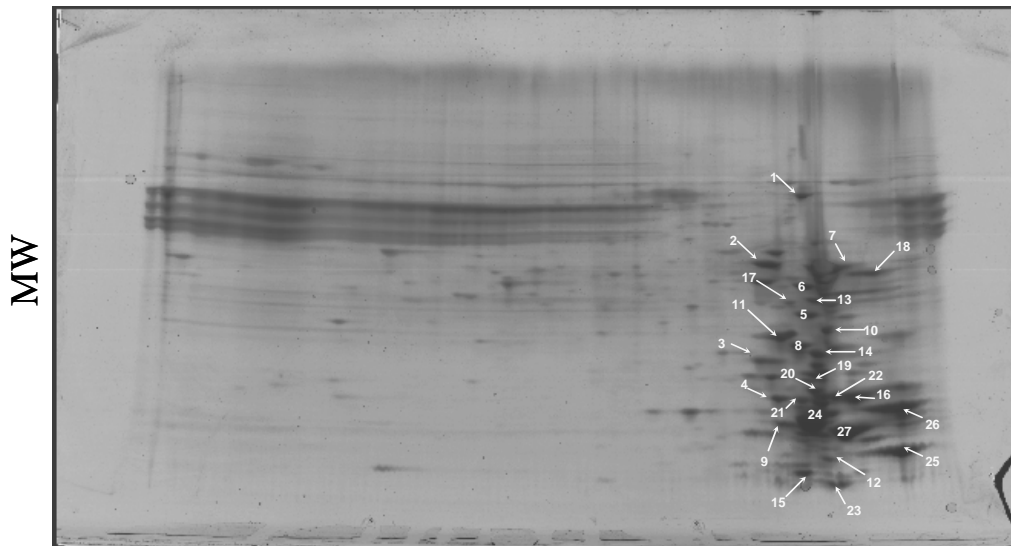
Reproducible Method for Isolation and Purification of Ribosomal

Proteins

Three methods for ribosome isolation were evaluated for purity. Figures 3.1-3.3 show the gels and list of proteins identified from each of the methods. In method one, of the 27 proteins which were identified, 24 were ribosomal. In method two, of the 24 proteins that were identified, 22 were ribosomal. In method three, of the 31 proteins that were identified, 29 were ribosomal.

Optimization of 2DGE and Protein Identification

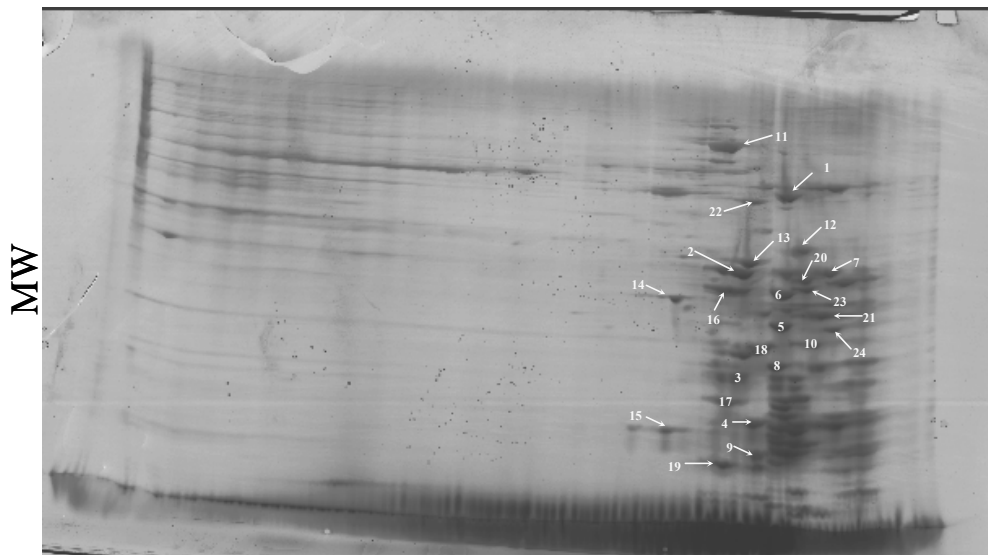
In this research, 2D gel electrophoresis and mass spectrometry are used to identify the ribosomal proteins as well as the post translational modifications and protein isoforms present in the ribosome of both the MCF-7 parental and drug resistance cell lines. Ribosomal proteins are known to be extremely basic and therefore do not resolve well in the first dimension of 2D gel electrophoresis. Multiple optimization steps were performed in order to produce reproducible gels in which the proteins were well resolved. The use of “zoom” isoelectric focusing strips, which have a pI range of 7-11, result in better resolution of the proteins than the wide range strips. Secondly, the amount of protein loaded on the gel was greatly reduced from the amount recommended in standard procedures. In many cases, a very complex sample mixture is applied to a gel, so the standard amount of 200ug of protein per gel with 1000-3000 spots give good resolution.



	Protein Name	MW (Da)	PI	# of peptides matched	Mascot Score
1	60S ribosomal protein L3	45440	10.16	4	99
2	40S ribosomal protein S3a	29795	9.75	6	212
3	60S ribosomal protein L11	19981	9.64	4	70
4	40S ribosomal protein S17	15409	9.85	3	67
5	60S ribosomal protein L10	24430	10.11	4	126
6	40S ribosomal protein S4, X isoform	29448	10.16	9	124
	40S ribosomal protein S4, Y isoform	29306	10.25	4	75
7	40S ribosomal protein S6	28663	10.85	6	159
8	60S ribosomal protein L17 (L23)	21252	10.18	4	97
9	40S ribosomal protein S20	13364	9.95	6	311
10	40S ribosomal protein S9	22447	10.66	6	102
11	40S ribosomal protein S5	22862	9.73	3	72
12	40S ribosomal protein L37a	10137	10.44	2	89
13	40S ribosomal protein S8	24509	10.32	7	140
14	60S ribosomal protein L21	18422	10.49	7	199
15	60S ribosomal protein L38	8082	10.10	2	62
16	40S ribosomal protein S18 (KE-3)	17708	10.99	5	108
17	60S ribosomal protein L10a (CSA-19)	24684	9.94	3	121
18	60S ribosomal protein L8	27876	11.03	6	180
19	40S ribosomal protein S11	18419	10.31	3	109
20	40S ribosomal protein S15	16898	10.39	3	70
21	40S ribosomal protein S25	13734	10.12	3	81
22	40S ribosomal protein L27a	16420	11.00	2	65
23	40S ribosomal protein S29	6541	10.17	4	132
24	40S ribosomal protein S16	16304	10.21	2	65
25	Histone H4	11229	11.36	4	208
26	Histone H3	15187	11.27	5	96
27	Histone H2A.e	13797	10.88	5	119

Figure 3.1 Evaluation of method 1 for isolation of ribosomal proteins

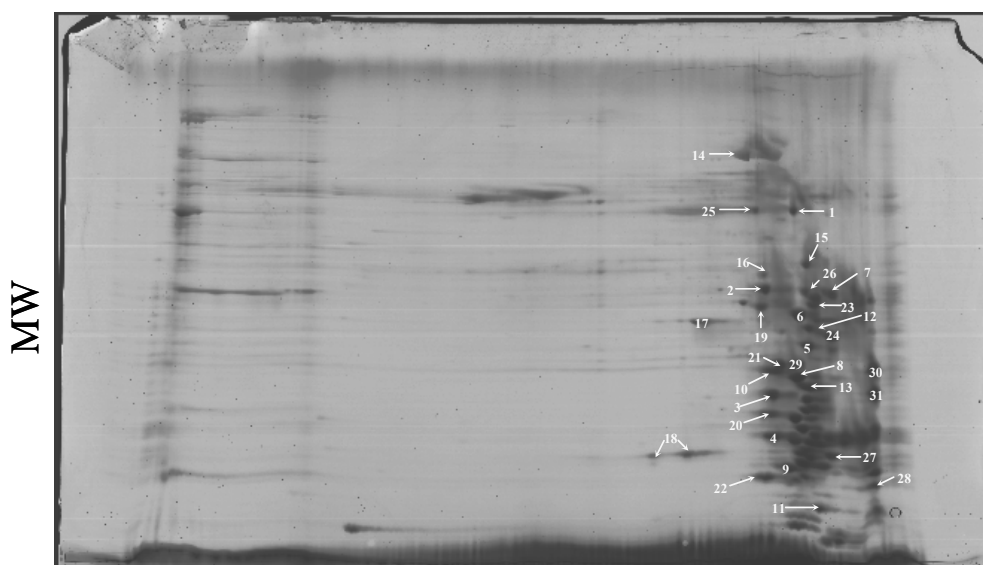
The gel was run with ribosomal proteins extracted using method 1. The protein list shows that 24 ribosomal proteins were identified. Three non-ribosomal proteins were identified.



	Protein Name	MW (Da)	PI	# of peptide matches	Mascot Score
1	60S ribosomal protein L3	45440	10.16	13	281
	60S ribosomal protein L3-like	46136	10.45	4	69
2	40S ribosomal protein S3a	29795	9.75	7	202
3	60S ribosomal protein L11	19981	9.64	3	104
4	40S ribosomal protein S17	15409	9.85	2	70
5	60S ribosomal protein L10	24430	10.11	4	98
6	40S ribosomal protein S4, X isoform	29448	10.16	4	123
7	40S ribosomal protein S6	28663	10.85	4	109
8	60S ribosomal protein L17 (L23)	21252	10.18	3	76
9	40S ribosomal protein S20	13364	9.95	4	84
10	40S ribosomal protein S9	22447	10.66	3	112
11	Polyadenate Binding Protein-1	61142	9.12	11	372
12	60S ribosomal protein L6	32577	10.59	11	271
13	60S ribosomal protein L5	34295	9.76	4	139
14	FK506-binding protein 3	25161	9.29	2	78
15	60S ribosomal protein L22	14647	9.22	2	104
16	40S ribosomal protein S3	26671	9.68	2	119
17	60S ribosomal protein L12	17808	9.48	2	69
18	40S ribosomal protein S7 (S8)	22113	10.09	2	62
19	60S ribosomal protein L30	12645	9.65	3	136
20	60S ribosomal protein L7a	29846	10.61	5	120
21	60S ribosomal protein L14	23160	10.94	3	130
22	DNA binding protein A	40036	9.77	1	102
23	60S ribosomal protein L7	29207	10.66	3	83
24	60S ribosomal protein L13a	23431	10.94	3	83

Figure 3.2 Evaluation of method 2 for isolation of ribosomal proteins

The gel was run with ribosomal proteins extracted using method 2. The protein list shows that 21 ribosomal proteins were identified. Three non-ribosomal proteins were identified



	Protein Name	MW (Da)	PI	# of peptide matches	Mascot Scores
1	60S ribosomal protein L3	45440	10.16	4	161
2	40S ribosomal protein S3a	29795	9.75	3	102
3	60S ribosomal protein L11	19981	9.64	8 (PMF)	92
4	40S ribosomal protein S17	15409	9.85	10 (PMF)	98
5	60S ribosomal protein L10	24430	10.11	3	146
6	40S ribosomal protein S4, X isoform	29448	10.16	3	103
7	40S ribosomal protein S6	28663	10.85	3	123
8	60S ribosomal protein L17 (L23)	21252	10.18	11 (PMF)	124
9	40S ribosomal protein S20	13364	9.95	3	170
10	40S ribosomal protein S5	22862	9.73	2	67
11	40S ribosomal protein L37a	10137	10.44	3	103
12	40S ribosomal protein S8	24509	10.32	8 (PMF)	88
13	60S ribosomal protein L21	18422	10.49	4	160
14	Polyadenate Binding Protein-1	61142	9.12	4	164
15	60S ribosomal protein L6	32577	10.59	3	79
16	60S ribosomal protein L5	34295	9.76	3	108
17	FK506-binding protein 3	25161	9.29	2	94
18	60S ribosomal protein L22	14647	9.22	2	111
19	40S ribosomal protein S3	26671	9.68	3	163
20	60S ribosomal protein L12	17808	9.48	6	74
21	40S ribosomal protein S7 (S8)	22113	10.09	2	70
22	60S ribosomal protein L30	12645	9.65	3	135
23	60S ribosomal protein L7a	29846	10.61	4	118
24	60S ribosomal protein L14	23160	10.94	3	134
25	Nuclease sensitive binding protein-1	35903	9.87	4	85
26	40S ribosomal protein S2 (S4)	31305	10.25	3	87
27	60S ribosomal protein L44 (L36a)	12302	10.59	2	73
28	60S ribosomal protein L35a	12530	11.07	4	194
29	60S ribosomal protein L9	21850	9.96	11 (PMF)	100
30	60S ribosomal protein L29	17610	11.66	3	100
31	60S ribosomal protein L24	17768	11.26	8	80

Figure 3.3 Evaluation of method 3 for isolation of ribosomal proteins

The gel was run with ribosomal proteins extracted using method 3. The protein list shows that 29 ribosomal proteins were identified. Two non-ribosomal proteins were identified.

Since the ribosome was enriched, the mixture of proteins is relatively simple. The protein amount can therefore be reduced leading to a much better resolution but still providing enough material to identify the proteins. Lastly, a DTT wick was applied to the cathode end of the focusing chamber. DTT migrates toward the anode during focusing, allowing the proteins left behind to be oxidized. The DTT supplied by the wick allows a constant supply of DTT to keep the proteins in the basic end reduced during isoelectric focusing. These optimization steps allowed for good resolution of the basic ribosomal proteins, which can be seen in Figure 3.4.

The ribosomal proteins were separated by 2DGE and the images were recorded. Figure 3.5 shows an annotated gel containing numbered protein spots which represent the spots that were cut, digested and subjected to mass spectrometry for identification. The proteins were identified by peptide mass fingerprinting or microsequencing.

At least 5 peptide mass matches in addition to a MASCOT score that allowed >95% confidence, were required for positive protein identification using peptide mass fingerprinting. A minimum of two sequence tags in addition to a significant MASCOT score were required for positive protein identification using the microsequencing technique. Fifty-one proteins were identified. Forty-nine were ribosomal proteins, while two are classified as ribosomal associated proteins. Table 3.1 shows the list of proteins identified using these methods.

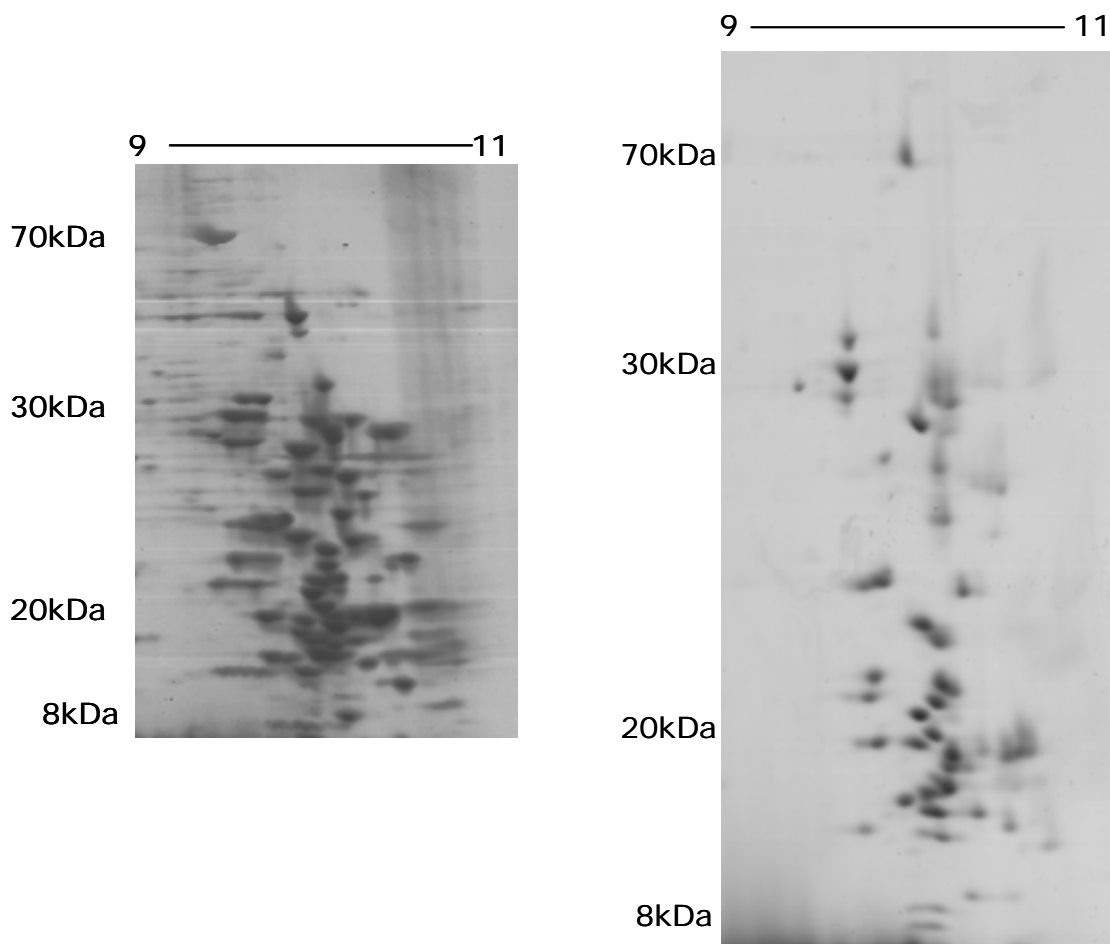


Figure 3.4 Comparison of 2D gel of ribosomal proteins before and after optimization

The picture on the left shows ribosomal proteins that are close together and there are many pairs of spots. The use of a large format gel allowed for better separation of the proteins. The DTT wick resulted in one population of the protein (no pairs of spots).

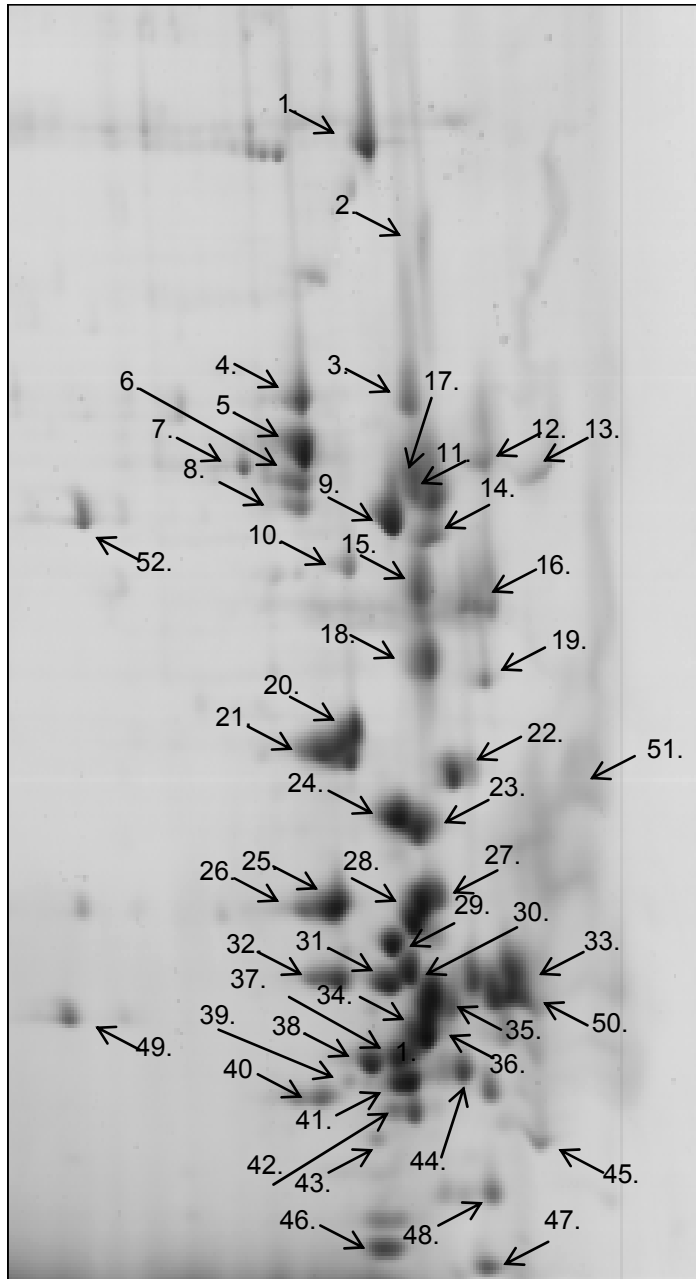


Figure 3.5 Annotated gel of ribosomal proteins

#	Protein (Isoform) Name	MW	PI	Sequence Tags	Mascot Score
1	Polyadenylate Binding Protein	70626	9.52	12	308
2	RPL3	45949	10.19	11	281
3	RPL6	32577	10.59	2	60
4	RPL5	34295	9.76	2	59
5	RPS3a	29795	9.75	4	72
6	RPS3	26671	9.68	10	635
7	RPS3	26671	9.68	9	556
8	RPS3	26671	9.98	5	288
9	RPS4X	29448	10.16	5	162
10	RPL10a	24684	9.94	5	351
	RPL13	24115	11.65	3	148
11	RPL7a	29207	10.66	6	210
12	RPS6	28663	10.85	3	123
13	RPL8	27876	11.03	6	180
14	RPL7	29207	10.66	3	83
15	RPS8	24059	10.32	5	228
16	RPL14	23144	10.94	3	81
17	RPS2	31305	10.25	5	193
18	RPL10	24430	10.11	7	200
19	RPL13a	23431	10.94	3	83
20	RPL9	21850	9.96	4	149
21	RPS5	22731	9.73	5	223
22	RPS9	22447	10.66	3	125
23	RPL21	18422	10.49	2	79
24	RPL17 (L23)	21252	10.18	3	114
25	RPL11	20109	9.64	2	117
26	RPL12	17808	9.48	3	95
27	RPL26/RPS26-like 1	17246	10.55	5	165
28	RPS11	18419	10.31	4	121
29	RPS10	18886	10.15	3	281
30	RPS15	16898	10.39	2	125
	RPS16	16304	10.21	3	144
	RPL27	15657	10.56	3	113
	RPS25	13734	10.12	2	109
	RPS15a	14699	10.14	5	224

Table 3.1 Proteins identified using the bottom-up approach from 2D gels

#	Protein (Isoform) Name	MW	PI	Sequence Tags	Mascot Score
31	RPS25	13734	10.12	4	138
32	RPS17	15409	9.85	5	282
33	RPS18	17708	10.99	7	235
34	RPS13	17081	10.53	5	149
35	RPL27	15657	10.56	5	173
36	RPL31	14454	10.54	5	166
	RPS14	16131	10.08	1	73
37	RPS16	16304	10.21	6	318
38	RPS20	13364	9.95	4	124
39	RPS10	18886	10.15	4	88
40	RPL30	12645	9.65	4	161
41	RPS19	16019	10.41	6	255
	RPS15a	14708	10.61	3	96
42	RPS15a	14708	10.61	3	98
43	RPS10	18886	10.15	3	72
44	RPL23	14856	10.51	5	118
45	RP35a	12530	11.07	7	236
46	RPL38	8082	10.10	2	62
47	RPS29	6541	10.17	4	132
48	RPL37a	10137	10.44	2	89
49	RPL22	14647	9.22	2	104
50	RPL36a	12302	10.59	2	73
51	RPL24	17768	11.26	8-PMF	80
52	FK506	25161	9.29	2	94

Table 3.1 Proteins identified using the bottom-up approach from 2D gels

#	Protein	Accession #	Sequence Covered	%
2	RPL3	P39023	SHRKFSAPRH GSLGFLPRKR SSRHRGKVKKS FPKDDPSKPV HLTAFILGYKA GMTHIVREVD RPGSKVNNKKE VVEAVTIVET PPMVVVGIVG YVETPRGLRT FKTVFAEHIS DECKRRFYKN WHKSKKKAFT KYCKKWQDED GKKQLEKDFS SMKKYCQVIR VIAHTQMRLI PLRQKKAHLM EIQVNGGTVA EKLDWARERL EQQVPVNQVF GQDEMIDVIG VTKGKGYKGV TSRWHTKKLP RKTHRGLRKY ACIGAWHPAR VAFSVARAGQ KGYHHRTEIN KKIYKIGQGY LIKDGKLIKNI NASTDYDLSK SINPLGGFV HYGEVTNDFV MLKGCVVGTK KRVLTLRKSL LVQTKRRALE KIDLKFIIDTT SKFGHGRFQT MEEKKAFMGP LKKDRIAKEE GA	62%
3	RPL6	Q02878	AGEKVEKPDY KEKKPEAKKV DAGGKVKKGN LKAKKPKKGG PHCSRNPVLV RGIGRYSRSA MYSRKAMYKR KYSAASKVE KKKKEKVLAT VTKPVGGDKN GGTRVVKLK MPRYYPTEDV PRKLLSHGKK PFSQHVRKLR ASITPGTILI ILTGRHRGKR VVFLKQLASG LLLVTGPLVL NRVPLRTHQ KFVIATSTKI DISNVKIPKH LTDAYFKKKK LRKPRHQEGE IFDTEKEKYE ITEQRKIDQK AVDSQILPKI KAIPQLQGYL RSVFALTNGI YPHKLVF	79%
4	RPL5	P46777	GFVKVVKNA YFKRYQVKFR RRREGKTDYY ARKRLVIQDK NKYNTPKYRM IVRVTNRDII CQIAYARIEG DMIVCARYAH ELPKYGVKVG LTNYAAAYCT GLLLARLLN RFGMDKIYEG QVEVTGDEYN VESIDGQPGA FTCYLDAGLA RTTTGNKVFG ALKGAVDGGL SIPHSTKRF GYDSESKEFN AEVHRKHIM QNVADYMYL MEEDEDAYKK QFSQYIKNSV TPDMMEMYK KAHAAIRENP VYEKKPKKEV KKKRWNRPKM SLAQKKDRVA QKKASFLRAQ ERAAES	68%
5	RPS3a	P61247	AVGKNKRLTK GGKKGAKKVV VDPFSKDWY DVKAPAMFNI RNIGKTLVTR TQGTKIASDG LKGRVFEVSL ADLQNDVAF RKFKLITEDV QGKNCLTNFH GMDLTRDKMC SMVKKWQTM EAHVDVKTDD GYLLRLFCVG FTKKRNNQIR KTSYAQHQQV RQIRKMMEI MTREVQTNDL KEVVNKLIPD SIGKDIEKAC QSIYPLHDFV VRKVKMLKKP KFELGKLMEL HEGSSSGKA TGDETGAKVE RADGYEPPVQ ESV	83%
6	RPS3	P23396	MAVQISKRRK FVADGIFKAE LNEFLTRELA EDGYSQVEVR VTPTRTEIII LATRTQNVLG EKGRRIRELT AVVQKRFQFP EGSVELYAEK VATRGLCAIA QAESLRYKLL GGLAVRRACY GVLRFIMESG AKGCEVVVSG KLRGQRAKSM KFVDGLMIHS GDPVNYVDV AVRHVLLRQG VLGIKVKIML PWDPTGKIGP KKPLPDHVS VEPKDEILPT TPISEQGGK PEPPAMPQPV PTA	92%

Table 3.2 Sequence coverage of proteins using the bottom-up approach.

#	Protein	Accession #	Sequence Covered	%
7	RPS3	P23396	MAVQISKRRK FVADGIFKAE LNEFLTRELA EDGYSGVEVR VTPTRTEIII LATRTQNVLG EKGRRIRELT AVVQKRFQFP EGSVELYAEK VATRGLCAIA QAESLRKLL GGLAVRACY GVLRFIMESG AKGCEVVVSG KLRGQRAKSM KFVDGLMIHS GDPVNYVDT AVRHVLLRQG VLGIKVKIML PWDPTGKIGP KKPLPDHVS VEPKDEILPT TPISEQGGK PEPPAMPQP PTA	67%
8	RPS3	P23396	MAVQISKRRK FVADGIFKAE LNEFLTRELA EDGYSGVEVR VTPTRTEIII LATRTQNVLG EKGRRIRELT AVVQKRFQFP EGSVELYAEK VATRGLCAIA QAESLRKLL GGLAVRACY GVLRFIMESG AKGCEVVVSG KLRGQRAKSM KFVDGLMIHS GDPVNYVDT AVRHVLLRQG VLGIKVKIML PWDPTGKIGP KKPLPDHVS VEPKDEILPT TPISEQGGK PEPPAMPQP PTA	48%
9	RPS4X	P62701	ARGPKKHLKR VAAPKHWMLD KLTGVFAPRP STGPHKLR EC LPLIIFLRNR LKYALTGDEV KKICMQRFIK IDGKVRDIT YPAGFMDVIS IDKTGENFRL IYDTKGRFAV HRITPEEAKY KLCKVRKIFV GTKGIPHLVT HDARTIRYPD PLIKVNDTIQ IDLETGKITD FIKFDTGNLC MVTGGANLGR IGVITNRERH PGSFVVHVK DANGNSFATR LSNIFVIGKG NKPWISLPRG KGIRLTIAEE RDKRLAAKQS SG	72%
10	RPL10a	P62906	SSKVSRTLY EAVREVLHGN QRKRRKFLET VELQISLKNY DPQDKRFSG TVRLKSTPRP KFSVCVLGDQ QHCDEAKAVD IPHMDIEALK KLNKNKLVK KLAKKYDAFL ASESLIKQIP RILGPGLNKA GKFPSSLTHN ENMVAKVDEV KSTIKFQMKK VLCLAVAVGH VKMTDDELVY NIHLAVNFLV SLLKKNWQNV RALYIKSTMG KPQRLY	72%
	RPL13	P26373	APSRNGMVLK PHFHKDWQRR VATWFNQPAR KIRRRKARQA KARRIAPRPA SGPIRPIVRC PTVRYHTKVR AGRGFSLEEL RVAGIHKVA RTIGISVDPR RRNKSTESLQ ANVQRLKEYR SKLILFPRKP SAPKKGSSA EELKLATQLT GPVMPVRNVY KKEKARVITE EEKNFKAFAS LRMARANARL FGIRAKRAKE AAEQDVEKKK	34%
11	RPL7a	P62424	PKGKAKGKK VAPAPAVVKK QEAKVVNPL FEKRPKNFGI GQDIQPKRDL TRFVKWPRYI RLQRQRAILY KRLKVPPAIN QFTQALDRQT ATQLLKLAKH YRPETKQEKQ QRLLARAEKK AAGKGDVPTK RPPVLRAGVN TVTTLVENKK AQLVVIADV DPELVVFLP ALCRKMGVPY CIKGGKARLG RLVHRKTCTT VAFQVNSD KGALAKLVEA IRTNYNDRYD EIRRHGGNV LGPKSVARIA KLEKAKAKEL ATKLG	59%

Table 3.2 Sequence coverage of proteins using the bottom-up approach

#	Protein	Accession #	Sequence Covered	%
12	RPS6	P62753	MKLNISFPAT GCQKLVVDD ERKLRTFYEK RMATEVAADA LGEWKGYYV RISGGNDKQG FPMKQGVLTG GRVRLLLSKG HSCYRPRRTG ERKRKSVRGC IVDANLSVLN LVIVKKGEKD IPGLTDTTVP RRLGPKRASR IRKLFNLSKE DDVRQYVVRK PLNKEGKKPR TKAPKIQRV TPRVLQHKRR RIALKKQRTK KNKEEAAEYA KLLAKRMKEA KEKRQEQIAK RRRLSSLRAS TSKSESSQK	60%
13	RPL8	P62917	GRVIRGQRKG AGSVFRAHVK HRKGAARLRA VDFAEERHGYI KGIVKDIHD PGRGAPLAKV VFRDPYRFKK RTELFIAAEG IHTGQFVYCG KKAQLNIGNV LPVGTMPGEGT IVCCLEEKPG DRGKLRASG NYATVISHNP ETKKTRVKLP SGSKKVISSA NRAVVGVVAG GGRIDKPIIK AGRAYHKYKA KRNCWPRVRG VAMNPVEHPF GGGNHQHIGK PSTIRRDAPA GRKVGLIAAR RTGRLRGTKT VQEKEN	64%
14	RPL7	P18124	MEGVEEKKKE VPAVPETLKK KRRNFABELKI KRLRKKFAQK MLRKARRKLI YEKAKHYHKE YRQMYRTEIR MARMARKAGN FYVPAEPKLA FVIRIRGING VSPKVRKVLQ LLRLRQIFNG TFVKLNKASI NMLRIVEPYI AWGYPNLKSV NELIYKRGYK KINKKR IALT DNALIARSLG KYGIICMEDL IHEIYTVGKR FKEANNFLWP FKLSSPRGGM KKKTTHFVEG GDAGNREDQI NRLIRRMN	72%
15	RPS8	P62241	GISRDNWHKR RKTGGKRKPY HKKRKYELGR PAANTKIGPR RIHTVVRGG NKKYRALRLD VGNFSWGSEC CTRKTRIIDV VYNASNNELV RTKTLVKNCI VLIDSTPYRQ WYESHYALPL GRKKGAKLTP EEEEILNKKR SKKIQKKYDE RKKNAKISSL LEEQFQQGKL LACIASRPGQ CGRADGYVLE GKELEFYLRK IKARKGK	74%
16	RPL14	P50914	VFRRFVEVGR VAYVSFGPHA GKLVAIVDVI DQNRALVDGP CTQVRRQAMP FKCMQLTDFI LKFPHSAHQK YVRQAWQKAD INTKWAATRW AKKIEARERK AKMTDFDRFK VMKAKKMRNR IIKNEVKKLQ KAALLKASP KAPGTKGTAA AAAAAAKVPK KKITAASKKA PAQKVPAQKA TGQKAAPAPK AQKGQKAPAQ KAPAPKASGK KA	43%
17	RPS2	P15880	MADDAGAAGG PGGPGGPGMG NRGGFRGGFG SGIRGRGRGR GRGRGRGRGA RGGKAEDKEW MPVTKLGRV KDMKIKSLEE IYLFSLPIKE SEIIDFFLGA SLKDEVKIM PVQKQTRAGQ RTRFKAFVAI GDYNGHVGLG VKCSKEVATA IRGAILAKL SIVPVRGYYW GNKIGKPHTV PCKVTGRGCS VLVRLIPAPR GTGIVSAPVP KLLMMAGID DCYTSARGCT ATLGNFATKAT FDAISKTYSY LTPDLWKETV FTKSPYQEFT DHLVKTHTRV SVQRTQAPAV ATT	55%

Table 3.2 Sequence coverage of proteins using the bottom-up approach

#	Protein	Accession #	Sequence Covered	%
18	RPL10	P27635	GRRPARCYRY CKNKPYPKSR FCRGVPDAKI RIFDLGRKKA KVDEFPLCGH MVSDEYEQLS SEALEAARIC ANKYMVKSCG KDFGHIRVRL HPFHVIRINK MLSCAGADRL QTGMRGAFGK PQGTVARVHI GQVIMSIRTK LQNKHEVIEA LRRAKFKFPG RQKIHISSKKW GFTKFNADF EDMVAEKRLI PDGCGVKYIP SRGPLDKWRA LHS	81%
19	RPL13a	P40429	AEVQVLVLDG RGHLLGR LAA IVAKQVLLGR KVVVVRCEGI NISGNFYR NK LK YLAFLR KR MNTNPSRGPY HFRAPSRIFW RTVRGMLPHK TKRGQAALDR LKVFDGIPPP YDKK KRMVVP AALKVVR LKP TRKFA YLR L AHEVGW KYQA VTATLEEK RK EKAKI HYR KK KQLMRL RKQA EKNVEKKIDK YTEVLKTHGL LV	39%
20	RPL9	P32969	MK TILSNQTV DIPENV DITL KGR TVIVKGP RGT LRDFNH INVELS LLGK KKKR LRVDKW WGNR KELATV RTICSH VQNM IKG VTLGFRY KMRSVYAHFP INVVIQENG S LVEIR NFLGE KYIRRV MRP GVACSV SQAQ KDELILEG ND IELVSNSAAL IQQATT VKNK DIRK FLDGIY VSEK GTVQQA DE	64%
21	RPS5	P46782	MTEWETAAPA VAETPD IKLF GK WSTDDVQI NDISLQ DYIA VKEKY AKYLP HSAGR YAAKR FRKA QCPIVE RL TNSMMMHG R NNGK KLMT V RIVKHAF EII HLLTGEN PLQ VLVNAI INSG PREDSTRIGR AGT VRQAVD VSPL RRVNQA IWLLCTGARE AAF RNIKTIA ECLADE LINA AKGSSNSYAI K KDELERVA KSNR	70%
22	RPS9	P46781	PVAR SWVCRK TYVTP RRPFE K SRLDQELKL IGEYGL RNKR EVWR VKFTLA KIRK AAARELL TLDEKDP RRL FEGNALL RRL VRIG VLDEGK MKLDYI LGLK IEDFL ERLQ TQV FKLGLAK SIHHAR VLIR QRHIR VRKQV VNIP SFIVRL DSQKHID FSL RSPYGG RRPG RVKR KNAKKG QGGAGAG DDE EED	87%
23	RPL21	P46778	TNTK GKRRGT RYMF SRPFRK HGVV PLATYM RIYK KGDIVD IKGM GTVQKG MPH KCYHGKT GRVYN VTQHA VGIV VNKQVK GKIL AKRINV RIEHIK HSKS RDS FLKRVKE NDQ KKKEAKE KGTW VQLKRQ PAPP REAHFV RTNG KEPELL EIPYEFMA	77%
24	RPL17 (L23)	P18621	VRYS LDPENP TK SCKSRGSN LR VHFKNTRE TAQA IKGMHI RKAT KYLKDV TL QKQCVFPR RYNGG VGRCA QAK QWGTQG RWPK KSAEFL LHML KNAESN AELK GLDVDS LVIE HIQVNK APKM RRRTYR AHGR INPYMS SPCHIE MILT EK EQIVPKPE EEVA QKKIS QK KLKQKLM ARE	72%

Table 3.2 Sequence coverage of proteins using the bottom-up approach

#	Protein	Accession #	Sequence Covered	%
25	RPL11	P62913	AQDQGEKENP MRELRIKLC LNICVGESGD RLTRAAKMLE QLTGQTPVFS KARYTVRSFG IRRNEKIAVH CTVRGAKAEE ILEKGLKVRE YELRKNFSD TGNFGFGIQE HIDLGIKYDP SIGIYGLDFY VVLGRPGFSI ADKKRRTGCI GAKHRISKEE AMRWFQKYD GIILPGK	68%
26	RPL12	P30050	MPPKFPDNEI KVVYLRCTGG EVGATSALAP KIGPLGLSPK KVGDDIAKAT GDWKGLRITV KLTIQNRQAQ IEVVPASAL IIKALKEPPR DRKKQKNIKH SGNITFDEIV NIARQMRHRS LARELSGTIK EILGTAQSVG CNVDGRHPHD IIDDINSGAV ECPAS	84%
27	RPL26	P61254	MKFNPFVTSR RSKNRKRHFN APSHIRKIM SSPLSKELRQ KYNVRSMP IR KDDEVQVVRG HYKGQQIGKV VQVYRKKYVI YIERVQREKA NGTTVHVGIIH PSKVVIIRLTK LDKDRKKILE RKAKSRQVVGK EKGKYKEETI EKMQE	59%
28	RPS11	P62280	MADIQTERAY QKQPTIFQNK KRVLLETGK EKLPRYKNI GLGFKTPKEA IEGTYIDKCC PFTGNVSIRG RILSGVVTM KMQR TIVIRR DYLHYIRKYN RFEKRHKNMS VHLSPCFRDV QIGDIVTVGE CRPLSKTVRF NVLKVTKAAG TKKQFQKF	76%
29	RPS10	P46783	MLMPKKNRIA IYELLFKEGV MVAKDVHMP KHPELADKNV PNLHVMKAMQ SLKSRGYVKE QFAWRHFYWY LTNEGIQYLR DYHLHLPPEIV PATLRRSRPE TGRPRPKGLE GERPARLTRG EADDRTYRRS AVPPGADKKA EAGAGSATEF QFRGGFGRGR GQPPQ	47%
30	RPS15	P62841	AEVEQKKKRT FRKFTYRGVD LDQLLDMSYE QLMQLYSARQ RRRRLNRGLRR KQHSLLKRLR KAKKEAPPME KPEVVKTHLR DMIILPEMVG SMVGVYNGKT FNQVEIKPEM IGHYLGFEFSI TYKPVKHGRP GIGATHSSRF IPLK	64%
31	RPS25	P62851	MPPKDDKKKK DAGKSAKKDK DPVNKSGGKA KKKKWSKGKV RDKLNNLVLF DKATYDKLCK EVPNYKLITP AVVSERLKIR GSLARAALQE LLSKGLIKLV SKHRAQVIYT RNTKGGDAPA AGEDA	52%
32	RPS17	P08708	GRVRTKTVKK AARVIEKYY TRLGNDFHTN KRVCEEIAII PSKKLRNKIA GYVTHLMKRI QRGPVRGISI KLQEEERERR DNYVPEVSAL DQEIIIEVDPD TKEMLLDF GSLSNLQVTQ PTVGMNFKTP RGPV	85%
33	RPS18	P62269	MSLVIPEKFQ HILRVLNTNI DGRRKIAFAI TAIKGVGRRY AHVVLKADI DLTKRAGELT EDEVERVITI MQNPRQYKIP DWFLNRQKDV KDGYSQVLA NGLDNKLRD LERLKKIRAH RGLRHFVGLR VRGQHTKTTG RRGRTVGVSK KK	69%

Table 3.2 Sequence coverage of proteins using the bottom-up approach

#	Protein	Accession #	Sequence Covered	%
34	RPS13	P62277	GRMHAPGKGL SQSALPYRRS VPTWLKLTSD DVKEQIYKLA KKGLTPSQIG VILRDSHGVA QVRFVTGNKI LRILKSKGLA PDLPEDLYHL IKKAVAVRKH LERNRKDKDA KFRLLILIESR IHLRLARYYKT KRVLPPNWKY ESSTASALVA	83%
35	RPL27	P61353	GKFMKPGKVV LVLAGRYSGR KAVIVKNIDD GTSDRPYSHA LVAGIDRYPR KVTAAAMGKKK IAKRSKIKSF VKVYNYNHLM PTRYSVDIPL DKTVVNKDVF RDPALKRKAR REAKVKFEER YKLGKKNWFF QKLR	67%
36	RPL31	P62899	MAPAKKGGEK KKGSAINEV VTREYNTINIH KR IHGVTGFKK RAPRALKEIR KFAMKEMGTP DVR IDTRLNK AVWAKGIRNV PYRIRVRLSR KRNEDEDSPN KLYTLVTYVP VTTFKNLQTV NVDEN	66%
	RPS14	P62263	APRKGKEKKE EQVISLGPQV AEGENVFGVC HIFASFNDTF VHVTDLSGKE TICRVTTGGMK VKADREDESS YAAMLAAQDV AQRCKELGIT ALHIKLRATG GNRTKTPGPG AQSALRALAR SGMKIGRIED VTPIPSDSTR RKGGRGRRL	46%
37	RPS16	P62249	PSKGPLQSVQ VFGRKKTATA VAHCKRGNGL IKVNGRPLEM IEPRTLQYKL LEPVLLLGKE RFAGVDIRVR VKGGGHVAQI YAIRQSISKA LVAYYQKYVD EASKKEIKDI LIQYDRLLV ADPRRCESKK FGGPGARARY QKSYR	60%
38	RPS20	P60866	MAFKDTGKTP VEPEVAIHR I RITLTSRNVK SLEKVCADLI RGAKKLNKLV KGPVRMPKKT LRITTRKTPC GEGSKTWDRF QMRIHKRLID LHSPSEIVKQ ITSISIEPGV EVEVTIADA	88%
39	RPS10	P46783	MLMPKKNRIA IYELLFKEGV MVAKKDVHMP KHPELADKNV PNLHVMKAMQ SLKSRGYVKE QFAWRHFYWY LTNEGIQYLR DYLLHLPPEIV PATLRRSRPE TGRPRPKGLE GERPARLTRG EADRDTYRRS AVPPGADKKA EAGAGSATEF QFRGGFGRGR GQPPQ	40%
40	RPL30	P62888	VAAKKTKSL ESINSRLQLV MKSGKYVLGY KQTLKMIRQG KAKLVILLANN CPALRKSEIE YYAMLAKTGV HHYSGNNIEL GTACGKYRIV CTLAIIDPGD SDIIRSMPEQ TGEK	84%
41	RPS19	P39019	PGVTVKDVNQ QEFVRLAAF LKKSGLKVP EWVDTVKLAK HKEELAPYDEN WFYTRAASTA RHLYLRGGAG VGSMTKIYGG RQRNGVMP SH FSRGSKSVAR RVLQALEGLK MVEKDQDGR KLTPQGQRDL DR IAGQVAAA NKKH	65%
42	RPS15a	P62244	VRMNVLADAL KSINNAEKRK KRQVLIRPCS KVIVRFLTVM MKHGYIGEFE IIDHRAGKI VVNLTGR LNK CGVISPRFDV QLKDLEKWQN NLLPSRQFGF IVLTTTSAGIM DHEEARRKHT GGKILGFFF	69%

Table 3.2 Sequence coverage of proteins using the bottom-up approach

#	Protein	Accession #	Sequence Covered	%
43	RPS10	P46783	MLMPKKNR IA IYELLFK EGV M VAKKD VHMP KHP ELADK NV PNLHVMKAMQ SLKSRGY VKE QFAWR H FYWY LTNEGIQYLR DYLHL PP IEIV PATL R RSRPE TGRPR P GLE GERPAR LTRG EADRDTYRRS AVPPGADKKA EAGAGSATEF QFRGGFGRGR GQPPQ	32%
44	RPL23	P62829	MSKR GRGGSS GAKFRISLGL PVGAVINCAD NTGAKNLYII SVKGIK GRLN RLPAA GVGDM VMATV KKGKP ELRKKVHPAV VIRQR KSYRR KDG VFLYFED NAGVIVNNKG EMKGS AITGP VAK ECADLWP RIASNAGSIA	46%
45	RPL35a	P18077	MSG R L WSKAI FAGYKRGLRN QREHTALLKI EGVYARDETE FYLGKRCAYV YKAKNNTVTP GGKPNKTRVI WGKVTRAHGN SGMVRAKFRS NLPAKAIGHR IRVMLYPSRI	87%
46	RPL38	P63173	PRK IEEIKDF LLTARRKDAK SVKIKKNKDN V KFKV RCSRY LYTLVITDKE KAELKQSLP PGLAVKELK	68%
47	RPS29	P62273	GHQQLYWSHP RKFGQGSRS C RVCSNRHGLI RKYGLNMCRQ CFRQYAKDIG FIKLD	87%
48	RPL37a	P61513	AKR TKKVGIV GKYGTRYGAS LRKMVKKIEI SQHAKYTCSF CGTKMKRRA VGIWHCGSCM KTVAGGAWTY NTTSAVTVKS AIRRLKELKD Q	82%
49	RPL22	P35268	APVKKLVVKG GKKKKQVLKF TLDCTHPVED GIMDAANFEQ FLQER IKVNG KAGNLGGGVV TIER SKSKIT VTSEVPFSKR YLKYLTKKYL KKNL RDWLR VVANSKESYE LRYFQINQDE EEEEDED	50%
50	RPL36a	P83881	VNVPK TRRTF CKKCGKHQPH KVTQYKKGKD SLYAQGKRRY DRKQSGYGGQ TKPIFRKKAK TTK KIVLRLE CVEPNCRSKR MLAIK RCKHF ELGGDKRKG QVIQF	49%
51	RPL24	P83731	MKVELCSFSG YKIYPGHGRR YARTDGKVFQ FLNAKCESAF LSKRNP RQIN WTVLYRRKHK KGQSEEIQK RTRRAVK FQR AITGASLADI MAKRNQPEV RKAQREQAIR AAKEAKKAKQ ASKK TAMAAA KAPTKAAPKQ KIVK PVKVSA PRVGGKR	66%

Table 3.2 Sequence coverage of proteins using the bottom-up approach.

The red peptides were matched by peptide mass fingerprint. The blue peptides were matched by performing microsequencing. The sequence coverage is the number of amino acids covered by identifying peptides in the mass spectra divided by the number of amino acids in the protein.

In addition to database searching, the sequence coverage for each protein was determined by performing an *in-silico* digest, and finding the matching peaks in the spectra obtained from each spot. Table 3.2 shows the sequence coverage obtained for each identified ribosomal protein. The range of sequence coverage is from 32% to 92%. The average and standard deviation of the percent sequence coverage is $66 \pm 15\%$ and the median is 67.5%.

Comparative Study Between Parental and Mitoxantrone^R MCF-7 Cells

Gels were acquired from both the parental MCF-7 cell line and the MCF-7 cell line selected for resistance. Figure 3.6 shows a zoomed picture of the 2D gel map from the parental cell line (left) and the mitoxantrone resistant cell line (right). Comparative densitometry was performed using the Compugen program to compare the protein abundance profiles between three different pairs of gels from each of three harvests. Three gels constituted each gel pair. Figure 3.7 shows a representative Compugen image of the comparison of a registered image of three gels of ribosomal proteins extracted from one harvest of the parental cell line with a registered image of three gels of ribosomal proteins extracted from one harvest of the drug resistant cell line. The yellow circles indicate a decrease in protein abundance with respect to the parental cell line. The red circles indicate the appearance of protein spots in the mitoxantrone resistant cell line not detected in the parental cell line.

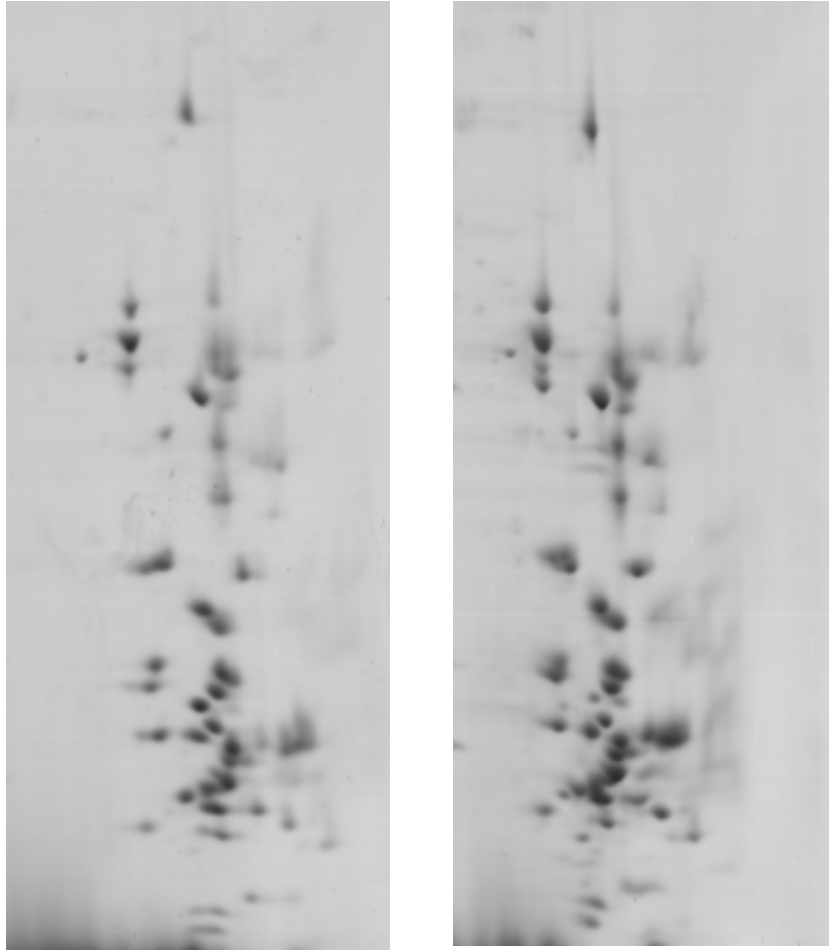


Figure 3.6 Zoomed views of the 2D gels of ribosomal proteins extracted from the parental cell line (left) and the mitoxantrone resistant cell line (right).

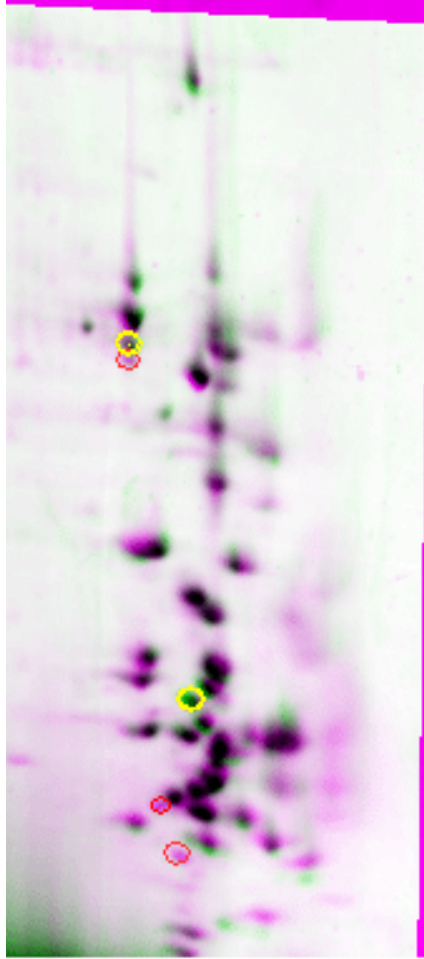


Figure 3.7 Compugen image of the comparison of the parental cell line and the mitoxantrone resistant cell line.

The yellow circles represent a decrease in protein abundance in the mitoxantrone resistant cell line with respect to the parental cell line. The red circles represent the appearance of proteins in the mitoxantrone resistant cell line with respect to the parental cell line.

Spot #	Protein Isoform	Parental Cell Line	Mitoxantrone ^R Cell Line
6	RPS3	1	0.43 ± 0.04
7	RPS3	Not Present	Present
29	RPS10	1	0.27
39	RPS10	Not Present	Present
43	RPS10	Not Present	Present

Table 3.3 Relative quantitation of proteins with altered abundances

The proteins with numbers for relative differences are present in both cell lines, and therefore a value can be obtained for differential abundance. Proteins that were only present in one cell line cannot be relatively quantified, since only one value is available.

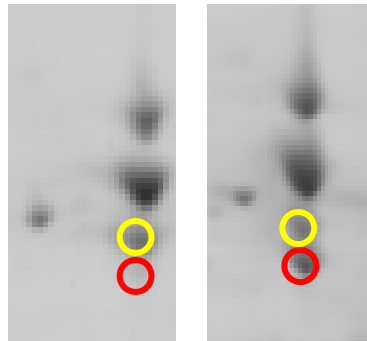


Figure 3.8 RPS3 protein abundance changes

The spot in the yellow circle decreases in the mitoxantrone resistant cell line (right panel) with respect to the parental cell line (left panel). The spot in the red circle was also identified as RPS3, but is not present in the parental cell line.

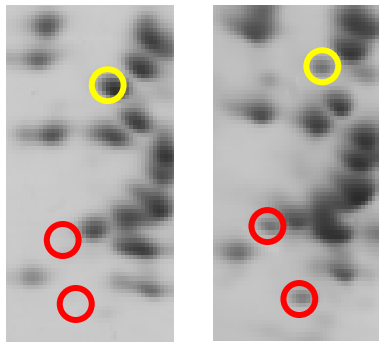


Figure 3.9 RPS10 protein abundance changes

The spot in the yellow circle decreases in the mitoxantrone resistant cell line (right panel) with respect to the parental cell line (left panel). The spots in the red circle was also identified as RPS10, but are not present in the parental cell line.

There are 5 differentially abundant spots detected in the mitoxantrone resistant cell line. Table 3.3 shows the differentially abundant proteins as well as their relative quantitation as determined by the Compugen program. Figure 3.8 shows the abundance changes in ribosomal protein S3 (RPS3). The spot circled in yellow decreases in intensity in the gel from the mitoxantrone resistant cell line. Conversely, the protein spot circled in red indicates the appearance of an isoform of RPS3 in the drug resistant cell line. The abundance changes in ribosomal protein S10 (RPS10) are shown in Figure 3.9. Again, the protein yellow circle indicates a decrease in abundance in the mitoxantrone resistant gel. The two red circles indicate the appearance of two isoforms of RPS10 in the drug resistant cell line.

Characterization of Protein Isoforms

A study was performed to test the extraction of the protein and determine the accuracy of the instrument. A standard protein, apomyoglobin, was run on a gel and extracted using the described procedure. The molecular weight of the protein was calculated to be 16952.27 Da, while the experimental molecular weight was 16953 Da as can be seen in Figure 3.10. This deviation in molecular weight represents a 0.004% error. A precision study was performed which tested the precision of the MALDI instrument. In this study, two proteins were extracted from a gel and spotted ten times on a MALDI plate and analyzed. Table 3.4 shows the results from this study.

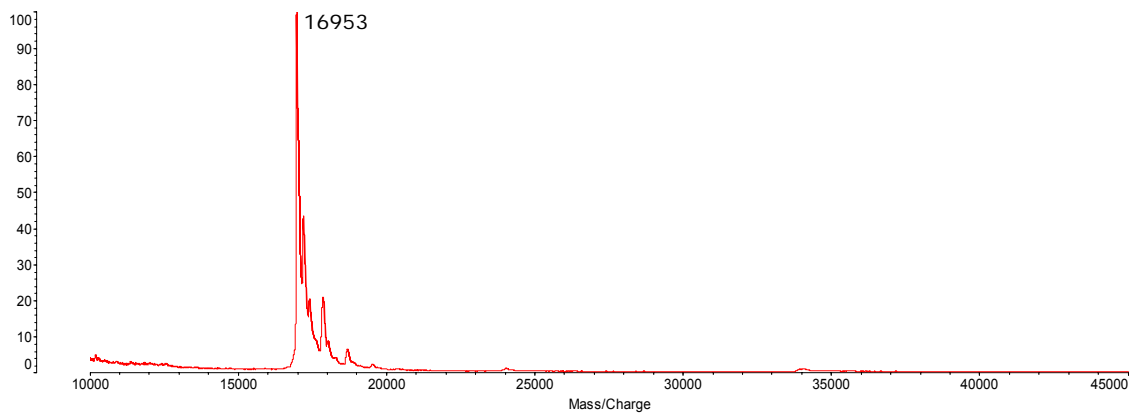


Figure 3.10 The intact molecular weight of the standard apomyoglobin

The calculated MW for apomyoglobin is 16952.27 Da. The observed molecular weight for apomyoglobin that was extracted from a 1D gel was 16953. This mass difference represents a 0.004% error.

Trial #	Mass Protein 1 (Da)	Mass Protein 2 (Da)
1	22215.3	21483.5
2	22220.9	21484.8
3	22202.1	21487.4
4	22217.7	21484.4
5	22215.7	21484.4
6	22220.6	21478.0
7	22217.6	21484.4
8	22212.1	21482.4
9	22225.1	21493.0
10	22227.9	21484.4
Avg	22218 ± 7	21485 ± 4

Table 3.4 Result of precision study of the MALDI-TOF

Two proteins were extracted and spotted on the MALDI plate 10 times. Ten measurements were made and recorded and the average and standard deviation were determined.

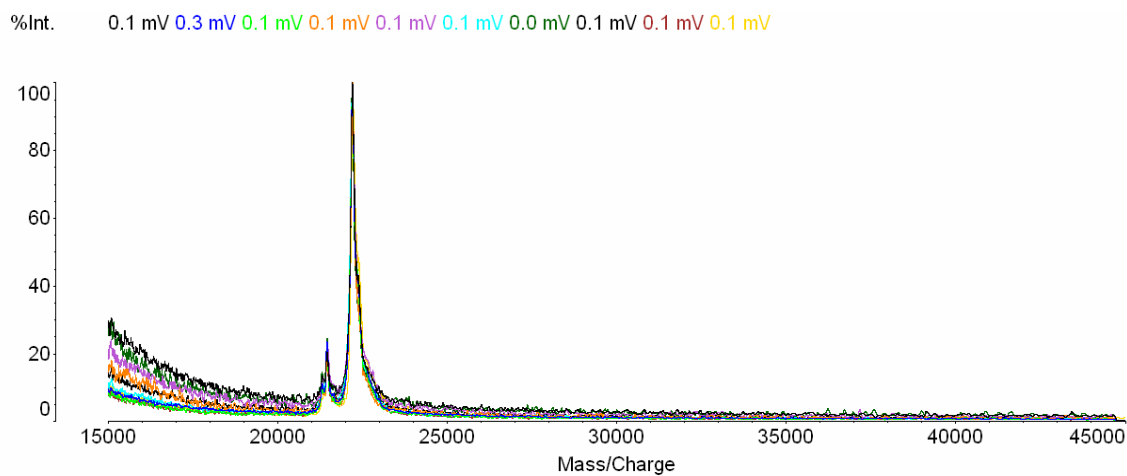


Figure 3.11 Overlay of the spectra from the precision study

The ten generated spectra were overlaid to obtain a visual description of the precision capabilities of the MALDI-TOF

Spot #	Protein Name	Calc Mass	Exp Mass	Potential Mods	Δ Da
3	RPL6	32634	32625		9
4	RPL5	34352	34447	1P, 1O	95
5	RPS3a	30023	30070	3O	47
6	RPS3	26728	26761	2O	33
7	RPS3	26785	26790		5
8	RPS3	26671	25723		-948
9	RPS4X	29619	29648	2O	29
10	RPL13	24343	24929		586
15	RPS8	24059	14298	C-term T 123-207	-9671
16	RPL14	23258	23260		2
18	RPL10	24886	24897	1O	11
20	RPL9	21964	22159		195
21	RPS5	22902	22977	1Ac, 2O	75
22	RPS9	22504	22500		4
24	RPL17 (L23)	21480	21523	3O	43
25	RPL11	20337	20384	2O, 1Me	47
26	RPL12	17922	17924		2
27	RPL26	17248	17291	2O, 1Me	43
28	RPS11	18533	18533		0
29	RPS10	18886	19020		134
30	RPS15	16898	17016	7O	118
31	RPS25	13791	13686	-Met,2Me	-105
32	RPS17	15466	15500	2O	44
33	RPS18	17708	17624	-Met, 1O, 2Me	-84
34	RPS13	17081	17083		2
35	RPL27	15657	15696	3Me	39
36	RPS14	16302	16337	2O	35
36	RPL31	14454	14183	-Met, -125	-271
37	RPS16	16418	16425		7
38	RPS20	13421	13422		1
39	RPS10	18886	15102	C-term T	-3784
40	RPL30	12816	12884	3O,1Me	68
41	RPS19	16019	15958		-61
42	RPS15a	14813	14874	3O, 1Me	61
43	RPS10	18886	14931		-3955
44	RPL23	14913	14932	1O	20
46	RPL38	8082	8154		-72
47	RPS29	6541	7982		1441
48	RPL37a	10137	10127		10
			9599		

Table 3.5 Intact molecular weights of the ribosomal proteins

It was determined that the standard deviation of protein 1 was 7Da, while the standard deviation of protein 2 was 4 Da. This shows that the instrument is capable of making precise measurements.

Top-down and bottom-up proteomic approaches were combined in an attempt to elucidate the structural changes in the protein isoforms that appear in the drug resistant cell line. The bottom-up approach involves protein digestion and subsequent mass spectrometry of peptides in an attempt to identify as many peptides as possible. The results of these analyses can be seen in Table 3.2. Molecular masses of peptides listed in red were matched to molecular masses of in-silico digestion. The blue entries were matched using sequence tags. Since not all peptides were found for the proteins, a top down approach was used to determine whether the protein appeared to be modified or unmodified. In this case the intact molecular weight of a gel extracted protein was determined using MALDI analysis. Table 3.5 shows the calculated and experimental molecular weights of ribosomal proteins, and a column which lists potential modifications, that could explain the observed mass differences. The last column shows the difference between the calculated and experimental masses of each protein.

Absolute Quantification of Ribosomes

The number of ribosomes per cell was determined for both the parental and drug resistant MCF-7 cell lines. This was achieved by counting the number of cells per harvest using a hemacytometer, then measuring the

number of ribosomes per harvest using a UV-Vis spectrophotometer. The two numbers can be divided to give the number of ribosomes per cell. Figure 3.12 shows a bar graph which represents the number of ribosomes per cell for parental (red columns) and mitoxantrone resistant (blue columns) cell lines. Figure 3.13 shows the bar graph representing the absorbances for the number of ribosomes per cell. Each column represents the average and standard deviation of eight measurements. Figure 3.14 shows the bar graph representing the number of cells per harvest. Each column represents the average and standard deviation of three cell counts. No change was observed in the number of ribosomes per cell.

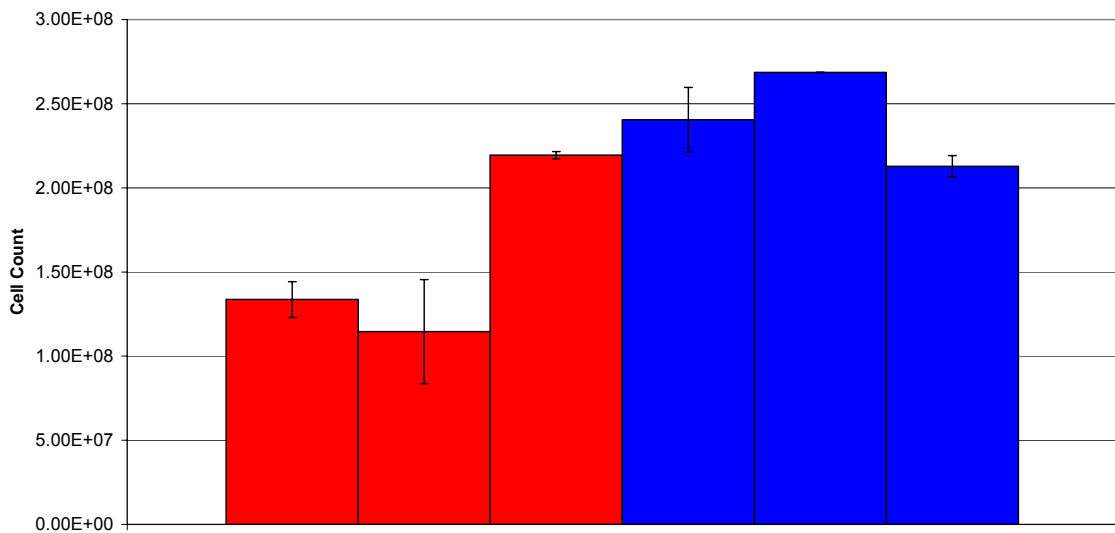


Figure 3.12 Bar graph representation of the number of cell per harvest

The number of cells per harvest was determined for three parental cell line harvests and three mitoxantrone resistant cell line harvests. The average and standard deviation of two measurements per harvest is shown in the bar graph.

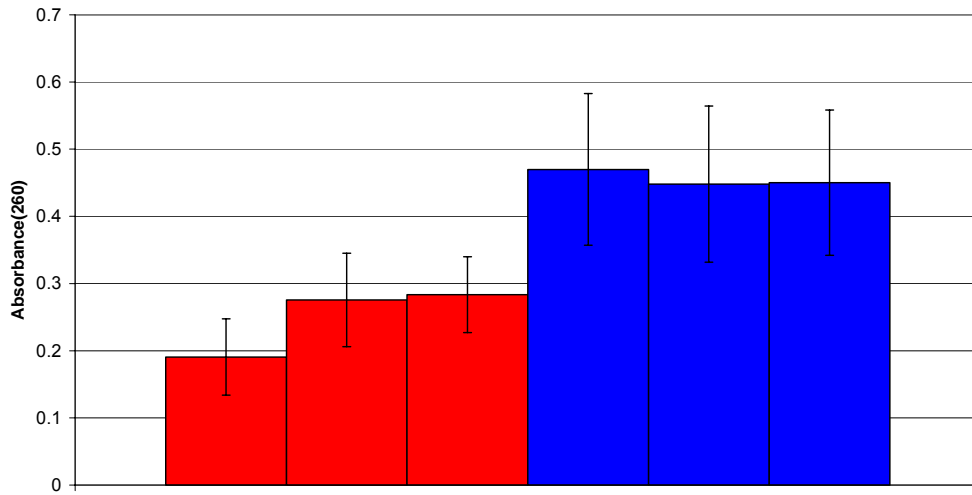


Figure 3.13 Bar graph representation of the number of ribosome per harvest

The number of ribosomes per harvest was determined for three parental cell line harvests and three mitoxantrone resistant cell line harvests. The average and standard deviation of eight measurements per harvest is shown in the bar graph.

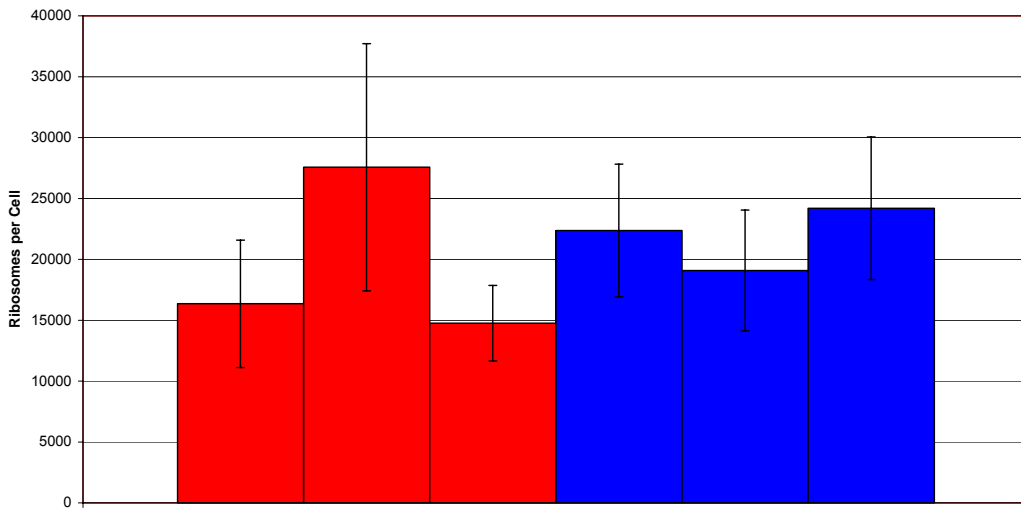


Figure 3.14 Bar graph representation of the number of ribosomes per cell

The number of ribosomes per cell was calculated for three parental cell line harvests and three mitoxantrone resistant cell line harvests. The average and standard deviation of the calculations are shown in the bar graph.

Chapter 4: Discussion

Characterization of the Ribosome

The ribosome is a cellular machine that synthesizes proteins. Since the function of this macromolecule remains constant, it would be easy to conclude that the structure would also remain constant. That is not the case, however, as it has been shown that structures of both the protein and rRNA content, which makes up the ribosome can differ under varying physiological conditions [20, 31, 34, 35, 98, 99]. Work has also been performed, which shows that the number of ribosomes in a cell can differ depending on various physiologic conditions [18, 100, 101]. Although the ribosome has been studied for 65 years, many of the details of its mechanism of protein synthesis are still undiscovered. Specifically, functions have not been described for ribosomal proteins of any species. Localizing the position of the proteins within the ribosome will aid in elucidation of their function, yet the crystal structures have only been reported for three organisms from archaea, and one bacterial. About 30% of *E. coli* ribosomal proteins have orthologous counterparts in eukaryotic ribosomes, which share about 30% sequence homology. The question remains whether assumptions can be made about eukaryotic ribosomes based on studies performed on bacterial or archaeic ribosomes.

Considering that ribosomal proteins change as a result of a change in specific conditions, and that the specific function of ribosomal proteins are unknown, characterizing the proteins found in ribosomes may provide insight

into specific functions. A method has been developed here, by which the ribosomal proteins of the MCF-7 drug susceptible and drug resistant cell lines were evaluated. The proteins were separated by 2D gel electrophoresis, which had been optimized to separate basic proteins. The proteins were identified using a “bottom-up” strategy. The state of the modifications of the ribosomal proteins was evaluated using a combined “top-down bottom-up” strategy.

Bottom-Up Characterization of the MCF-7 Ribosome

Bottom-up characterization is used to identify proteins by analysis of the peptides produced by protease digestion. The proteins can be identified by submitting a list of peptide masses to a database, by obtaining sequence tags using tandem mass spectrometry and submitting to a database or by submitting the tandem mass spectra to a search engine. In this study, protein spots were cut from 2D gels and peptides were generated by in-gel digestion.

Optimization of 2D Gel Analysis

The lack of reproducibility and poor resolution of proteins in the basic region of 2D gels has been widely reported [49-56]. Many factors contribute to the poor first dimension separation. The first factor is the migration of the reducing agent dithiothreitol towards the anode of the focusing chamber during isoelectric focusing. The results of this migration are the formation of intra- and inter- molecular disulphide bridges in the unprotected protein. This

produces proteins in various states of oxidation and therefore multiple populations of a single protein are visible on the gel. A second factor resulting in poor resolution of basic proteins by 2D gel electrophoresis is the amount of protein loaded onto the first dimension strip. Experiments have shown that loading a smaller protein amount leads to increased resolution in the basic region of the gel [54, 55]. These limitations were overcome by using a DTT saturated wick at the cathode end of the focusing tray and decreasing the amount of protein loaded onto the gel.

It was reported that using longer immobilized pH gradient strips or large format gels decreased the quality of the gel because longer strips increase the amount of horizontal streaking observed in the gel [55]. Once the optimization steps discussed above were applied to the electrophoresis, a large format gel could be used without the excessive horizontal streaking that was previously described. The effect was better resolution of the protein spots and more space between each of the protein spots. The final result was that ribosomal proteins were able to be separated and well-resolved by 2D gel electrophoresis, which can be seen in Figure 3.4.

Identification of Proteins

Due to an apparent heterogeneity of the human ribosome, a definitive number of proteins expected in the ribosome has not been determined to date [4, 20, 21, 98]. The number of proteins in the *E. coli* ribosome was determined in 1970 by Kaltschmidt and Wittman using 2D gel electrophoresis [14]. The

same method was applied to ribosomes harvested from rat liver in 1972, and 69 proteins were found [13]. Early reports of the number of ribosomal proteins in HeLa cells reported 34 proteins in the large ribosomal subunit and 17-20 proteins that always occurred in the small subunit [21]. In addition, there were 10 proteins that were sometimes found in the ribosomal fraction. It has since been determined that all mammalian ribosomes consist of about 78-80 ribosomal proteins per ribosome [4]. Recent reports which evaluate either the small subunit [41] or the large subunit [36] have found 31 and 46 ribosomal proteins respectively.

The SwissProt database contains 84 ribosomal protein entries, which are listed in Table 4.1. Using a theoretical isoelectric point calculator, [102] it was determined that 45 of these ribosomal proteins are in the pI range 7-11. This is significant because it was the pI range of the first dimension gel used in this work. Forty-nine ribosomal proteins were identified, and are red in color in Table 4.1. Thirty-six were calculated to be in the pI range of 7-11. Thirteen ribosomal proteins were identified, whose calculated pI's were determined to be higher than 11. Nine ribosomal proteins, whose calculated pI's are in the range, were not identified and are blue in color in Table 4.1.

Structural redundancy, in which more than one ribosomal protein has a very similar sequence to another, is a common theme observed in human ribosomal proteins. For example, ribosomal protein S4 has three isoforms; S4X, S4Y1, and S4Y2. Since these proteins share such high homology, it would be reasonable to assume that they would perform similar functions. As

a result, only one of the three protein isoforms might be observed in the ribosomes. Four of the proteins that were expected, but not identified, had a high level of sequence homology with proteins that were identified.

Another possible reason for not observing all of the proteins that were expected in this region is the method for isolation of the ribosomal proteins. The classic method of ribosomal isolation is using acetic acid to remove the ribosomal RNA followed by acetone to precipitate the proteins [94]. Suh et al. investigated other methods and reagents to obtain ribosomal proteins prior to mass spectrometry [42]. They concluded that even with many optimization steps, only 90% of the expected ribosomal proteins could be observed in the mass spectrum. In addition, they found that the low molecular weight ribosomal proteins were more sensitive to sample preparation and therefore less likely to be seen in the spectrum. These results are consistent with what was observed in this work. Four of the proteins that were expected, but not identified had molecular weights below 10kDa. A theoretical digest was performed using the PeptideCutter program to compare the number of peptides generated from the small ribosomal proteins using three different proteases. The results are shown in Table 4.2.

The results show that a similar number of peptides are generated in the detectable range of 600-3000 Da whether trypsin or lys-c are used as a protease. Glu-C produces fewer, much larger peptides.

Protein Name	MW	PI	Accession Number
RPL3	45949	10.62	P39023
RPL4	47697	11.5	P36578
RPL5	34295	10.05	P46777
RPL6	32577	11.03	Q02878
RPL7	29207	11.07	P18124
RPL7A	29846	11.06	P62424
RPL8	27876	11.45	P62917
RPL9	21850	10.37	P32969
RPL10	24430	10.49	P27635
RPL10A	24684	10.36	P62906
RPL11	20109	9.96	P62913
RPL12	17808	9.9	P30050
RPL13	24130	12.06	P26373
RPL13A	23446	11.36	P40429
RPL14	23158	11.41	P50914
RPL15	24015	12.02	P61313
RPL17	21266	10.6	P18621
RPL18	21503	12.13	Q07020
RPL18A	20762	11.15	Q02543
RPL19	23466	11.89	P84098
RPL21	18434	10.91	P46778
RPL22	14656	9.61	P35268
RPL23	14865	10.94	P62829
RPL23A	17695	10.89	P62750
RPL24	17779	11.69	P83731
RPL26	17248	10.98	P61254
RPL26-I	17246	10.98	Q9UNX3
RPL27	15657	10.98	P61353
RPL27A	16430	11.42	P46776
RPL28	15616	12.42	P46779
RPL29	17621	12.08	P47914
RPL30	12645	9.96	P62888
RPL31	14454	10.97	P62899
RPL32	15729	11.74	P62910
RPL34	13162	11.88	P49207
RPL35	14420	11.48	P42766
RPL35A	12530	11.46	P18077
RPL36	12123	12	Q9Y3U8
RPL36A	12302	11.03	P83881
RPL36A-I	12338	11.1	Q969Q0
RPL37	10947	12.15	P61927
RPL37A	10137	10.44	P61513
RPL38	8085	10.56	P63173
RPL39	6275	12.96	P62891
RPL39-I	6161	12.81	Q96EH5
RPL40	6181	10.73	P62987
RPL41	3456	13.36	P62945
RPSA	32723	4.95	P08865
RPS2	31305	10.65	P15880
RPS3	26671	10.04	P23396
RPS3A	29795	10.04	P61247
RPS4X	29448	10.59	P62701
RPS4Y	29324	10.68	P22090
RPS4Y2	29164	10.51	Q8TD47

Table 4.1 The list of human ribosomal proteins in the SwissProt database

RPS5	22731	10.09	P46782
RPS6	28663	11.29	P62753
RPS7	22127	10.58	P62081
RPS8	24059	10.72	P62241
RPS9	22447	11.09	P46781
RPS10	18886	10.51	P46783
RPS11	18419	10.71	P62280
RPS12	14395	6.34	P25398
RPS13	17081	10.94	P62277
RPS14	16131	10.53	P62263
RPS15	16898	10.79	P62841
RPS15A	14699	10.61	P62244
RPS16	16304	10.57	P62249
RPS17	15409	10.24	P08708
RPS18	17708	11.42	P62269
RPS19	16109	10.73	P39019
RPS20	13364	10.44	P60866
RPS21	9111	8.89	P63220
RPS23	15676	10.96	P62266
RPS24	15423	11.24	P62847
RPS25	13734	10.58	P62851
RPS26	12884	11.42	P62854
RPS27	9330	9.84	P42677
RPS27A	9418	10.22	P62979
RPS28	7841	11.15	P62857
RPS29	6541	10.17	P62273
RPS30	6648	12.56	P62861
RPP0	34274	5.6	P05388
RPP1	11514	4	P05386
RPP2	11665	4.18	P05387

Table 4.1 The list of human ribosomal proteins in the SwissProt database.

The proteins highlighted in red were identified in this study. The proteins highlighted in blue were in the pI range evaluated in this study, but were not identified.

seqRPS4X	ARGPKKHLKR	VAAPKHWMLD	KLTGVFAPRP	STGPHKLREC	LPLIIFLRNR
seqRPS4Y1	ARGPKKHLKR	VAAPKHWMLD	KLTGVFAPRP	STGPHKLREC	LPLIVFLRNR
seqRPS4Y2	ARGPKKHLKR	VAAPKHWMLD	KLTGVFAPRP	STGPHKLREC	LPLIVFLRNR
seqRPS4X	LKYALTGDEV	KKICMQRFIK	IDGKVRTDIT	YPAGFMDVIS	IDKTGENFRL
seqRPS4Y1	LKYALTGDEV	KKICMQRFIK	IDGKVRVDVT	YPAGFMDVIS	IEKTGEHFRL
seqRPS4Y2	LKYALTGDEV	KKICMQHFLK	IDGKVRVDIT	YPAGFIDVIS	IEKTGEHFRL
seqRPS4X	IYDTKGRFAV	HRITPEEAKY	KLCKVRKIFV	GTKGIPHLVT	HDARTIRYPD
seqRPS4Y1	VYDTKGRFAV	HRITVEEAKY	KLCKVRKITV	GVKGIPHLVT	HDARTIRYPD
seqRPS4Y2	VYNTKGCFAV	HRITVEEAKY	KLCKVRKITV	GTKGIPHLVT	HDARTIRYPD
seqRPS4X	PLIKVNDTIQ	IDLETGKITD	FIKFDTGMLC	MVTGGANLGR	IGVITNRERH
seqRPS4Y1	PVIKVNDTVQ	IDLGTGKIIN	FIKFDTGMLC	MVIGGANLGR	VGVITNRERH
seqRPS4Y2	PLIKVNDTVQ	IDLGTGKITS	FIKFDTGMLC	MVIAGANLGR	VGVITNRERH
seqRPS4X	PGSFDVVHVK	DANGNSFATR	LSNIFVIGKG	NKPWISLPRG	KGIRLTIAEE
seqRPS4Y1	PGSFDVVHVK	DANGNSFATR	LSNIFVIGNG	NKPWISLPRG	KGIRLTVAEE
seqRPS4Y2	PGSCDVVHVK	DANGNSFATR	ISNIFVIGNG	NKPWISLPRG	KGIRLTIAEE
seqRPS4X	RDKRLAAKQS	SG			
seqRPS4Y1	RDKRLATKQS	SG			
seqRPS4Y2	RDKRLAAKQS	SG			

Figure 4.1 A ClustLW sequence alignment of three isoforms of ribosomal protein S4.

The green boxes highlight the differences that exist between the isoforms.

Sequence Coverage

The usual goal of bottom-up analysis of proteins is to identify the protein. This requires a minimum of two sequence tags or five peptide mass matches [73]. Tryptic peptides of basic ribosomal proteins are particularly small due to the frequent occurrence of lysine and arginine residues. Two sequence tags or five peptides would not represent or cover a very large portion of the sequence of the protein.

Ribosomal proteins are known to contain many post-translational modifications (PTM's). Many recent papers that identify the proteins also make an attempt to identify the PTM's [36-39, 41, 42, 84, 85]. Identifying a few out of many possible peptides would not likely lead to identification of the PTM's. For that reason, analyses were performed in ways designed to maximize the number of peptides identified for each protein. One report in the literature cites 14-70% sequence coverage for ribosomal proteins, with more than half of the proteins having over 41% sequence coverage [35].

For 37 of the proteins studied here, at least 60 % of the sequence was covered in the spectra of the peptides of those proteins. The general trend is that for proteins with less intense spots on the gel, less of the sequence was characterized. For intense spots on the gel, better sequence coverage was obtained. The identification of PTM's can be supported by database searching. When submitting tandem MS data in our study, the following modifications were entered for consideration by

	Number of Peptides in Mass Range of Detection		
	Trypsin	Lys-C	Glu-C
RPS21	7	8	5
RPS27	11	11	3
RPS27a	7	6	5
RPL40	3	5	1

Table 4.2 In-silico digest of small molecular weight ribosomal proteins in the detectable range

The detectable range is 600Da to 3000Da. Although Lys-C only cuts at lysine residues, it makes about the same amount of peptides as trypsin. Glu-C make fewer peptides, which are larger in size.

the search: acetylation, methylation, and phosphorylation. These modifications are the most common modifications reported on ribosomal proteins.

Top-Down Characterization of the MCF-7 Ribosome

The goal of the proteomic top-down approach is to experimentally obtain an intact molecular weight for a protein, followed by gas phase fragmentation and sequencing of the protein. Two common methods are applied in this way. The first is a one or two dimensional gel electrophoresis experiment. Molecular mass is estimated by movement of the protein, and a limitation of this method is the error, up to 10%, in the determination of molecular weights. Proteins are identified following excision from the gel and trypsin digestion.

In the second method the molecular weight of the intact protein is obtained using mass spectrometry. This measurement has a 0.05-0.1% error for proteins under 30kDa. In the latter approach, after determination of the intact molecular weight, the protein is fragmented in the gas phase [75, 81, 83, 103]. As in bottom-up analysis, 100% sequence coverage of the protein is desired. An additional objective of this method is to induce cleavages at every peptide bond. This allows very specific localization of post-translational modifications. In practice, 137 of the possible 258 amide bonds were cleaved for carbonic anhydrase [75] in one study, while 250 of the possible 258 amide bonds were cleaved for carbonic anhydrase in a later study [77].

In addition, the reports of high levels of cleavage usually involve the use of high amounts of purified protein standards. The application of these techniques to mixtures of harvested proteins has not proven to be nearly as successful. The most useful piece of information gathered from top-down experiments with “wild-type” proteins is the intact molecular weight. Determining the experimental molecular weight for a protein is a way of scanning whether the protein is modified or unmodified. In addition, if the experimental molecular weight does not agree with the theoretical molecular weight, the amount of deviation will narrow down the potential post-translational modifications. For instance, if the deviation from the theoretical molecular weight is 44 Da, phosphorylation (addition of 80 Da) is not the modification. Researchers have employed this approach to narrow down the proteins which required further characterization of post-translational modifications [104, 105].

In this work, intact molecular weights were determined for 41 ribosomal proteins. The proteins were already identified by bottom-up analysis by in-gel digestion. Since the protein spots had been identified, the calculated molecular weight for each protein could be determined. The intact proteins were extracted from the gel spots and their molecular weights were determined using MALDI.

Optimization of Extraction of Ribosomal Proteins from Gels

Since the ribosomal proteins had already been identified in the gel, a method was desired in which the intact protein could be extracted from the gel for analysis. This tactic simplifies the correlation between the protein's identification and its molecular weight. Multiple approaches exist in the literature. In one approach, MALDI analysis was performed on the protein that was still in the gel [106-109]. The gels were usually soaked in MALDI matrix, and mounted onto the MALDI plate. In a second approach, the proteins were blotted from the gel to a membrane such as PVDF or nitrocellulose. MALDI analysis can then be performed directly from the membrane [110-112], or the protein can be extracted from the membrane and analysed [113, 114]. The third approach involves the direct extraction of the protein from the gel into solution. Two methods have been employed: electroelution, or chemical elution. The commercial electrelutor applies a voltage creating an electric field which elutes the protein from the gel and dialyses it into the buffer of choice [115]. In passive elution, the gel piece containing the protein is soaked in an extraction solution to recover the protein [96, 107, 113, 116-119]. It is noteworthy that all of the solution extraction analyses were performed using proteins recovered from one dimensional gels.

The first approach, performing mass spectrometric analysis directly on the gel, was not attempted. Since the analyzer on our MALDI instrument is time-of-flight, distance from the point of ionization to the detector determines

the mass accuracy of the measurement. It has been determined that when the thickness of a MALDI matrix spot differs, mass accuracy and resolution will vary as well [120]. It was therefore decided that the thickness of the gel would invite variations that could be avoided.

The second approach of electroblotting the proteins to a membrane was attempted. Using the method based on Towbin [121], the gel was electroblotted onto PVDF membranes. An attempt was made to remove the protein from the membrane for subsequent mass spectrometric analysis. The piece of PVDF membrane with the protein spot was placed in an extraction solution. The blotting itself was efficient as determined by using colorimetric standards. The extraction from the membrane was evaluated by the disappearance of the color from the membrane. This approach did not provide a good mass spectrum.

The third approach proved to be the most successful. Although solution extraction methods from multiple groups were evaluated, the method Mirza et al. was the only one that provided results with our proteins [96]. This method has a fairly extensive destaining process, followed by a simple extraction using 50%ACN/0.1% TFA, which is the solvent for MALDI matrix. The method effectively destained and extracted the proteins from the gel pieces and allowed for MALDI analyses of intact molecular weights from the ribosomal proteins.

MALDI optimization for molecular mass determination

Mass spectrometry was optimized by adjusting the solubilizing solutions. It was determined that using a 50% ACN with 1%TFA for solubilizing the matrix resulted in a much improved MS signal intensity. In addition, mixing Triton X-100 with the extracted sample to a final concentration of 2.5% resulted in increased MS signals as well as increases in resolution. There was a very noticeable decrease in the width of the peak as well as a decrease in the adduct peaks observed. The addition of Triton X-100 produced a doubly-charged protein peak in many instances.

Intact Molecular Weights

Obtaining intact molecular weights for ribosomal proteins provides insight into the level of post-translational modification of the proteins. This approach has been taken to analyze *E. coli* proteins [37, 42, 84, 85] and proteins from the microbe *Rhodopseudomonas palustris*, which is environmentally important and has a completely sequenced genome [38]. Post-translational modifications such as loss of N-terminal methionine, methylation, and acetylation, loss of signal peptide, B-methylthiolation, and C-terminal truncation were all hypothesized as modifications which lead to the differences between experimental masses and calculated masses in these prokaryotic proteins.

Fewer reports exist on the intact molecular weight determination of eukaryotic ribosomal proteins. The yeast large subunit ribosomal proteins

were analyzed by LC-MS and intact molecular weight determination revealed PTM's such as acetylation and methylation [39]. In addition, 58 protein isoforms were identified, 9 masses were not correlated with a protein, and 6 proteins were not associated with a mass. This is a strong indication of various forms of truncation or a large amount of processing, which could not be resolved.

The small ribosomal subunit of the rat ribosome was analyzed using an LC-MS based system [34]. In this case, 41 total proteins were observed. Thirty-six proteins were correlated to the 32 rat liver small ribosomal subunit proteins. Four proteins were observed to have two isoforms. Twelve proteins exhibited masses that were consistent with the calculated mass; 15 differed by mass increments readily assignable to PTM, while seven showed masses that were inconsistent with known modifications. Five masses could not be correlated with any protein in the database. In this case, multiple isoforms of some ribosomal proteins could be resolved.

Proteins from the small subunit of human ribosomes have been analyzed using N-terminal sequencing and mass spectrometry [40] and top-down bottom-up analysis [41]. In the former study, 32 ribosomal proteins from human placenta were separated by offline HPLC and analyzed. Two proteins were found to have different N-terminal sequences than what was present in the database. One protein, RPS24, was found to have a 318 Da mass difference between calculated and observed molecular weights.

In the latter study, 31 ribosomal proteins were identified using the top-down, bottom-up approach. N-terminal methionine loss, acetylation and methylation were detected. Two proteins were found to be differentially modified between the healthy and ribosomes from Hepatitis C infected cell small subunits, RP25 and RP29. Of the 22 proteins identified using the top-down approach, all of them contained post-translational modifications. Thirty-one proteins were identified using the bottom-up approach, and all but one was modified. Many of the peptides containing the modifications were not discovered.

These and other literature reports demonstrate the variability of ribosomes found in all types of organisms. They have shown that the number of detected ribosomal proteins varies, the masses vary, the isoforms vary, and the sequences vary. In one 2D gel based bottom-up study performed on *Arabidopsis thaliana*, 25% of the proteins has mass or charge differences [35]. More than 18 ribosomal proteins were identified in more than one spot on the gel, meaning that multiple populations existed for those 18 proteins. This observation indicates biochemical variation. Depending on the method of detection, data obtained from the proteins is often not correlated with proteins because of the degree of variation. The results obtained in this study are consistent with those that are published as can be seen in Table 3.5. Some of the ribosomal proteins have molecular weights that are so different than the calculated molecular weight the modifications cannot be deduced or hypothesized.

Implications for Methods to Multidrug Resistance in Breast Cancer

Multi-drug resistance is the most common cause of cancer treatment failure. The cytotoxicity of most chemotherapy drugs initiates apoptosis in non-resistant cells [122]. A defect in the apoptotic pathway can lead to tumorigenesis and progression of the disease that results from the mutation. In addition tumors must circumvent cellular responses such as hypoxia, nutrient deprivation, changes in adhesion, and immune attacks to progress and metastasize [123]. Each of these obstacles acts as a selective pressure to alter the apoptotic pathway or promote other mechanisms of resistance.

The amount of ribosomes in a cell is a factor that has been reported to change based on various cellular changes. One such study reports an increase in the number of ribosomes as a result of an increase in calcium influx [18]. Another study reports that an increase in the number of ribosomes was observed when a DNA inverting enzyme, which stimulates the production of rRNA, was overexpressed [100].

The number of cells in a harvest was counted using a hemacytometer. Ribosomes were quantitated after isolation by taking the absorbance reading at 260nm. One Absorbance unit at 260nm is equal to 19 pmol of ribosomes [97]. Using this conversion, the number of ribosomes in a harvest could be calculated. The procedure was performed for both the parental MCF-7 as well as the mitoxantrone resistance MCF-7 cells. It was determined that the number of ribosomes per cell was not statistically different between the cell lines.

Ribosomal proteins are known to be involved in apoptosis and, thus potentially, multidrug resistance. Ribosomal protein S3, which was found to be modified in the present work, and ribosomal proteins S13 and L23 reportedly promote multidrug resistance by suppressing drug induced apoptosis [124-126].

Alternative isoforms of RPS3 and RPS10 appeared in the gel of the drug resistant cell line, which can be seen circled in red in Figures 3.8 and 3.9. Although functional studies have not yet been performed for most eukaryotic ribosomal proteins, the literature reports of these proteins provide insight into their functions in varying experimental conditions. In addition, literature reports indicate altered structures for these ribosomal proteins in other circumstances.

RPS3

In the drug resistant cell line, the RPS3 spot found in the parental cell line decreased in abundance, while another RPS3 isoform appeared. The novel isoform had a molecular mass that was 948 daltons less than the calculated molecular weight. The literature indicates that modifications of RPS3 are variable and that the type of modifications cannot be directly discerned because of the large molecular weight changes. As evaluated by migration in a 2D gel, Chang et.al. determined a mass shift in RPS3 [35]. The intact molecular weight of RPS3 was not determined using the top-down approach by Yu et al, because a molecular weight corresponding to that

protein was not found [41]. A mass difference of (+) 228 Da was reported in a human ribosomal protein by Vladimirov et.al. [40]. In a rat protein, a mass difference of (-) 362.1 Da was observed in one isoform of RPS3 [34]. The second identified isoform of RPS3 had a mass difference of (-) 74.9 Da as determined by Louie et.al. [34]. It is clear that RPS3 is commonly reported as modified and that the nature of the modification varies.

RPS10

Two additional isoforms of RPS10 appeared in the drug resistant cell line. The spot identified as RPS10 in the drug susceptible cell line was decreased in abundance in the drug resistant cell line relative to the drug susceptible cell line. The molecular masses of the two novel isoforms were 14931 Da and 15102 Da. This represents a decrease from the expected molecular weight of 3784 Da and 3955 Da respectively. Chang et. al. observed a mass shift in ribosomal protein S10 based on its migration in a 2D gel [35]. Using mass spectrometry, an increase in mass corresponding to the addition of a methyl group and an acetyl group were observed by Yu et al [41]. In the work performed by Vladimirov et al. ribosomal protein S10 was not determined because at the time of publication, the sequence of RPS10 was unknown [40]. In the work performed by Louie et al., RPS10 was determined to have a mass change of (+) 57 Da [34]. Again it is apparent that the changes in RPS10 can be difficult to characterize.

The changes in the ribosome observed in this study need to be considered in the context of changes in other parts of the cell. The cell is a functioning unit therefore the changes that take place as a result of multidrug resistance will be global. In addition, drug resistance in cancer is multifactorial, meaning that differing mechanisms of resistance are simultaneously working to create a state of drug resistance in the cell. No single protein is ever completely responsible for drug resistance in a cell.

Conclusion

The conclusion can be made that changes in abundance of ribosomal protein isoforms in the MCF-7 cell line are associated with resistance to mitoxantrone. Studies are planned to test for corresponding changes in ribosomal function.

References

1. Nissen, P., J. Hansen, N. Ban, P.B. Moore, and T.A. Steitz, *The structural basis of ribosome activity in peptide bond synthesis*. Science, 2000. **289**(5481): p. 920-30.
2. Hansen, J.L., T.M. Schmeing, P.B. Moore, and T.A. Steitz, *Structural insights into peptide bond formation*. Proc Natl Acad Sci U S A, 2002. **99**(18): p. 11670-5.
3. Lafontaine, D.L. and D. Tollervey, *The function and synthesis of ribosomes*. Nat Rev Mol Cell Biol, 2001. **2**(7): p. 514-20.
4. Spirin, A., *Ribosomes*. Cellular Organelles, ed. P. Siekevitz. 1999, New York: Kluwer Academic.
5. Spahn, C.M., R. Beckmann, N. Eswar, P.A. Penczek, A. Sali, G. Blobel, and J. Frank, *Structure of the 80S ribosome from *Saccharomyces cerevisiae*--tRNA-ribosome and subunit-subunit interactions*. Cell, 2001. **107**(3): p. 373-86.
6. Bulygin, K.N., M.N. Repkova, A.G. Ven'yaminova, D.M. Graifer, G.G. Karpova, L.Y. Frolova, and L.L. Kisselev, *Positioning of the mRNA stop signal with respect to polypeptide chain release factors and ribosomal proteins in 80S ribosomes*. FEBS Lett, 2002. **514**(1): p. 96-101.
7. Schuwirth, B.S., M.A. Borovinskaya, C.W. Hau, W. Zhang, A. Vila-Sanjurjo, J.M. Holton, and J.H. Cate, *Structures of the bacterial ribosome at 3.5 Å resolution*. Science, 2005. **310**(5749): p. 827-34.
8. Yusupov, M.M., G.Z. Yusupova, A. Baucom, K. Lieberman, T.N. Earnest, J.H. Cate, and H.F. Noller, *Crystal structure of the ribosome at 5.5 Å resolution*. Science, 2001. **292**(5518): p. 883-96.
9. Wimberly, B.T., D.E. Brodersen, W.M. Clemons, Jr., R.J. Morgan-Warren, A.P. Carter, C. Vonrhein, T. Hartsch, and V. Ramakrishnan, *Structure of the 30S ribosomal subunit*. Nature, 2000. **407**(6802): p. 327-39.
10. Pioletti, M., F. Schlunzen, J. Harms, R. Zarivach, M. Gluhmann, H. Avila, A. Bashan, H. Bartels, T. Auerbach, C. Jacobi, T. Hartsch, A. Yonath, and F. Franceschi, *Crystal structures of complexes of the small ribosomal subunit with tetracycline, edeine and IF3*. Embo J, 2001. **20**(8): p. 1829-39.
11. Harms, J., F. Schlunzen, R. Zarivach, A. Bashan, S. Gat, I. Agmon, H. Bartels, F. Franceschi, and A. Yonath, *High resolution structure of the large ribosomal subunit from a mesophilic eubacterium*. Cell, 2001. **107**(5): p. 679-88.
12. Ban, N., P. Nissen, J. Hansen, P.B. Moore, and T.A. Steitz, *The complete atomic structure of the large ribosomal subunit at 2.4 Å resolution*. Science, 2000. **289**(5481): p. 905-20.
13. Sherton, C.C. and I.G. Wool, *Determination of the number of proteins in liver ribosomes and ribosomal subunits by two-dimensional polyacrylamide gel electrophoresis*. J Biol Chem, 1972. **247**(14): p. 4460-7.

14. Kaltschmidt, E. and H.G. Wittmann, *Ribosomal proteins. XII. Number of proteins in small and large ribosomal subunits of Escherichia coli as determined by two-dimensional gel electrophoresis*. Proc Natl Acad Sci U S A, 1970. **67**(3): p. 1276-82.
15. Wilson, D.N. and K.H. Nierhaus, *Ribosomal proteins in the spotlight*. Crit Rev Biochem Mol Biol, 2005. **40**(5): p. 243-67.
16. Gorelic, L., *Photoinduced cross-linkage, in situ, of Escherichia coli 30S ribosomal proteins to 16S rRNA: identification of cross-linked proteins and relationships between reactivity and ribosome structure*. Biochemistry, 1976. **15**(16): p. 3579-90.
17. Baumert, H.G., S.E. Skold, and C.G. Kurland, *RNA-protein neighbourhoods of the ribosome obtained by crosslinking*. Eur J Biochem, 1978. **89**(2): p. 353-9.
18. Zhang, Y. and S.A. Berger, *Increased calcium influx and ribosomal content correlate with resistance to endoplasmic reticulum stress-induced cell death in mutant leukemia cell lines*. J Biol Chem, 2004. **279**(8): p. 6507-16.
19. Giavalisco, P., D. Wilson, T. Kreitler, H. Lehrach, J. Klose, J. Gobom, and P. Fucini, *High heterogeneity within the ribosomal proteins of the Arabidopsis thaliana 80S ribosome*. Plant Mol Biol, 2005. **57**(4): p. 577-91.
20. Bickle, T.A., G.A. Howard, and R.R. Traut, *Ribosome heterogeneity. The nonuniform distribution of specific ribosomal proteins among different functional classes of ribosomes*. J Biol Chem, 1973. **248**(13): p. 4862-4.
21. McConkey, E.H. and E.J. Hauber, *Evidence for heterogeneity of ribosomes within the HeLa cell*. J Biol Chem, 1975. **250**(4): p. 1311-8.
22. Preiherr, J., T. Hildebrandt, S. Klostermann, S. Eberhardt, S. Kaul, and U.H. Weidle, *Transcriptional profiling of human mammary carcinoma cell lines reveals PKW, a new tumor-specific gene*. Anticancer Res, 2000. **20**(4): p. 2255-64.
23. Vaarala, M.H., K.S. Porvari, A.P. Kyllonen, M.V. Mustonen, O. Lukkarinen, and P.T. Vihko, *Several genes encoding ribosomal proteins are over-expressed in prostate-cancer cell lines: confirmation of L7a and L37 over-expression in prostate-cancer tissue samples*. Int J Cancer, 1998. **78**(1): p. 27-32.
24. Shuda, M., N. Kondoh, K. Tanaka, A. Ryo, T. Wakatsuki, A. Hada, N. Goseki, T. Igari, K. Hatsuse, T. Aihara, S. Horiuchi, M. Shichita, N. Yamamoto, and M. Yamamoto, *Enhanced expression of translation factor mRNAs in hepatocellular carcinoma*. Anticancer Res, 2000. **20**(4): p. 2489-94.
25. Kondoh, N., M. Shuda, K. Tanaka, T. Wakatsuki, A. Hada, and M. Yamamoto, *Enhanced expression of S8, L12, L23a, L27 and L30 ribosomal protein mRNAs in human hepatocellular carcinoma*. Anticancer Res, 2001. **21**(4A): p. 2429-33.

26. Kondoh, N., C.W. Schweinfest, K.W. Henderson, and T.S. Papas, *Differential expression of S19 ribosomal protein, laminin-binding protein, and human lymphocyte antigen class I messenger RNAs associated with colon carcinoma progression and differentiation*. *Cancer Res*, 1992. **52**(4): p. 791-6.
27. Khanna, N., V.G. Reddy, N. Tuteja, and N. Singh, *Differential gene expression in apoptosis: identification of ribosomal protein S29 as an apoptotic inducer*. *Biochem Biophys Res Commun*, 2000. **277**(2): p. 476-86.
28. Bortoluzzi, S., F. d'Alessi, C. Romualdi, and G.A. Danieli, *Differential expression of genes coding for ribosomal proteins in different human tissues*. *Bioinformatics*, 2001. **17**(12): p. 1152-7.
29. Brown, K.J. and C. Fenselau, *Investigation of doxorubicin resistance in MCF-7 breast cancer cells using shot-gun comparative proteomics with proteolytic 18O labeling*. *J Proteome Res*, 2004. **3**(3): p. 455-62.
30. Kasai, H., D. Nadano, E. Hidaka, K. Higuchi, M. Kawakubo, T.A. Sato, and J. Nakayama, *Differential expression of ribosomal proteins in human normal and neoplastic colorectum*. *J Histochem Cytochem*, 2003. **51**(5): p. 567-74.
31. Wiene, B., R. Ehrlich, M. Stoffler-Meilicke, G. Stoffler, I. Smith, D. Weiss, R. Vince, and S. Pestka, *Ribosomal protein alterations in thiostrepton- and Micrococin-resistant mutants of Bacillus subtilis*. *J Biol Chem*, 1979. **254**(16): p. 8031-41.
32. Gregory, S.T. and A.E. Dahlberg, *Mutations in the conserved P loop perturb the conformation of two structural elements in the peptidyl transferase center of 23 S ribosomal RNA*. *J Mol Biol*, 1999. **285**(4): p. 1475-83.
33. Gabashvili, I.S., S.T. Gregory, M. Valle, R. Grassucci, M. Worbs, M.C. Wahl, A.E. Dahlberg, and J. Frank, *The polypeptide tunnel system in the ribosome and its gating in erythromycin resistance mutants of L4 and L22*. *Mol Cell*, 2001. **8**(1): p. 181-8.
34. Louie, D.F., K.A. Resing, T.S. Lewis, and N.G. Ahn, *Mass spectrometric analysis of 40 S ribosomal proteins from Rat-1 fibroblasts*. *J Biol Chem*, 1996. **271**(45): p. 28189-98.
35. Chang, I.F., K. Szick-Miranda, S. Pan, and J. Bailey-Serres, *Proteomic characterization of evolutionarily conserved and variable proteins of Arabidopsis cytosolic ribosomes*. *Plant Physiol*, 2005. **137**(3): p. 848-62.
36. Odintsova, T.I., E.C. Muller, A.V. Ivanov, T.A. Egorov, R. Bienert, S.N. Vladimirov, S. Kostka, A. Otto, B. Wittmann-Liebold, and G.G. Karpova, *Characterization and analysis of posttranslational modifications of the human large cytoplasmic ribosomal subunit proteins by mass spectrometry and Edman sequencing*. *Journal of Protein Chemistry*, 2003. **22**(3): p. 249-258.

37. Arnold, R.J. and J.P. Reilly, *Observation of Escherichia coli ribosomal proteins and their posttranslational modifications by mass spectrometry*. Anal Biochem, 1999. **269**(1): p. 105-12.
38. Strader, M.B., N.C. Verberkmoes, D.L. Tabb, H.M. Connelly, J.W. Barton, B.D. Bruce, D.A. Pelletier, B.H. Davison, R.L. Hettich, F.W. Larimer, and G.B. Hurst, *Characterization of the 70S Ribosome from Rhodospseudomonas palustris using an integrated "top-down" and "bottom-up" mass spectrometric approach*. J Proteome Res, 2004. **3**(5): p. 965-78.
39. Lee, S.W., S.J. Berger, S. Martinovic, L. Pasa-Tolic, G.A. Anderson, Y. Shen, R. Zhao, and R.D. Smith, *Direct mass spectrometric analysis of intact proteins of the yeast large ribosomal subunit using capillary LC/FTICR*. Proc Natl Acad Sci U S A, 2002. **99**(9): p. 5942-7.
40. Vladimirov, S.N., A.V. Ivanov, G.G. Karpova, A.K. Musolyamov, T.A. Egorov, B. Thiede, B. Wittmann-Liebold, and A. Otto, *Characterization of the human small-ribosomal-subunit proteins by N-terminal and internal sequencing, and mass spectrometry*. Eur J Biochem, 1996. **239**(1): p. 144-9.
41. Yu, Y., H. Ji, J.A. Doudna, and J.A. Leary, *Mass spectrometric analysis of the human 40S ribosomal subunit: native and HCV IRES-bound complexes*. Protein Sci, 2005. **14**(6): p. 1438-46.
42. Suh, M.J. and P.A. Limbach, *Investigation of methods suitable for the matrix-assisted laser desorption/ionization mass spectrometric analysis of proteins from ribonucleoprotein complexes*. Eur J Mass Spectrom (Chichester, Eng), 2004. **10**(1): p. 89-99.
43. Ruggero, D. and P.P. Pandolfi, *Does the ribosome translate cancer?* Nat Rev Cancer, 2003. **3**(3): p. 179-92.
44. Loreni, F., G. Thomas, and F. Amaldi, *Transcription inhibitors stimulate translation of 5' TOP mRNAs through activation of S6 kinase and the mTOR/FRAP signalling pathway*. Eur J Biochem, 2000. **267**(22): p. 6594-601.
45. Williams, A.J., J. Werner-Fraczek, I.F. Chang, and J. Bailey-Serres, *Regulated phosphorylation of 40S ribosomal protein S6 in root tips of maize*. Plant Physiol, 2003. **132**(4): p. 2086-97.
46. Pandey, A. and M. Mann, *Proteomics to study genes and genomes*. Nature, 2000. **405**(6788): p. 837-46.
47. O'Farrell, P.H., *High resolution two-dimensional electrophoresis of proteins*. J Biol Chem, 1975. **250**(10): p. 4007-21.
48. Gorg, A., W. Weiss, and M.J. Dunn, *Current two-dimensional electrophoresis technology for proteomics*. Proteomics, 2004. **4**(12): p. 3665-85.
49. Friso, G. and L. Wikstrom, *Analysis of proteins from membrane-enriched cerebellar preparations by two-dimensional gel electrophoresis and mass spectrometry*. Electrophoresis, 1999. **20**(4-5): p. 917-27.

50. Bae, S.H., A.G. Harris, P.G. Hains, H. Chen, D.E. Garfin, S.L. Hazell, Y.K. Paik, B.J. Walsh, and S.J. Cordwell, *Strategies for the enrichment and identification of basic proteins in proteome projects*. *Proteomics*, 2003. **3**(5): p. 569-79.
51. Hoving, S., B. Gerrits, H. Voshol, D. Muller, R.C. Roberts, and J. van Oostrum, *Preparative two-dimensional gel electrophoresis at alkaline pH using narrow range immobilized pH gradients*. *Proteomics*, 2002. **2**(2): p. 127-34.
52. Gorg, A., C. Obermaier, G. Boguth, A. Csordas, J.J. Diaz, and J.J. Madjar, *Very alkaline immobilized pH gradients for two-dimensional electrophoresis of ribosomal and nuclear proteins*. *Electrophoresis*, 1997. **18**(3-4): p. 328-337.
53. Bjellqvist, B., M. Linderholm, K. Ostergren, and J. Strahler, *Moving and stationary boundaries in immobilized pH gradients*. *Electrophoresis*, 1988. **9**(9): p. 453-63.
54. Pennington, K., E. McGregor, C.L. Beasley, I. Everall, D. Cotter, and M.J. Dunn, *Optimization of the first dimension for separation by two-dimensional gel electrophoresis of basic proteins from human brain tissue*. *Proteomics*, 2004. **4**(1): p. 27-30.
55. Olsson, I., K. Larsson, R. Palmgren, and B. Bjellqvist, *Organic disulfides as a means to generate streak-free two-dimensional maps with narrow range basic immobilized pH gradient strips as first dimension*. *Proteomics*, 2002. **2**(11): p. 1630-2.
56. Luche, S., H. Diemer, C. Tastet, M. Chevallet, A. Van Dorsselaer, E. Leize-Wagner, and T. Rabilloud, *About thiol derivatization and resolution of basic proteins in two-dimensional electrophoresis*. *Proteomics*, 2004. **4**(3): p. 551-61.
57. Fenn, J.B., M. Mann, C.K. Meng, S.F. Wong, and C.M. Whitehouse, *Electrospray ionization for mass spectrometry of large biomolecules*. *Science*, 1989. **246**(4926): p. 64-71.
58. Karas, M. and F. Hillenkamp, *Laser desorption ionization of proteins with molecular masses exceeding 10,000 daltons*. *Anal Chem*, 1988. **60**(20): p. 2299-301.
59. Tanaka, K.W., H; Ido, Y; Akita, S; Yoshida, Y; Yoshida, T; Matsuo, T, *Protein and polymer analyses up to m/z 100 000 by laser ionization time-of-flight mass spectrometry*. *Rapid Communications in Mass Spectrometry*, 1988. **2**(8): p. 151-153.
60. Spengler, B., *The Basics of Matrix-Assisted Laser Desorption, Ionization Time-of-Flight Mass Spectrometry and Post-Source Decay Analysis*. *Proteome Research: Mass Spectrometry*, ed. P. James. 2001, Berlin: Springer-Verlag.
61. Mann, M., R.C. Hendrickson, and A. Pandey, *Analysis of proteins and proteomes by mass spectrometry*. *Annu Rev Biochem*, 2001. **70**: p. 437-73.
62. Mann, M. and O.N. Jensen, *Proteomic analysis of post-translational modifications*. *Nat Biotechnol*, 2003. **21**(3): p. 255-61.

63. Sun, Z.W. and C.D. Allis, *Ubiquitination of histone H2B regulates H3 methylation and gene silencing in yeast*. Nature, 2002. **418**(6893): p. 104-8.
64. Yuan, Z.L., Y.J. Guan, D. Chatterjee, and Y.E. Chin, *Stat3 dimerization regulated by reversible acetylation of a single lysine residue*. Science, 2005. **307**(5707): p. 269-73.
65. Oda, Y., K. Huang, F.R. Cross, D. Cowburn, and B.T. Chait, *Accurate quantitation of protein expression and site-specific phosphorylation*. Proc Natl Acad Sci U S A, 1999. **96**(12): p. 6591-6.
66. Ji, X., J. Kong, and S.A. Liebhaber, *In vivo association of the stability control protein alphaCP with actively translating mRNAs*. Mol Cell Biol, 2003. **23**(3): p. 899-907.
67. Salek, M., A. Alonso, R. Pipkorn, and W.D. Lehmann, *Analysis of protein tyrosine phosphorylation by nanoelectrospray ionization high-resolution tandem mass spectrometry and tyrosine-targeted product ion scanning*. Anal Chem, 2003. **75**(11): p. 2724-9.
68. Wilkins, M.R., E. Gasteiger, A.A. Gooley, B.R. Herbert, M.P. Molloy, P.A. Binz, K. Ou, J.C. Sanchez, A. Bairoch, K.L. Williams, and D.F. Hochstrasser, *High-throughput mass spectrometric discovery of protein post-translational modifications*. J Mol Biol, 1999. **289**(3): p. 645-57.
69. Jensen, O.N., *Modification-specific proteomics: characterization of post-translational modifications by mass spectrometry*. Curr Opin Chem Biol, 2004. **8**(1): p. 33-41.
70. Seo, J. and K.J. Lee, *Post-translational modifications and their biological functions: proteomic analysis and systematic approaches*. J Biochem Mol Biol, 2004. **37**(1): p. 35-44.
71. Schweppe, R.E., C.E. Haydon, T.S. Lewis, K.A. Resing, and N.G. Ahn, *The characterization of protein post-translational modifications by mass spectrometry*. Acc Chem Res, 2003. **36**(6): p. 453-61.
72. Eng, J.K., A.L. McCormack, and J.R. Yates, *An Approach to Correlate Tandem Mass-Spectral Data of Peptides with Amino-Acid-Sequences in a Protein Database*. Journal of the American Society for Mass Spectrometry, 1994. **5**(11): p. 976-989.
73. Mann, M. and M. Wilm, *Error-tolerant identification of peptides in sequence databases by peptide sequence tags*. Anal Chem, 1994. **66**(24): p. 4390-9.
74. Liebler, D., *Introduction to Proteomics: Tools for the New Biology*. 2002, Totowa, NJ: Humana Press.
75. Kelleher, N.L., H.Y. Lin, G.A. Valaskovic, D.J. Aaserud, E.K. Fridriksson, and F.W. McLafferty, *Top down versus bottom up protein characterization by tandem high-resolution mass spectrometry*. Journal of the American Chemical Society, 1999. **121**(4): p. 806-812.
76. Kelleher, N.L., *Top-down proteomics*. Anal Chem, 2004. **76**(11): p. 197A-203A.

77. Sze, S.K., Y. Ge, H. Oh, and F.W. McLafferty, *Top-down mass spectrometry of a 29-kDa protein for characterization of any posttranslational modification to within one residue*. Proc Natl Acad Sci U S A, 2002. **99**(4): p. 1774-9.
78. Zhai, H., X. Han, K. Breuker, and F.W. McLafferty, *Consecutive ion activation for top down mass spectrometry: improved protein sequencing by nozzle-skimmer dissociation*. Anal Chem, 2005. **77**(18): p. 5777-84.
79. Demirev, P.A., A.B. Feldman, P. Kowalski, and J.S. Lin, *Top-down proteomics for rapid identification of intact microorganisms*. Anal Chem, 2005. **77**(22): p. 7455-61.
80. Vaidyanathan, S., D.B. Kell, and R. Goodacre, *Selective detection of proteins in mixtures using electrospray ionization mass spectrometry: influence of instrumental settings and implications for proteomics*. Anal Chem, 2004. **76**(17): p. 5024-32.
81. Reid, G.E. and S.A. McLuckey, *'Top down' protein characterization via tandem mass spectrometry*. J Mass Spectrom, 2002. **37**(7): p. 663-75.
82. Nemeth-Cawley, J.F. and J.C. Rouse, *Identification and sequencing analysis of intact proteins via collision-induced dissociation and quadrupole time-of-flight mass spectrometry*. J Mass Spectrom, 2002. **37**(3): p. 270-82.
83. Resing, K.A. and N.G. Ahn, *Proteomics strategies for protein identification*. FEBS Lett, 2005. **579**(4): p. 885-9.
84. Moini, M. and H. Huang, *Application of capillary electrophoresis/ electrospray ionization-mass spectrometry to subcellular proteomics of Escherichia coli ribosomal proteins*. Electrophoresis, 2004. **25**(13): p. 1981-7.
85. Millea, K.M., I.J. Kass, S.A. Cohen, I.S. Krull, J.C. Gebler, and S.J. Berger, *Evaluation of multidimensional (ion-exchange/reversed-phase) protein separations using linear and step gradients in the first dimension*. J Chromatogr A, 2005. **1079**(1-2): p. 287-98.
86. *PROCLAME: Protein Cleavage and Modification Engine*. 2006.
87. *ProSight PTM*. 2006.
88. Perkins, D.N., D.J. Pappin, D.M. Creasy, and J.S. Cottrell, *Probability-based protein identification by searching sequence databases using mass spectrometry data*. Electrophoresis, 1999. **20**(18): p. 3551-67.
89. Creasy, D.M. and J.S. Cottrell, *Error tolerant searching of uninterpreted tandem mass spectrometry data*. Proteomics, 2002. **2**(10): p. 1426-34.
90. Aebersold, R. and M. Mann, *Mass spectrometry-based proteomics*. Nature, 2003. **422**(6928): p. 198-207.
91. Bommer, U.B., N; Junemann, R; Spahn, C; Triana-Alonso, F and Nierhaus, K, *Ribosomes and Polysomes*. Subcellular Fractionation: A Practical Approach, ed. J.M.G.a.D. Rickwood. 1997, Oxford: Oxford University Press.

92. Siegmann, M. and G. Thomas, *Separation of multiple phosphorylated forms of 40 S ribosomal protein S6 by two-dimensional polyacrylamide gel electrophoresis*. *Methods Enzymol*, 1987. **146**: p. 362-9.
93. Spector, D.G., R; Leinwand, L, *Subcellular Fractionation*. Culture and Biochemical Analysis of Cells, ed. K. Janssen. Vol. 1. 1998, Cold Spring Harbor: Cold Spring Harbor Laboratory Press.
94. Hardy, S.J., C.G. Kurland, P. Voynow, and G. Mora, *The ribosomal proteins of Escherichia coli. I. Purification of the 30S ribosomal proteins*. *Biochemistry*, 1969. **8**(7): p. 2897-905.
95. Shevchenko, A., M. Wilm, O. Vorm, and M. Mann, *Mass spectrometric sequencing of proteins silver-stained polyacrylamide gels*. *Anal Chem*, 1996. **68**(5): p. 850-8.
96. Mirza, U.A., Y.H. Liu, J.T. Tang, F. Porter, L. Bondoc, G. Chen, B.N. Pramanik, and T.L. Nagabhushan, *Extraction and characterization of adenovirus proteins from sodium dodecylsulfate polyacrylamide gel electrophoresis by matrix-assisted laser desorption/ionization mass spectrometry*. *J Am Soc Mass Spectrom*, 2000. **11**(4): p. 356-61.
97. Meskauskas, A., J.W. Harger, K.L. Jacobs, and J.D. Dinman, *Decreased peptidyltransferase activity correlates with increased programmed -1 ribosomal frameshifting and viral maintenance defects in the yeast Saccharomyces cerevisiae*. *Rna*, 2003. **9**(8): p. 982-92.
98. Sherton, C.C. and I.G. Wool, *A comparison of the proteins of rat skeletal muscle and liver ribosomes by two-dimensional polyacrylamide gel electrophoresis. Observations on the partition of proteins between ribosomal subunits and a description of two acidic proteins in the large subunit*. *J Biol Chem*, 1974. **249**(7): p. 2258-67.
99. Wilcox, S.K., G.S. Cavey, and J.D. Pearson, *Single ribosomal protein mutations in antibiotic-resistant bacteria analyzed by mass spectrometry*. *Antimicrob Agents Chemother*, 2001. **45**(11): p. 3046-55.
100. Richins, R. and W. Chen, *Effects of FIS overexpression on cell growth, rRNA synthesis, and ribosome content in Escherichia coli*. *Biotechnol Prog*, 2001. **17**(2): p. 252-7.
101. Dong, H., L. Nilsson, and C.G. Kurland, *Gratuitous overexpression of genes in Escherichia coli leads to growth inhibition and ribosome destruction*. *J Bacteriol*, 1995. **177**(6): p. 1497-504.
102. *Compute pI/Mw Tool*. 2006.
103. Wysocki, V.H., K.A. Resing, Q. Zhang, and G. Cheng, *Mass spectrometry of peptides and proteins*. *Methods*, 2005. **35**(3): p. 211-22.
104. Misek, D.E., R. Kuick, H. Wang, V. Galchev, B. Deng, R. Zhao, J. Tra, M.R. Pisano, R. Amunugama, D. Allen, A.K. Walker, J.R. Strahler, P. Andrews, G.S. Omenn, and S.M. Hanash, *A wide range of protein isoforms in serum and plasma uncovered by a quantitative intact protein analysis system*. *Proteomics*, 2005. **5**(13): p. 3343-52.

105. Wang, Y., B.M. Balgley, P.A. Rudnick, E.L. Evans, D.L. DeVoe, and C.S. Lee, *Integrated capillary isoelectric focusing/nano-reversed phase liquid chromatography coupled with ESI-MS for characterization of intact yeast proteins*. J Proteome Res, 2005. **4**(1): p. 36-42.
106. Xu, Y., M.W. Little, D.J. Rousell, J.L. Laboy, and K.K. Murray, *Direct from polyacrylamide gel infrared laser desorption/ionization*. Anal Chem, 2004. **76**(4): p. 1078-82.
107. Loo, J.A., J. Brown, G. Critchley, C. Mitchell, P.C. Andrews, and R.R. Ogorzalek Loo, *High sensitivity mass spectrometric methods for obtaining intact molecular weights from gel-separated proteins*. Electrophoresis, 1999. **20**(4-5): p. 743-8.
108. Loo, R.R., J.D. Cavalcoli, R.A. VanBogelen, C. Mitchell, J.A. Loo, B. Moldover, and P.C. Andrews, *Virtual 2-D gel electrophoresis: visualization and analysis of the E. coli proteome by mass spectrometry*. Anal Chem, 2001. **73**(17): p. 4063-70.
109. Loo, R.R.O., L. Yam, J.A. Loo, and V.N. Schumaker, *Virtual two-dimensional gel electrophoresis of high-density lipoproteins*. Electrophoresis, 2004. **25**(14): p. 2384-2391.
110. Strupat, K., M. Karas, F. Hillenkamp, C. Eckerskorn, and F. Lottspeich, *Matrix-Assisted Laser-Desorption Ionization Mass-Spectrometry of Proteins Electroblotted after Polyacrylamide-Gel Electrophoresis*. Analytical Chemistry, 1994. **66**(4): p. 464-470.
111. Vestling, M.M. and C. Fenselau, *Polyvinylidene difluoride (PVDF): an interface for gel electrophoresis and matrix-assisted laser desorption/ionization mass spectrometry*. Biochem Soc Trans, 1994. **22**(2): p. 547-51.
112. Botting, C.H., *Improved detection of higher molecular weight proteins by matrix-assisted laser desorption/ionization time-of-flight mass spectrometry on polytetrafluoroethylene surfaces*. Rapid Commun Mass Spectrom, 2003. **17**(6): p. 598-602.
113. Jorgensen, C.S., M. Jagd, B.K. Sorensen, J. McGuire, V. Barkholt, P. Hojrup, and G. Houen, *Efficacy and compatibility with mass spectrometry of methods for elution of proteins from sodium dodecyl sulfate-polyacrylamide gels and polyvinylidene difluoride membranes*. Anal Biochem, 2004. **330**(1): p. 87-97.
114. Jonsson, A.P., Y. Aissouni, C. Palmberg, P. Percipalle, E. Nordling, B. Daneholt, H. Jornvall, and T. Bergman, *Recovery of gel-separated proteins for in-solution digestion and mass spectrometry*. Anal Chem, 2001. **73**(22): p. 5370-7.
115. Yefimov, S., A.L. Yergey, and A. Chrambac, *Transfer of SDS-proteins from gel electrophoretic zones into mass spectrometry, using electroelution of the band into buffer without sectioning of the gel*. J Biochem Biophys Methods, 2000. **42**(1-2): p. 65-78.
116. Ehring, H., S. Stromberg, A. Tjernberg, and B. Noren, *Matrix-assisted laser desorption/ionization mass spectrometry of proteins extracted*

- directly from sodium dodecyl sulphate-polyacrylamide gels. *Rapid Commun Mass Spectrom*, 1997. **11**(17): p. 1867-73.
117. Jin, Y. and T. Manabe, *High-efficiency protein extraction from polyacrylamide gels for molecular mass measurement by matrix-assisted laser desorption/ionization-time of flight-mass spectrometry*. *Electrophoresis*, 2005. **26**(6): p. 1019-28.
 118. Cohen, S.L. and B.T. Chait, *Mass spectrometry of whole proteins eluted from sodium dodecyl sulfate-polyacrylamide gel electrophoresis gels*. *Anal Biochem*, 1997. **247**(2): p. 257-67.
 119. Yang, E.C., J. Guo, G. Diehl, L. DeSouza, M.J. Rodrigues, A.D. Romaschin, T.J. Colgan, and K.W. Siu, *Protein expression profiling of endometrial malignancies reveals a new tumor marker: chaperonin 10*. *J Proteome Res*, 2004. **3**(3): p. 636-43.
 120. Ramirez, J. and C. Fenselau, *Factors contributing to peak broadening and mass accuracy in the characterization of intact spores using matrix-assisted laser desorption/ionization coupled with time-of-flight mass spectrometry*. *J Mass Spectrom*, 2001. **36**(8): p. 929-36.
 121. Towbin, H., T. Staehelin, and J. Gordon, *Electrophoretic transfer of proteins from polyacrylamide gels to nitrocellulose sheets: procedure and some applications*. *Proc Natl Acad Sci U S A*, 1979. **76**(9): p. 4350-4.
 122. Hengartner, M.O., *The biochemistry of apoptosis*. *Nature*, 2000. **407**(6805): p. 770-6.
 123. Johnstone, R.W., A.A. Ruefli, and S.W. Lowe, *Apoptosis: a link between cancer genetics and chemotherapy*. *Cell*, 2002. **108**(2): p. 153-64.
 124. Kim, H.D., J.Y. Lee, and J. Kim, *Erk phosphorylates threonine 42 residue of ribosomal protein S3*. *Biochem Biophys Res Commun*, 2005. **333**(1): p. 110-5.
 125. Shi, Y., H. Zhai, X. Wang, Z. Han, C. Liu, M. Lan, J. Du, C. Guo, Y. Zhang, K. Wu, and D. Fan, *Ribosomal proteins S13 and L23 promote multidrug resistance in gastric cancer cells by suppressing drug-induced apoptosis*. *Exp Cell Res*, 2004. **296**(2): p. 337-46.
 126. Kim, T.S., C.Y. Jang, H.D. Kim, J.Y. Lee, B.Y. Ahn, and J. Kim, *Interaction of Hsp90 with ribosomal proteins protects from ubiquitination and proteasome-dependent degradation*. *Mol Biol Cell*, 2006. **17**(2): p. 824-33.